THE PHYSIOLOGICAL RESPONSE OF PICOPHYTOPLANKTON TO LIGHT, TEMPERATURE AND NUTRIENTS, INCLUDING CLIMATE CHANGE MODEL SIMULATIONS

Thesis for the Degree of

Doctor of Philosophy

Submitted to the School of Environmental Sciences

at the University of East Anglia

by

Beate Stawiarski

September 2014

The physiological response of picophytoplankton to light, temperature and nutrients, including climate change model simulations

Doctor of Philosophy

University of East Anglia, School of Environmental Sciences

Beate Stawiarski, 2014

Abstract

Laboratory experiments on the physiological response of picophytoplankton to light, temperature and nutrient limitations were conducted. The impact of climate change in a RCP8.5 model scenario simulation was investigated. An acclimated and a dynamic photosynthesis response model reproduce the physiological response to light. Long-term damage (accumulated over days) through photoinhibition is underestimated by the dynamic model. The maximum rate of photosynthesis is significantly lower for picoprokaryotes (0.81 − 1.44 d^{-1}) than for picoeukaryotes (1.93 − 4.93 d^{-1}). Also, their affinity for light is higher (7.15 − 12.42 g C m^2 (mol photons g Chl)$^{-1}$ compared to 3.42 − 9.81 g C m^2 (mol photons g Chl)$^{-1}$). Optimum growth rates differ significantly between the groups (0.47 ± 0.17 d^{-1} for picoprokaryotes and 1.05 ± 0.47 d^{-1} for picoeukaryotes). The temperature tolerance range is higher for picoeukaryotes (2.8°C − 32.4°C compared to 13.7°C − 27°C). The maximum picophytoplankton community growth has a Q_{10} value of 2.3. For picoprokaryotes the Q_{10} value is even higher (4.9). The cell composition in both groups deviates significantly from the Redfield ratio under nutrient saturated conditions with a lower phosphorus demand in picoprokaryotes. Under nutrient limitation nitrogen: carbon is reduced by 15 − 42%, and phosphorus: carbon by 37 − 65%. Chlorophyll *a*: carbon is significantly lower under both nitrogen (-50 − -82%) and phosphorus (-62 − -91 %) limitations. The half-saturation constants are in the range between 0.01 ± 0.02 and 0.19 ± 0.23 µmol NH_4^+ L^{-1} for individual picoeukaryotes. These findings agree with theoretical assumptions related to size with an advantage in subtropical oligotrophic light limited environments and highlight the requirement of data on picoeukaryotes. Climate change leads to enhanced stratification of the water column, reduced availability of nutrients and an increased contribution of picophytoplankton to total phytoplankton biomass weakening the biological pump.

TABLE OF CONTENTS

LIST OF FIGURES

LIST OF TABLES

Acknowledgements

I would like to extend my warmest thanks and appreciation to my supervisory team of Dr Erik Buitenhuis and Professor Corinne Le Quéré of the Tyndall Centre for Climate Change Research at the University of East Anglia. I have benefitted from their patience, kindness, knowledge and combined experience and I feel truly honoured and grateful to have completed my PhD thesis under their direction. Thank you for giving me constant motivation, freedom to develop my interests and skills and for having an open door and ear at any time!

I thank Dr. Laurent Bopp for his supervision during my secondment at LSCE in Paris and for an excellent introduction into the world of climate modelling. It was a pleasure for me to join the group.

Big thanks to my colleagues Moritz, Sian and Raffaela for an exciting and joyful time during long hours of laboratory work which never got boring. A very special thank to Rob, for the excellent support in setting up experiments, looking after the cultures and dealing with any trouble. Lots of things would not have been possible without his help. I also thank Peter for being a good organizer and friend during conference trips and for his never ending coffee supply. I thank everybody who was part of the Greencycles II network for being friends and colleagues and for a good time during workshops, conferences and summer schools. I also thank my friends in Paris who made the summer of 2014 with an exciting football world cup unforgettable while writing up the thesis. Thanks to everybody who was a good friend during the past 4 years and gave me constant motivation.

Außerdem möchte ich meiner Familie für ihre moralische Unterstützung, aber auch für ihre Hilfe bei den Umzügen auf die Insel und wieder zurück und für ihre kontinuierliche Versorgung mit Köstlichkeiten aus der Heimat danken.

I would also like to thank both PhD examiners, Professor Colin Brownlee and Professor Mike Zubkov for an interesting discussion during my PhD viva and lots of valuable comments on my thesis.

The research leading to these results has received funding from the European Community's Seventh Framework Programme (FP7 2007-2013) under grant agreement n° 23836.

1. INTRODUCTION

1.1. Marine climate-carbon cycle feedback

Enhanced atmospheric emissions of greenhouse gases (especially CO_2) by anthropogenic activities, including fossil fuel burning and land-use change during recent decades, lead to an increase in global warming. Since climate change has a positive feedback on the global carbon cycle (Friedlingstein et al. 2001), there is an urgent need for understanding and assessing this system with all its pools, fluxes and vulnerability to predict future carbon-climate feedbacks. The main focus lies on CO_2, as it accounts for 80% of global warming from all greenhouse gases (Canadell et al. 2010).

The natural equilibrium for the distribution of CO_2 between ocean and atmosphere is controlled by temperature, salinity and alkalinity of the surface ocean. Before industrialization inorganic carbon was naturally pumped into the ocean with cold deep water formation in high latitudes, transported to warmer lower latitudes by thermohaline circulation and the same amount (1 Pg C $year^{-1}$) was returned to the atmosphere by upwelling of CO_2 supersaturated water masses. This process was compensated by the flux of 1 Pg C $year^{-1}$ from low to high latitudes in the atmosphere and altogether known as the *solubility pump* (Raven & Falkowski 1999).

Approximately 26% of all anthropogenic CO_2 emissions between 1750 and 2000 (450 Pg C) have been dissolved in the oceans (Le Quéré et al. 2005). More alarming is that its function as a sink for CO_2 decreases significantly with ongoing global warming (Friedlingstein et al. 2001; Le Quéré et al. 2010)

The major drivers of this reduced uptake capacity of the ocean are: increased surface temperature, which decreases the solubility of CO_2 in water, enhanced stratification which restricts the export of carbon to the deep ocean and changes in its biogeochemical cycling within the water column (Friedlingstein et al. 2001).

The global biogeochemical cycling of elements is controlled by food web dynamics. Phytoplankton forms the base of the marine food web (Doney 2006). Even though it accounts for only 0.2% of the global primary producer biomass, half of the global primary production (58 ±7 Pg C $year^{-1}$) is located in the oceans due to faster turnover times (Field

1998; Buitenhuis et al. 2013). Hence, these organisms play an important role in the global carbon cycle.

1.2. The marine carbon cycle

Dissolved inorganic carbon in the upper water column is fixed by phytoplankton, converted into organic matter and passed on to higher trophic levels. Particulate organic matter is released from different trophic levels and is either exported to depth, or recycled by heterotrophic bacteria within the microbial loop (Figure 1. 1). On global average 15% of the phytoplankton biomass, produced at the surface sinks down and is remineralized in the interior ocean, and is eventually returned as inorganic nutrients into the surface by vertical mixing (Falkowski & Oliver 2007). Especially in oligotrophic regions the regeneration of nutrients via the microbial loop is essential (Fenchel 2008).

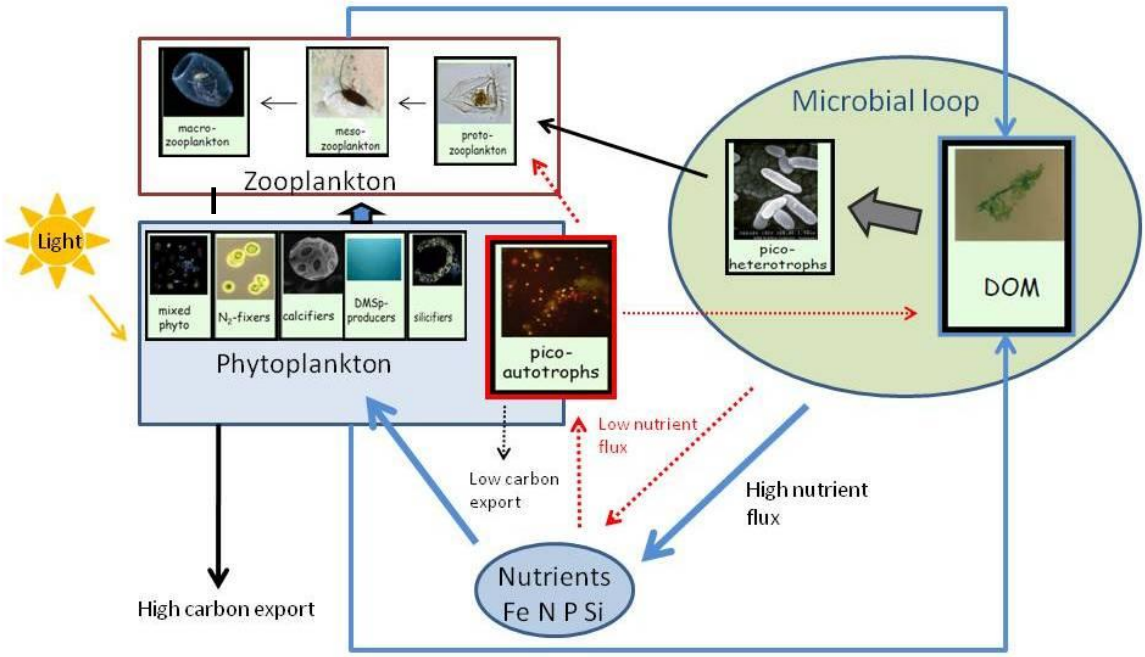

Figure 1. 1 Simplified biogeochemical fluxes between Plankton Functional Types included in the PlankTOM10 model. (Modified after Enright et al. 2009) DOM: Dissolved organic matter

The phytoplankton community structure regulates the export of organic carbon to the deep ocean. This is, because the constitution of the sinking particles defines their depth of degradation (Ploug et al. 2008; Dutkiewicz et al. 2009). This export process is defined as the *biological pump* and mainly driven by the availability of nutrients such as nitrogen or phosphorus (Raven & Falkowski 1999).

Picoprokaryotes (autotrophic bacteria) have been discovered to be an important component of the microbial loop (Jiao et al. 2005; Follows et al. 2007; Azam et al. 1983). With their small size, they have lower sinking rates and the advantage over other phytoplankton groups by taking up nutrients more efficiently (Raven 1998). Like heterotrophic bacteria, they are grazed by protozooplankton.

In oligotrophic ocean areas picophytoplankton, including picoprokaryotes and picoeukaryotes dominate the phytoplankton biomass (Partensky et al. 1999a; Agawin et al. 2000) and have a substantial influence on the biogeochemical cycles. However, quantitative food web dynamics and especially fluxes through the microbial loop are still not fully understood (Marañón 2005).

1.3. Environmental control on primary production

Primary production by photosynthesis is controlled by environmental conditions represented by light, temperature and nutrient availability.

Light is the energy source for all photosynthetic organisms, which is required to convert H_2O and CO_2 into biomass. Its intensity declines exponentially with depth (Lambert-Beer law) due to attenuation by water, dissolved and particulate organic components. It is generally assumed that photosynthesis can be maintained up to depths at which the light intensity decreases down to 1%. This threshold marks the bottom of the euphotic layer, may reach depths up to 200m and is defined as the compensation depth (Sommer 2005). This depth differs significantly between different phytoplankton groups (Speight & Henderson 2010).

Phytoplankton is maintained within the euphotic zone, through vertical stratification of the water column if the mixed surface layer is shallower than the depth of the euphotic zone. Temperature and salinity gradients result in a density gradient across the water column with an upper mixed layer. Within this mixed layer the temperature is nearly constant. A permanent thermocline is present between 200 and 1000m depth over much of the ocean. In mid-latitudes seasonality leads to a shallower seasonal mixed layer in summer. The temperature is lower in these latitudes than in the tropics. In high latitudes the water temperature varies only slightly throughout the water column and is substantially colder than in the other regions (Sommer 2005). Temperature influences the biogeographical distribution of different plankton groups through having an effect on

photosynthesis and growth rates but also on biochemical reactions within the cells (Eppley 1972; Bissinger et al. 2008; Raven & Geider 1988). Phytoplankton groups differ in optimum temperatures, Q_{10} and temperature tolerance ranges. Hence, picoprokaryotes are more restricted towards warmer regions (Buitenhuis et al. 2012), while diatoms and coccolithophores can be found globally in different ecological niches, with high abundances in higher latitudes (Partensky et al. 1999a; Agawin et al. 2000; Buitenhuis et al. 2012).

Furthermore, the limitation by nutrients sets limits to photosynthesis. Carbon, hydrogen and oxygen are the major components of biomass (90%), but also major elements Ca, K, Mg, N, S, P, and trace elements such as e.g. Fe are required. For silicifiers also Si needs to be included as a major nutrient (Sommer 2005).

Nitrogen is the limiting nutrient for photosynthesis over most of the ocean, while iron and phosphorus are important as well. Nitrogen and phosphorus were found to be incorporated into biomass on average with a ratio of 106:16:1 (Redfield 1958), while the importance of iron has been established more recently (Martin & Fitzwater 1988).

In the stratified tropical and mid-latitudes the surface concentrations of nitrogen and phosphorus are very low, sometimes even undetectable (Libes 2009). If there is only low mixing of the water column and no entrainment with external nutrients at the bottom of the mixed layer, primary production in those areas will rely on the remineralisation of organic components and losses will be very low (Fenchel 2008; Falkowski et al. 1998).

There are also ocean regions where the concentration of these two nutrients is higher, but primary production is low. These areas are defined as high nutrients, low chlorophyll regions and limited by the trace element, iron (Martin & Fitzwater 1988), which is essential for the built-up of chlorophyll *a* and photosynthesis. Biologically available iron is limiting due to its low solubility in the ocean water. Hence, the major sources of iron in the ocean are riverine inflows of suspended material, which is more limited to coastal areas or atmospheric dust deposition(Poulton & R. 2002; Kraemer 2004).

1.4. The implication of climate change on environmental conditions

Climate change induced warming of the surface ocean leads to an enhanced stratification of the water column. This causes a reduction in nutrient influx into the surface in mid-latitudes and tropics and consequently a decline in phytoplankton productivity. However

it has also been suggested that the increase in nitrogen fixing organisms in oligotrophic regions may enhance primary productivity where nitrogen is the ultimately limiting nutrient. In this case also the availability of iron, which is essential for chlorophyll *a* synthesis, other trace elements, or phosphorus may control primary production (Karl et al. 1997). At higher latitudes, where the water column exhibits strong mixing and phytoplankton is light limited, climate warming and enhanced fresh water influx from melting sea ice improve the stability of the surface waters and results in an increased phytoplankton biomass (Doney 2006, Figure 1. 2).

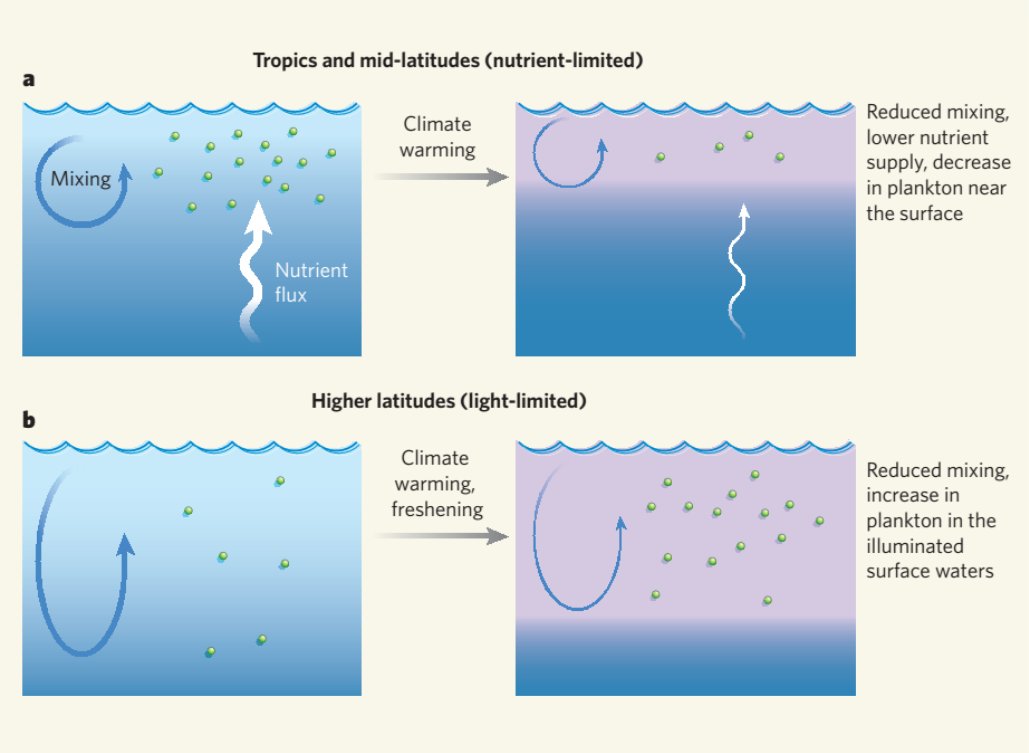

Figure 1. 2 The impact of climate change on the water colum stratification and phytoplankton biomass in tropics and mid-latitudes and higher latitudes (taken from (Doney 2006, Figure 1)

These changes in environmental conditions also have an impact on the community structure (Dutkiewicz et al. 2009) with an increased shift towards smaller phytoplankton and a significant increase in the contribution of picophytoplankton to total phytoplankton biomass in the global ocean (Morán et al. 2010; Agawin et al. 2000). As the efficiency of the biological pump in these communities is decreased, it leads to a positive feedback of climate on the carbon cycle (Bopp et al. 2005).

1.5. Characteristics of picophytoplankton

Picophytoplankton are the smallest component of the phytoplankton community with a size less than 2 - 3 µm depending on definition. They include the two picoprokaryotic genera *Prochlorococcus* (Chisholm et al. 1988) and *Synechococcus* (Nägeli 1849) between 0.6 - 1µm and a variety of larger picoeukaryotes, belonging to the divisions *Chlorophyta*, *Cryptophyta*, *Haptophyta* and *Heterokontophyta* (Vaulot et al. 2008).

Prochlorococcus is the smallest picoprokaryote (0.6µm) and the most abundant phytoplankter in the marine environment. Both picoprokaryotes are also known as cyanobacteria, which translates from Greek into blue bacteria. However, they are also commonly described as blue-green algae. This name relates to the unique derivates of chlorophyll *a* and *b* in *Prochlorococcus*, which allow the identification in field samples by e.g. HPLC (Partensky et al. 1999b) or by satellite observations (Alvain et al. 2005). *Prochlorococcus* reaches the smallest possible size, while containing all essential photosynthetic and metabolic apparatus to maintain cell functioning and convert photosynthetic products into growth (Raven 1998).

There are two *Prochlorococcus* ecotypes, which can be distinguished by their adaptation to high-light (HL) and low-light (LL) environments (Moore & Chisholm 1999). The photosynthetic properties vary only slightly between them with a higher photosynthetic efficiency, but stronger light inhibition in the low light ecotype due to differences in their pigment composition (Veldhuis et al. 2005) with a higher Chl b_2 to Chl $a_2$ratio in the low light ecotype (Partensky et al. 1999b).

Cyanobacteria are the oldest know fossils on earth. They were the first organism which were able to conduct oxygenic photosynthesis and convert H_2O into oxygen and hence created an atmosphere which was favourable for later life forms. Their long evolutionary history made them the most successful organisms on earth (Duarte 2012).

The fist picoeukaryote has been described in 1952 with the discovery of *Chromulina pusilla* (Butcher 1952), which was later renamed to *Micromonas pusilla* (Manton & Parke 1960). With the improvement of isolation techniques from dilution techniques towards the use of flow cytometry sorting and molecular techniques still only 72 picoeukaryotic species have been described by 2008 (Vaulot et al. 2008).

Picoeukaryotes include representatives from various taxa with different pigment compositions and physiological characteristics and many are not yet available in culture. Their cells are more complex than those of prokaryotes including a nucleus and cell

organelles. *Micromonas pusilla* is an important ubiquitous representative of the most abundant group of picoeukaryotes, consisting of a single chloroplast, mitochondrium and golgi apparatus. It also possesses a flagellum like some other picoeukaryotes (Worden 2008). Altogether, picophytoplankton have an advantage over larger cells in light limited environments because of the small package effect, which leads to an increased efficiency in light acquisition (Raven 1998).

Their large surface to volume ratio also allows them to acquire nutrients efficiently and is beneficial in resource limited environments (Raven 1998). In addition, *Prochlorococcus* is able to substitute phospholipids for sulfolipids which is a competitive advantage in the oligotrophic subtropical gyres (Van Mooy et al. 2006).

1.6. Picophytoplankton biomass and distribution

Picophytoplankton are found in all marine environments with contrasting light and nutrient regimes in both strongly vertically mixed and stratified water columns (Veldhuis et al. 2005). Their biomass accounts for 0.53 - 1.32 Pg C globally of which 17 - 39 % is attributed to *Prochlorococcus* 12 - 15% to *Synechococcus* and 49 - 69 % to picoeukaryotes (Buitenhuis et al. 2012).

Together they contribute substantially (26 - 56%) to both phytoplankton biomass and primary production in oligotrophic areas which constitute ~ 70 % of the ocean surface such as the subtropical gyres (Alvain et al. 2005; Buitenhuis et al. 2013; Grossman et al. 2010) and high nutrient low chlorophyll ocean waters (Le Quéré et al. 2005) with slightly decreasing biomass from the tropics polewards (Buitenhuis et al. 2012).

Over a horizontal gradient, their contribution to total phytoplankton biomass is inversely related to nutrient concentration (Raven 1998). In all environments, both prokaryotes are more abundant than picoeukaryotes (Veldhuis et al. 2005), but constitute a smaller biomass (Buitenhuis et al. 2012). Picoprokayrotes are more restricted in geographical distribution towards lower latitudes, while picoeukaryotes can also be found in polar regions (Veldhuis et al. 2005). On average, the biomass of *Prochlorococcus* decreases more slowly with depth than of *Synechococcus* or picoeukaryotes. It dominates at the deep chlorophyll maximum together with picoeukaryotes (Buitenhuis et al. 2012).

1.7. Picophytoplankton diversity in this study

The picophytoplankton species which are used in this study include one high light adapted and one low light adapted *Prochlorococcus sp.* strain and one *Synechococcus sp.* strain as representatives for the group of picoprokaryotes, as well as 6 picoeukaryotes (Table 1. 1). Those strains were isolated by different isolators and have been in culture for 3-23 years until this study started. They were grown at a temperature of either 15, 20 or 22°C and light levels of 20, 35, 100 or 150 µmol photons m^{-2} s^{-1}. The stocks remained at these or very similar conditions during the entire study. Further information about the location and depth of isolation can be found in Figure 3. 1 and Table 3. 1.

The 6 picoeukaryotes cover the size spectrum of this group (1.2 – 3µm) and belong to 3 out of 4 divisions and 6 out of 12 classes of which representatives of picophytoplankton have been described (Table 1. 2). Species from classes with a high and a low number of representatives (Vaulot et al. 2008) have been chosen. Also, the pigment composition of those representatives covers the full range of chlorophylls of picoeukaryotes available in culture with the exception of Chl c_3 containing species (see Table 6.1 in Worden 2008).

Even though there is only very limited information available on the relative contribution of each group to picophytoplankton biomass in the ocean, studies based on e.g. 18S rRNA gene sequences revealed that *Prasinophyceae* account for the highest relative biomass (Figure 1. 3). Together with two other *Mamiellales* species *Micromonas pusilla* accounts for 90% of analyzed gene sequences in the samples of small phytoplankton (≤ 3µm), with higher contributions in temperate and polar areas (Vaulot et al. 2008) as well as the English Channel (Marie et al. 2010). Other studies confirmed the dominance of *Prasinophyceae* in the South Atlantic with highest contributions of *Mamiellales* clade II in mesotrophic temperate waters (Gómez-Pereira et al. 2013). Further, an arctic ecotype of *Micromonas* was shown to dominate in the polar region, where species diversity is lower than in subtropical oligotrophic waters (Balzano et al. 2012). *Dinophyceae* and Diatoms (*Bacillariophyceae*) will not be investigated within this study as other PhD projects investigate those classes in detail, together with larger representatives as calcifying or silicifying plankton functional types. Even though *Dinophyceae* have a relatively high contribution to gene sequences in the review of Vaulot et al. (2008), Massana (2011) argues that their global contribution (5%) results from artefacts in the sampling techniques. Significantly lower contributors are made by the remaining groups (Figure 1. 3). C*ryptophyceae*, *Bolidophyceae*, *Trebouxiophyceae* and *Eustigmatophyceae*

are found to be more abundant in coastal waters, the Prymnesiophyte *Imantonia rotunda* has been reported in temperate and Arctic waters before (Vaulot et al. 2008). However, the study by Vaulot et al. (2008) was biased towards coastal areas and the results concerning picoeukarote distribution patterns are not always consistent with the locations from which strains were initially isolated. For example, *Eustigmatophyceae* were frequently isolated from coastal environments but were not present in their dataset. Hence the link to geographical distribution should be regarded with caution. A more recent review by Massana (2011) confirms the dominance of *Prasinophyceae* in coastal areas but states that *Haptophyta, Pelagophyceae* and *Chrysophyceae* are of higher importance in open ocean waters with global contributions of 15%, 32%, 26% and 21% respectively to autotrophic picophytoplankton communities. Unfortunately, he does not give numbers for the other groups.

The strains used in this study were isolated from tropical, subtropical and temperate, open ocean and coastal areas (Figure 3. 1). Based on the understanding of the contribution of picoeukaryote classes to gene sequences in the review by Vaulot et al. (2008) (Figure 1. 3), the sum of the shown classes *Prasinophyceae, Prymnesiophyceae, Bolidophyceae, Trebouxiophyceae* which are used in this study equals 49.5% of the gene sequences. Also a Haptophyte as an important contributor offshore is included in the experiments and hence the selection of species can be regarded as representative for the investigation of the physiology of the whole group of picoeukaryotes.

Table 1. 1 Picophytoplankton species used within this study including isolation date, light and temperature conditions they were held at in the culture collection and the name of the isolator

Strain	Isolation date	Light µmol photons m^{-2} s^{-1}	Temperature °C	Isolator
Prochlorococcus sp. (HL)	01.04.1990	20	20	Partensky F.
Prochlorococcus sp. (LL)	n/a	20	20	Shimada, A.
Synechococcus sp.	09.10.1987	100	22	Vaulot D., Courties C.
Bolidomonas pacifica	13.11.1994	100	20	Vaulot D.
Micromonas pusilla	11.07.2007	35	15	Foulon, E. Masquelier, S.
Picochlorum sp.	10.11.1994	100	20	Vaulot D.
Nannochloropsis granulata	21.12.2000	100	20	Guillou L.
Imantonia rotunda	09.06.2000	150	15	Le Gall F.
Phaomonas sp.	25.06.2001	100	20	Guillou L.

Table 1. 2 Classification of autotrophic eukaryotic picophytoplankton species used in this study. The list is extended by all classes of which representatives with a cell size < 3µm have been described (after Table 1 in Vaulot et al. 2008). *Phaeomonas sp.* was included in the number of described species.

Division	Class	Genus	Species	Reference	described species
Chlorophyta	Prasinophyceae	*Micromonas*	*Pusilla*	(Butcher 1952; Manton & Parke 1960)	14
	Trebouxiophyceae	*Picochlorum*	*sp.*	(Butcher 1952; Henley et al. 2004)	7
	Pedinophyceae	-	-	-	2
Cryptophyta	Cryptophyceae	-	-	-	1
Haptophyta	Prymnesiophyceae	*Imantonia*	*Rotunda*	(Reynolds 1974)	10
Heterokontophyta	Bacillariophyceae	-	-	-	19
	Bolidophyceae	*Bolidomonas*	*Pacifica*	(Guillou et al. 1999)	2
	Eustigmatophyceae	*Nannochloropsis*	*Granulata*	(Karlson et al. 1996)	3
	Pelagophyceae	-	-	-	4
	Pinguiphyceae	*Phaeomonas*	*sp.*	(Honda and Inouye 2002)	3
	Chrysophyceae	-	-	-	6
	Dictyochophyceae	-	-	-	1

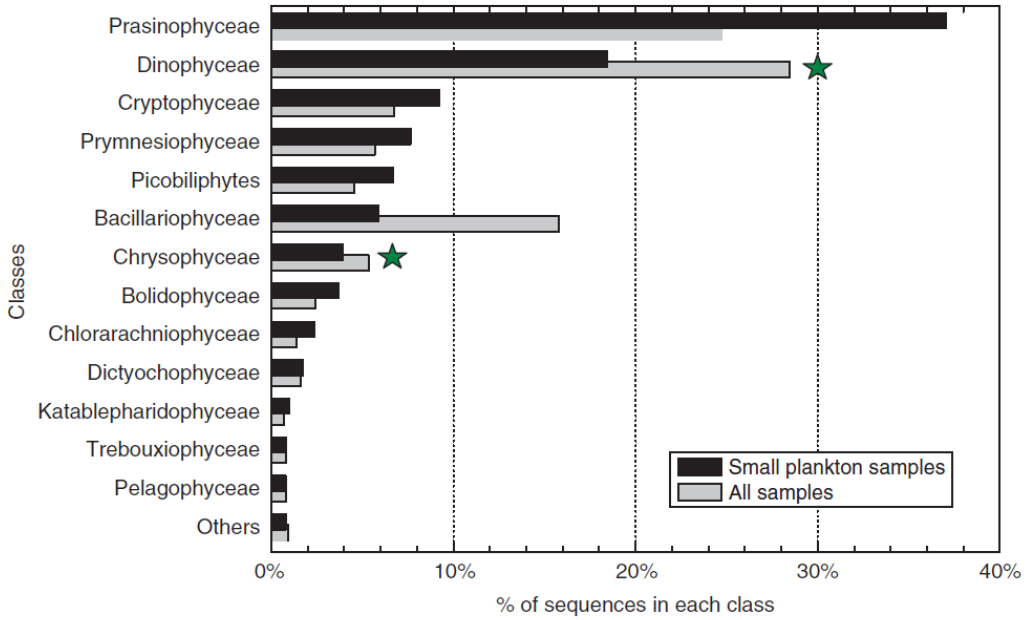

Figure 1. 3 Relative contribution of each picophytoplankton class in predominantly coastal field samples based on a 18S rRNA gene sequence analysis from (Vaulot et al. 2008, Figure 5)

1.8. Studying the physiology of phytoplankton inthe laboratory

Physiological experiments on picophytoplankton can be either conducted in the field to investigate the response to a multiple set of environmental factors on their growth rates or can more specifically treat individual communities or representatives (single strain cultures) in laboratory experiments to focus on the individual impact of one parameter. For example, if the research question addresses the direct impact of light on a picophytoplankton cell, temperature and nutrient conditions will be chosen at favourable levels to avoid a co-limitation by a second parameter.

These approaches help to gain a mechanistic understanding of single processes in the cells which altogether define the physiological response to a whole set of environmental conditions. Observed differences between different groups may then lead to a better comprehension of the underlying processes which govern community structure in the field.

It is challenging to create laboratory conditions which can simulate the physiological response of living organisms in their natural environment and researchers need to be aware of potential adaptation and evolutionary processes which may cause changes in genotype diversity of the phytoplankton culture. These processes are driven by spontaneous mutations, recombination, selection, genetic drift and inbreeding (Lakeman et al. 2009). A small size of the inoculum is one selective process but also changes in environmental parameters compared to those present at the location of isolation or during culturing may favour different genotypes. Also, the transition through different growth phases with high stress potential during stationary phase is influential (Lakeman et al. 2009). Lakeman et al. (2009) published a detailed description about the potential genetic forces on laboratory strains which have been observed for specific taxa. The highest diversity in potential physiological changes due to genetic adaptation has been reported for diatoms. For the two classes (*Chlorophyceae* and *Prymnesiophyceae*) which include picophytoplankton representatives, which are used within this study, a potential adaptation to solid culturing medium would be possible. Also the loss of biomineralization, changes in life cycle phase and changes in ploidity have been reported.

For a representative physiological study on species from a large spatial scale isolates should be sampled close in time and culture conditions should try to be identical to those at the sampling location. In addition, multiple stocks should be maintained if not cryopreserved (Lakeman et al. 2009). This would be the ideal situation. However, for

studying a broad range of species researchers depend on strains which are available in culture collections.

In this case an adequate acclimation period under experimental conditions is mandatory to remove the effect of culturing history on the parameter of interest, even though acclimation may select for a certain genotype. Hence, sub-cultures from stocks should be taken for different experimental setups which require acclimation and replicates should be produced (Lakeman et al. 2009).

1.9. Thesis objectives

It has been shown that climate change has profound implications on phytoplankton because of their high sensitivity to changing environmental conditions (Hays et al. 2005) and causes a shift in community structure towards smaller phytoplankton with a significant increase in the contribution of picophytoplankton (Morán et al. 2010) and a positive climate-carbon cycle feedback (Bopp et al. 2005).

Marine biogeochemical models investigate the interactions of biological communities represented by different plankton functional types and environmental variables to represent biogeochemical fluxes (e.g. Le Quéré et al. 2005) which are affected by physical and chemical settings of the environment and its variability (Dutkiewicz et al. 2009).

To parameterize these models to understand the implications of ongoing changes of the global climate on the carbon cycle, physiological information from laboratory cultures is required (Follows et al. 2007). While most studies focus on picoprokaryotes when investigating the physiology of picophytoplankton, there is a requirement for data of the picoeukaryotes to be included in climate models (Timmermans et al. 2005).

The aim of this study is to investigate the impact of changes in environmental conditions on the physiology of prokaryotic and eukaryotic picophytoplankton to improve their representation in marine biogeochemical models and the understanding of the microbial loop within the carbon cycle on a long term perspective. Further differences between the two picophytoplankton groups are examined to find out if a classification into one plankton functional type is legitimate.

For this, light, temperature and nutrient limitation experiments are conducted on up to 3 picoprokaryotes and 6 picoeukaryotes (Table 1. 1).

Light limitation experiments (Chapter 2) are conducted over a range of light intensities as they are represented in the euphotic zone of the ocean. Growth rates are measured in cultures which have been acclimated to specific light intensities together with an instantaneous photosynthesis response to changes in light. From this, photosynthetic parameters are derived for an acclimated and dynamic response. The following hypotheses are discussed

- We are able to reproduce the physiological response of picophytoplankton to changing environmental conditions with a dynamic photosynthesis model. With the inclusion of a light inhibition term and validation against this extensive new dataset I am able to improve the understanding on translating chlorophyll *a* concentration into carbon biomass and primary production

- Picoeukaryotes differ significantly from picoprokaryotes in terms of physiological parameterization in specific light environments

Temperature experiments (Chapter 3) are conducted over a temperature gradient to test whether Eppley's assumptions

- The temperature dependent maximum growth rates of single phytoplankton species follow an optimum function.

- The temperature dependent maximum growth rates of a phytoplankton community approach an exponential function

can be applied to picophytoplankton in the laboratory and quantify physiological parameters of picoprokaryotes and picoeukaryotes.

Nitrogen and phosphorus limitation experiments (Chapter 4) are conducted in chemostats to compare the nutrient stoichiometry of both groups to results obtained under nutrient saturated conditions. The flexibility of the cells is investigated over a broad range of light (Chapter 2) and temperature (Chapter 3) conditions as they occur in the ocean. This has not been reported before in a single study and will address the hypothesis that

- Both groups show a high flexibility in their nutrient stoichiometry under a broad light and temperature range under nutrient replete conditions, but picoprokaryotes have lower phosphorus requirements.

- Nutrient limitation affects C: N: P ratios and leads to a decrease in Chlorophyll *a*: carbon ratios.

Finally, the physiological parameters derived from the light and temperature experiments are implemented into the marine biogeochemical model PISCES (Chapter 5). Preindustrial conditions in 1800 are compared to a high emission scenario (RCP 8.5) in 2100 to identify if

- Climate change has an influence on the relative contribution of picophytoplankton to total phytoplankton biomass and as a consequence, on the export of carbon to the deep ocean.

A general summary and conclusions, together with an outlook on future research are summarized in Chapter 6. The thesis ends with References.

2. THE INFLUENCE OF LIGHT ON THE PHYSIOLOGY OF PICOPHYTOPLANKTON

2.1. Abstract

We measured both the acclimated and dynamic response of 7 strains of picophytoplankton to light intensity. We derive five photophysiological parameters, maximum photosynthesis rate (P^C_{max}), respiration (resp), the initial slope (α^{chl}), light inhibition (β^{chl}) and maximum chlorophyll to carbon ratio (θ_{max}) using a dynamic photosynthesis model. We also obtain the first four parameters directly from curve fits to the photosynthesis versus light (PI) curves. The parameters from the two methods are comparable for P^C_{max} and α^{chl}, but are different for resp and β^{chl}. Photoinhibition was not represented as strongly in instantaneous photosynthesis measurements as in acclimated growth response curves and led to the underestimation of long term damage due to acclimation to high light conditions in the dynamic model. The maximum carbon specific rate of photosynthesis is significantly lower for picoprokaryotes (0.81 - 1.44 d^{-1}) than for picoeukaryotes (1.93 - 4.93 d^{-1}). The initial slope of the photosynthesis-light curve is higher for picoprokaryotes (7.15 - 12.42 g C m^2 (mol photons g Chl)$^{-1}$) than for picoeukaryotes (3.42 - 9.81 g C m^2 (mol photons g Chl)$^{-1}$). This results in lower light saturation levels (19 - 65 µmol photons m^{-2} s^{-1}) for picoprokaryotes compared to 170- 367 µmol photons m^{-2} s^{-1} for picoeukaryotes. These findings agree with theoretical assumptions related to size which give picoprokaryotes an advantage in oligotrophic light limited environments. There are no differences in maximum chlorophyll to carbon ratios (θ_{max}) between the two groups (0.058 ± 0.016 g Chl g^{-1} C).

2.2. Introduction

Biogeochemical processes and the cycling of elements are both regulated by microbial communities and highly dependent on their community structure (Follows et al. 2007). They consist of various groups of phytoplankton, which are distinguished by specific traits related to biogeochemical processes or size. In ecosystem models these groups are expressed as plankton functional types (PFTs) (Le Quéré et al. 2005; Follows & Dutkiewicz 2011).

Picophytoplankton include cells with a diameter $\leq 3\mu m$ (e.g. Vaulot et al. 2008) and consist of picoprokaryotes represented by *Prochlorococcus* and *Synechococcus* and picoeukaryotes. Picophytoplankton contribute substantially to both phytoplankton biomass and primary production in oligotrophic areas such as the subtropical gyres (Alvain et al. 2005) and high nutrient low chlorophyll ocean waters (Le Quéré et al. 2005) with slightly decreasing biomass from the tropics polewards (Buitenhuis et al. 2012).

As a central part of the microbial loop they regulate the export of organic carbon which is produced in the upper ocean (Morán et al. 2010). Unlike larger organisms, it is assumed that picophytoplankton supply less carbon to the deep ocean as a consequence of small size, lower sinking and higher turnover rates, channelling energy back into higher trophic levels (Fenchel 2008).

While *Prochlorococcus* and picoeukaryotes dominate at the deep chlorophyll maximum in equatorial regions, *Synechococcus* biomass increases towards the surface. In all environments, both prokaryotic cyanobacteria, *Prochlorococcus* and *Synechococcus*, are more abundant than picoeukaryotes (Veldhuis et al. 2005), but constitute a smaller biomass (Buitenhuis et al. 2012).

Changing environmental conditions have a strong influence on the biogeochemical composition of the cells, changing major nutrient stoichiometry of carbon, nitrogen and phosphorus as well as pigmentation (including chlorophyll *a* concentration) as a consequence of acclimation to the prevailing conditions (Veldhuis et al. 2005), which influences the physiological response to light. Additionally, different ecotypes of a single species can be distinguished, which differ in terms of physiological properties such as high light-adapted and low light-adapted ecotypes of *Prochlorococcus* (Johnson et al. 2006).

While previous studies focused on picoprokaryotes in terms of their physiology, there is less data available on picoeukaryotes (Veldhuis et al. 2005). Hence, there is a need to investigate this group more extensively to improve the representation of picophytoplankton in ocean biogeochemical models (Timmermans et al. 2005).
In this study, laboratory experiments on picophytoplankton, including prokaryotic and eukaryotic species, are conducted to investigate the influence of light on their physiology. For this, both an acclimated and a dynamic model are used to obtain 5 parameters: the maximum carbon specific rate of photosynthesis (P^c_m), the initial slope of the PI curve, showing the affinity to light (α^{Chl}), the light inhibition parameter (β^{chl}), the maximum chlorophyll to carbon ratio (θ_{max}), and the specific respiration rate (resp). Three derived parameters are also presented: the maximum growth rate (μ_{max}), the light intensity at which photosynthesis is saturated (I_k) and at its optimum if photoinhibition is included (I_{opt}). The results are used to discuss the following research questions:

1) Are we able to reproduce the physiological response of picophytoplankton to changing environmental conditions by a dynamic model to improve the understanding on translating chlorophyll *a* concentration into carbon biomass and primary production?

2) Do picoeukaryotes differ significantly from picoprokaryotes in terms of physiological parameterization in specific light environments?

The influence of light on the specific cell components (C, N, P) will be discussed in the nutrient chapter of this thesis.

2.2.1. Physiological response of (Pico-) phytoplankton to light

Under nutrient saturated conditions, photosynthesis rate can be regarded as a function of light intensity (Photosynthesis vs. Irradiance (PI) curve, Figure 2. 1) increasing asymptotically from oxygen consumption in darkness to a light saturated maximum oxygen production level. In these light-limited conditions, the slope indicates the affinity for light, which is dependent on the Chlorophyll to carbon ratio (θ) of the organism (Geider et al. 1998). Above light saturation (I_{Opt}) light inhibition described by a light

inhibition parameter (β^{chl}) reduces photosynthesis rate (Platt et al. 1980). If β^{chl} is very low, as in most of the species we measured, the point at which α^{chl} intercepts $P_m^C - resp$ equals light saturation.

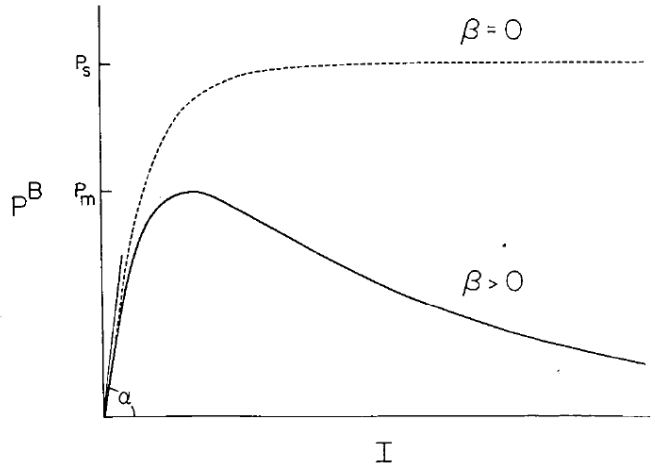

Figure 2. 1 Photosynthesis vs. Irradiance (PI) curve. Initial slope (α) indicates the affinity for light, maximum rate of Photosynthesis (here represented by PB) is reached under optimum light conditions, high light levels may induce light inhibition represented by β (figure 1 in Platt et al. 1980)

The ability to photosynthesize over the range of irradiances (1 - 1500 µmol photons m^{-2}), as they occur in natural environments, is a consequence of photoacclimation to the prevailing conditions, which affects their cell properties (Partensky et al. 1993). It causes a decline in pigment content, such as chlorophyll a, with increasing light intensity together with an increase of energy storage components (Geider 1987).

2.2.2. A dynamic photosynthesis model with light inhibition

Chlorophyll *a* is widely used as an indicator of phytoplankton biomass and, by inference, of carbon concentration. However, it is a highly variable cell component that only accounts for 0.1 - 5% of organic biomass within phytoplankton cells (Geider et al. 1997) and was found to be 2.1 ± 1.1% of C biomass in our experiments. The chlorophyll to carbon ratio increases with decreasing light intensity, increasing temperature and nutrient saturation (Geider et al. 1997). Despite this variability, it is still commonly used in research because of the ease with which chlorophyll *a* concentration can be measured by

satellite or shipboard observations. Better observational constraints on the controls that environmental conditions, species and ecotype distributions exert on the chlorophyll to carbon ratio would improve the usefulness of these observations.

Earlier studies found that the acclimated rate of photosynthesis, normalized to chlorophyll *a* content can simply be described by an exponential function of irradiance (Cullen 1990; Falkowski & La Roche 1991). These steady-state models were used to describe the photosynthetic response under time independent acclimated chlorophyll: carbon ratios and balanced growth conditions.

Later, improvements towards dynamic photosynthesis models were made. With these, environmental feedback on pigment and nutrient stoichiometry within the cells can also be considered over time under unbalanced growth conditions (Geider et al. 1998).

Here, we add a dynamic representation of light inhibition to this photosynthesis model, and evaluate it against picophytoplankton data that were measured in this study under nutrient saturated growth conditions.

2.3. Material and Methods

2.3.1. Cultures and growth rates

Picophytoplankton strains were obtained from the Roscoff culture collection (Vaulot et al. 2004). They include 3 strains of prokaryotes, *Synechococcus* sp. (RCC 30) and a high light and a low light ecotype of *Prochlorococcus sp.* (RCC 296 and 162) as well as the 4 picoeukaryotes, *Bolidomonas pacifica* (RCC 212), *Micromonas pusilla* (RCC 1677), *Picochlorum sp*. (RCC 289), and *Nannochloropsis granulata* (RCC 438).

Cultures were grown in conical flasks (400ml) at a constant temperature of 22°C. Artificial seawater medium (ESAW) (Berges et al. 2001) with ammonium (882 µM $(NH_4)_2SO_4$) as the single nitrogen source and selenium (10 nM Na_2SeO_3) was used. The cultures were grown at up to 7 light intensities between 13 and 720 µmol photons $m^{-2}s^{-1}$ provided by fluorescent tubes (Mitsubishi/Osram FC40ss.W/37) and dimmed by neutral density film in a 14: 10 light: dark cycle. Experiments were conducted in a Sanyo incubator (Versatile Environmental test chamber). Cultures were acclimated for at least 5 divisions. Light intensities were measured with a Radiometer (Biospherical Instruments Inc. QSL - 2101). In vivo fluorescence of acclimated cultures was measured daily in 4 ml samples in a Turner Design Fluorometer (10 AU). Growth rates were calculated during exponential growth phase by taking the logarithm of the in vivo fluorescence values and applying a linear regression through at least three consecutive measurements.

2.3.2. Instantaneous Photosynthetic activity

Instantaneous photosynthetic activity was measured during exponential growth phase after at least 6 hours of light. For this, two oxygraph systems (Hansatech Instruments ltd, DW1/AD electrode chamber) were used. The oxygraph chambers were filled with 3 ml of culture and run at light intensities between 0 and 2000 µmol photons m^{-2} s^{-1} at 21°C. Light levels were increased every 10 minutes by changing neutral density filters in front of a 3 Watt white LED lamp (Deltech GU10-1HP3W). Rates of oxygen production were calculated from the last 5 minutes. Oxygen consumption by the electrodes was measured in filtered culture medium, and used to correct photosynthesis rates.

2.3.3. Sampling

All cultures were sampled for Chlorophyll a, particulate organic carbon (POC), nitrogen (PON) and phosphorus (POP) content. Sampling took place at the same time as the oxygraphs were run. POC/PON samples were collected on precombusted 13 mm GF/F filters for all species. *Prochlorococcus* cells were too small to remain on the filters, but preliminary tests showed that no cells passed through if a layer of 3 filters was used. Chlorophyll a and POP samples were collected on precombusted 25 mm GF/F filters, while *Prochlorococcus* was sampled on 25 mm polycarbonate filters (0.2µm). Between 5 and 20 ml were filtered, depending on the cell density, and rinsed with Milli-Q water. All filters were frozen immediately after sampling in liquid nitrogen and stored at -80°C until analyses. Cell numbers were measured by flow cytometry (BD Biosciences FACSCalibur, flow cytometer). Flow rate was calibrated using the method by Marie et al. (2005) .

2.3.4. Elemental analysis

POC/PON samples were dried at 40°C for 24 hours, placed into precombusted tin capsules and analysed with an elemental analyser (Exeter Analytical, CE-440 Elemental Analyser), which was calibrated with acetanilide (Exeter Analytical). Results were corrected for blank filters. For POP analysis and the results of PON and POP see the nutrient chapter.

2.3.5. Chlorophyll analysis

Chlorophyll samples were extracted in 10 ml of Acetone in 15 ml centrifuge tubes and disintegrated by shaking and vortexing. Tubes were wrapped in aluminium foil and stored at 4°C for 24 hours. For analysis samples were centrifuged and the supernatant was analysed in a Fluorescence Spectrometer (PerkinElmer LS 45 Luminescence Spectrometer). After reading a sample 3 drops of 8% HCl were added into the cuvette to correct for chlorophyll degradation products. The concentration of the calibration standard (SIGMA product No C5753) was obtained prior to analyses (Parson et al. 1984).

2.3.6. Calculations

The instantaneous rates of photosynthesis (mol O_2 s^{-1}) were converted into carbon specific production (d^{-1}). A photosynthetic quotient of 1.1 mol O_2 mol^{-1} CO_2 (Laws 1991) was used as cultures were grown on ammonium as a nitrogen source, together with the measured cell densities and POC content per cell.

We formulate a new dynamic photosynthesis equation (Equation 2. 1), which predicts the dependence of instantaneous photosynthesis (P^C) on the chlorophyll to carbon ratio (θ) and irradiance.

Equation 2. 1

$$P^C = P_m^C \left(1 - exp\left(\frac{-\alpha^{chl} I\theta}{P_m^C}\right)\right) \exp\left(\frac{-\beta^{Chl} I\theta}{P_m^C}\right) - resp$$

See Table 2. 1 for an explanation of the symbols. Equation 2. 1 is based on the dynamic photosynthesis equation developed by Geider and colleagues (Geider et al. 1997). It is extended by a light inhibition term which we obtained by reformulating the steady state light inhibition equation (Platt et al. 1980) to match the dependence on a variable chlorophyll *a* to carbon ratio in the dynamic photosynthesis equation.

We used two different models for estimating the five photosynthetically relevant parameters (α^{chl}, β^{chl}, P^C_m, resp, θ_{max}). The acclimated model uses the measured chlorophyll to carbon ratio and estimates the other four parameters for individual photosynthesis versus irradiance curves by minimizing the residual sum of squares (RSS) between the model and the observations of instantaneous photosynthetic activity (PI curve) for each sample. Parameters for each species were then calculated as the mean of the results for each PI curve. We estimated θ_{max} from linear regression of $\frac{1}{\theta}$ versus I. We also calculated a single parameter set to fit all photosynthesis curves normalized to θ, but found that β^{chl} became negative in five out of seven species which is inconsistent with theoretical expectations. For completeness we summarized those results in the appendix (Table 2. 5).

The second model, the dynamic model estimates all five parameters using a random parameter generation combined with a golden section search to minimize the residual sum of squares between model and observations of instantaneous photosynthesis rate, growth rate and θ (Buitenhuis & Geider 2010). Chlorophyll synthesis was formulated as in

Geider et al. (1997). Because there were many more instantaneous photosynthesis rate measurements that have a larger relative error, they dominated the RSS, while the other measurements, with their smaller errors in fact provided better constraints on the parameters. The average relative standard deviation of the replicate measurements which were used in both models was 11.8 % for growth rates, 15.6 % for θ and 70 % for photosynthesis rates. In addition, the contribution of θ was also lower because it has smaller numerical values. Therefore, growth rates were weighted 30 times more in the RSS and chlorophyll to carbon ratio ratios 50 times more. With these weights the contribution of growth rates was 21 ± 12% of RSS, and of θ 1 ± 1 %.

Table 2. 1 Definition of parameters

Parameter	Definition	Unit
α^{chl}	Chlorophyll specific initial slope of the photosynthesis vs. irradiance curve	g C g^{-1} Chl m^2 mol^{-1} photons
β^{Chl}	Chlorophyll specific light inhibition parameter	g C g^{-1} Chl m^2 mol^{-1} photons
P_m^C	Carbon specific maximum rate of photosynthesis	d^{-1}
P^C	Carbon specific instantaneous rate of photosynthesis	d^{-1}
P_m^{Chl}	Chlorophyll specific maximum rate of photosynthesis	mg C h^{-1} (mg Chl a)$^{-1}$
$resp$	Respiration rate	d^{-1}
θ	Chlorophyll: carbon ratio	g Chl *a* g^{-1} C
θ_{max}	Maximum chlorophyll: carbon ratio	g Chl a g^{-1} C
μ_{max}	Maximum growth rate	d^{-1}
I_{opt}	Light intensity of growth saturation	µmol photons $m^{-2}s^{-1}$
I_k	Light intensity of growth saturation without light inhibition	µmol photons $m^{-2}s^{-1}$

The maximum growth rate was also calculated by Equation 2. 2

Equation 2. 2

$$\mu_{max} = P_m^C \times \left(\frac{14}{24}\right) - resp$$

The light intensity at growth saturation (I_{opt}) can be described by Equation 2.3. If β^{chl} is very low, the optimum light intensity will approach infinity. In that case the point of light saturation can also be described by Equation 2.4.

Equation 2. 3 (Platt et al. 1980)

$$I_{Opt} = \left(\frac{P_m^{Chl}}{\alpha^{chl}}\right) ln\left(\frac{\alpha^{chl} + \beta^{Chl}}{\beta^{Chl}}\right)$$

Equation 2. 4 (Talling 1957)

$$I_k = \left(\frac{P_m^{Chl}}{\alpha^{chl}}\right)$$

Equation 2. 5

$$P_m^{Chl} = \left(\frac{P_m^C}{\theta_{Opt}}\right)$$

P_m^C was converted into P_m^{Chl} by division by chlorophyll *a* to carbon ratio at optimum light intensity (θ_{Opt}) using Equation 2.5. As the calculation of θ_{Opt} requires an input of I_{Opt}, iterations were conducted until a further step would change I_{Opt} by less than 1%.

For measuring statistically significant differences between groups a non-parametric test (Mann-Whitney U test) was used. The tests were conducted with the software Mystat, version 12.

2.4. Results

2.4.1. Instantaneous photosynthetic response of acclimated cells to changes in light

As described in 2.2.1 the chlorophyll concentration within the cells will affect the rate of photosynthesis at a given light intensity. Therefore instantaneous response measurements of photosynthesis were conducted with acclimated cells. For the acclimated model we use measured chlorophyll concentration while the dynamic model uses a dynamically estimated concentration to parameterize Equation 2. 1. Species specific photosynthesis versus irradiance curve parameters are shown in (Table 2. 1 and Table 2. 3).

2.4.2. Acclimated photosynthesis response model with steady state chlorophyll to carbon ratio

The parameterization of the acclimated model (Table 2. 2) showed significant differences ($p < 0.01$) in P^C_m between both groups. Prokaryotes have mean values of 1.22 ± 0.26 d^{-1} with both *Prochlorococcus* ecotypes exceeding the rate of *Synechococcus.* Eukaryotes show higher values of 3.14 ± 1.94 d^{-1}.

The initial slope of the PI-curve is 8.9 ± 6.7 g C m^2 (mol photons g Chl)$^{-1}$ and 5.04 ± 3.78 g C m^2 (mol photons g Chl)$^{-1}$ and also significantly different between the groups ($p < 0.01$). The high standard deviation of the eukaryotes can be explained by the extreme value of *Bolidomonas pacifica,* which had the fewest photosynthesis measurements. Excluding this single value makes α^{chl} lower for the latter group (4.08 ± 2.03 g C m^2 (mol photons g Chl)$^{-1}$).

None of the remaining parameters (respiration, β^{chl} or θ_{max}) are significantly different between both groups. Therefore they can be summarized as respiration= 0.59 ± 0.51 d^{-1}, $\beta^{chl} = 0.07 \pm 0.25$ g C m^2 (mol photons g Chl)$^{-1}$ and $\theta_{max}= 0.047 \pm 0.014$ g Chl g^{-1} C. It has to be mentioned that β^{chl} became negative for *Bolidomonas pacifica* and *Nannochloropsis granulata*, which is inconsistent with theoretical expectations. None of the β^{chl} values is significantly different from 0.

Photosynthesis parameters of individual species and acclimation light intensities are included in the appendix (Figure 2. 8).

Table 2. 2 Parameterization of the acclimated model

Species	size	P_m^C	α^{chl}	β^{chl}	respiration	θ_{max}
	µm	d^{-1}	gC m^2 (mol photons g Chl)$^{-1}$	gC m^2 (mol photons g Chl)$^{-1}$	d^{-1}	g Chl g^{-1} C
Prochlorococcus (HL)	0.6	1.36 (0.68)	7.15 (5.20)	0.02 (0.09)	0.41 (0.41)	0.070 (0.029)
Prochlorococcus (LL)	0.6	1.44 (0.55)	10.09 (9.19)	0.03 (0.08)	0.65 (0.35)	0.044 (0.010)
Synechococcus	1	0.98 (0.58)	9.16 (5.34)	0.12 (0.27)	0.49 (0.61)	0.027 (0.002)
Bolidomonas pacifica	1.2	2.78 (0.51)	13.95 (4.71)	- 0.08 *10^{-2} (0.17)	1.34 (0.64)	0.027 (0.003)
Micromonas pusilla	1.5	4.93 (3.00)	3.77 (1.89)	0.22 (0.36)	0.58 (0.26)	0.057 (0.009)
Picochlorum sp.	2	1.93 (0.96)	4.17 (2.29)	0.19 (0.33)	0.42 (0.25)	0.052 (0.010)
Nannochloropsis granulata	2	2.97 (0.94)	4.25 (2.00)	-0.06 (0.11)	0.68 (0.57)	0.060 (0.003)

2.4.3. Dynamic photosynthesis response model

Using the dynamic model to estimate photosynthetic parameters (Table 2. 3), the maximum carbon specific rate of photosynthesis is again significantly lower ($p < 0.05$) for picoprokaryotes (1.00 ± 0.26 d^{-1}) than for picoeukaryotes (2.89 ± 0.63 d^{-1}). The low light *Prochlorococcus* ecotype shows the lowest value, which is 38% lower than the high light ecotypes.

α^{chl} is higher ($p = 0.289$) for picoprokaryotes (11.5 ± 1.4 g C m² (mol photons g Chl)$^{-1}$) than for picoeukaryotes (8.2 ± 6.5 g C m² (mol photons g Chl)$^{-1}$). Like in the acclimated model, this difference is even amplified ($p = 0.05$) if the extreme value of *Bolidomonas pacifica* is removed (5.0 ± 1.7 g C m² (mol photons g Chl)$^{-1}$).

Respiration is higher for picoprokaryotes (0.18 ± 0.16 d^1) than for picoeukaryotes (0.07 ± 0.12 d^{-1}), again the difference is greater without *Bolidomonas pacifica* (0.01 ± 0.02 d^{-1}).

Photoinhibition is strongly present in *Synechococcus sp.* and *Picochlorum sp.* (1.46 and 0.47 g C m² (mol photons g Chl)$^{-1}$) while the other species have much lower values in the range of 0.006 ± 0.013 g C m² (mol photons g Chl)$^{-1}$. Chlorophyll to carbon ratio is estimated to be 0.06 ± 0.02 g C g^{-1} Chl.

Table 2. 3 Parameterization of the dynamic model

	size	P_m^C	α^{chl}	β^{chl}	Respiration	θ_{max}
	µm	d^{-1}	gC m^2 (mol photons g Chl)$^{-1}$	gC m^2 (mol photons g Chl)$^{-1}$	d^{-1}	g Chl g^{-1} C
Prochlorococcus (HL)	0.6	1.30	12.14	$5.48 * 10^{-10}$	0.31	0.086
Prochlorococcus (LL)	0.6	0.81	12.42	$2.86 * 10^{-2}$	0.22	0.066
Synechococcus	1	0.90	9.81	0.47	$2.64 * 10^{-6}$	0.041
Bolidomonas pacifica	1.2	2.27	17.71	$5.27 *10^{-17}$	0.25	0.044
Micromonas pusilla	1.5	2.89	3.42	$1.1 * 10^{-14}$	$1.42 * 10^{-4}$	0.053
Picochlorum sp.	2	3.76	6.77	1.46	$1.01 *10^{-6}$	0.067
Nannochloropsis granulata	2	2.63	4.83	$4.07 *10^{-12}$	0.03	0.052

The instantaneous response of photosynthesis to light was plotted vs. θ * I (Figure 2. 2). It illustrates the decrease in light requirement with increasing θ as predicted by Equation 2. 1 (cf. Buitenhuis & Geider 2010). That means that with this normalization all curves of all incubations at different light intensities of one species should match. There is good agreement in the data at low light levels but more scatter at higher θ * I. At low θ * I measured rates of both groups are very close to each other. Picoprokaryotes have a slightly steeper slope and reach saturation at a lower light level (Figure 2. 2). They also reach a lot lower photosynthesis rates than the other group.

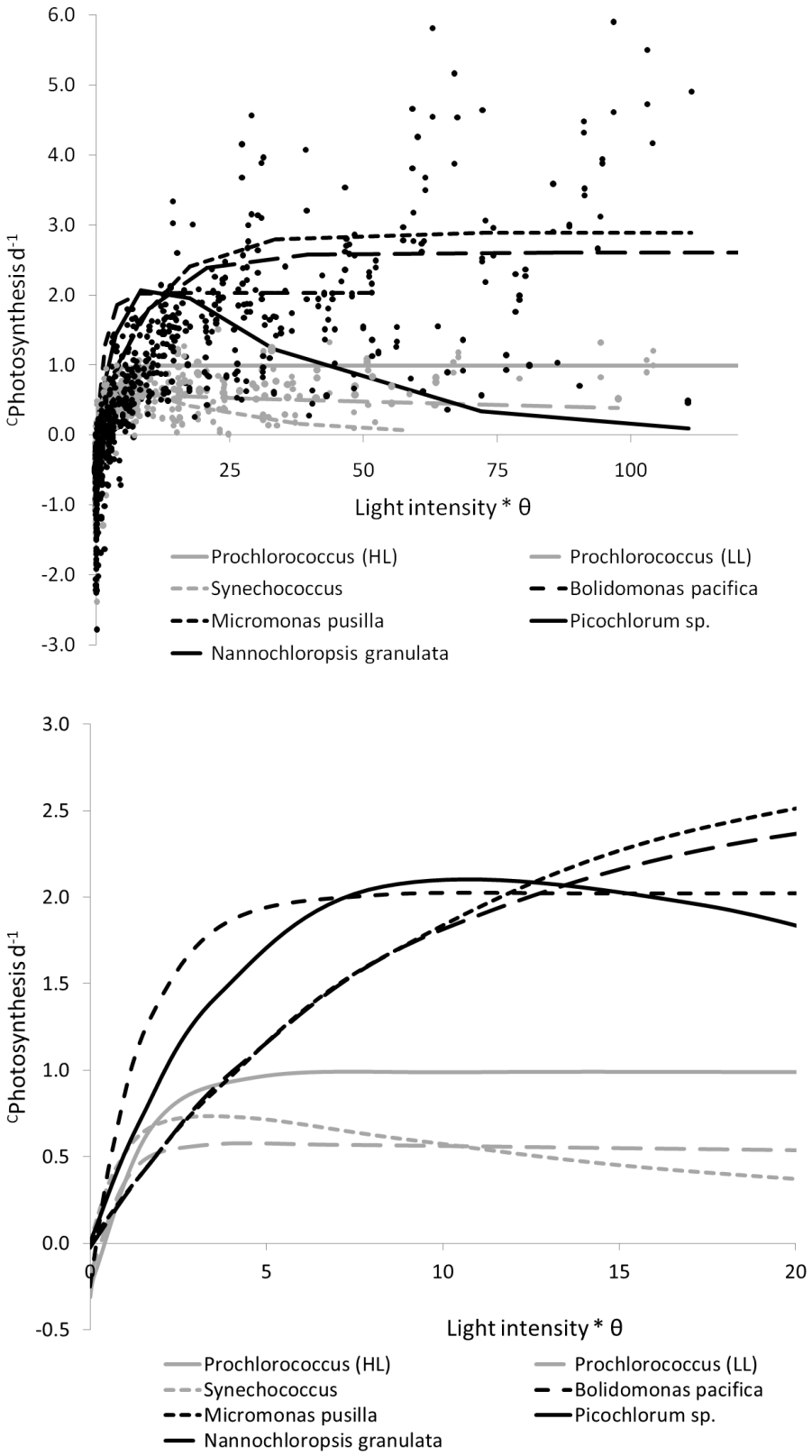

Figure 2. 2Top: Photosynthesis light response normalised to chlorophyll to carbon ratio. circles: measured rates , lines: dynamic model fits. black: picoeukaryotes, grey: picoprokaryotes, bottom: Photosynthesis light response fits normalized to chlorophyll *a* to carbon ratio at low light intensities only.

2.4.4. Comparison of both models

We compare each parameter estimated by both models in (Figure 2. 3). It can be recognised that P^{C}_{m} ,α^{chl}, θ_{max} agree well between the models while resp and β^{chl} are much lower in the dynamic model. The latter only agrees for *Prochlorococcus* (LL). Higher μ_{max} are calculated (μ_{dyn}) than measured (μ_{acc}) if the parameters of the dynamic model are used in Equation 2. 2.

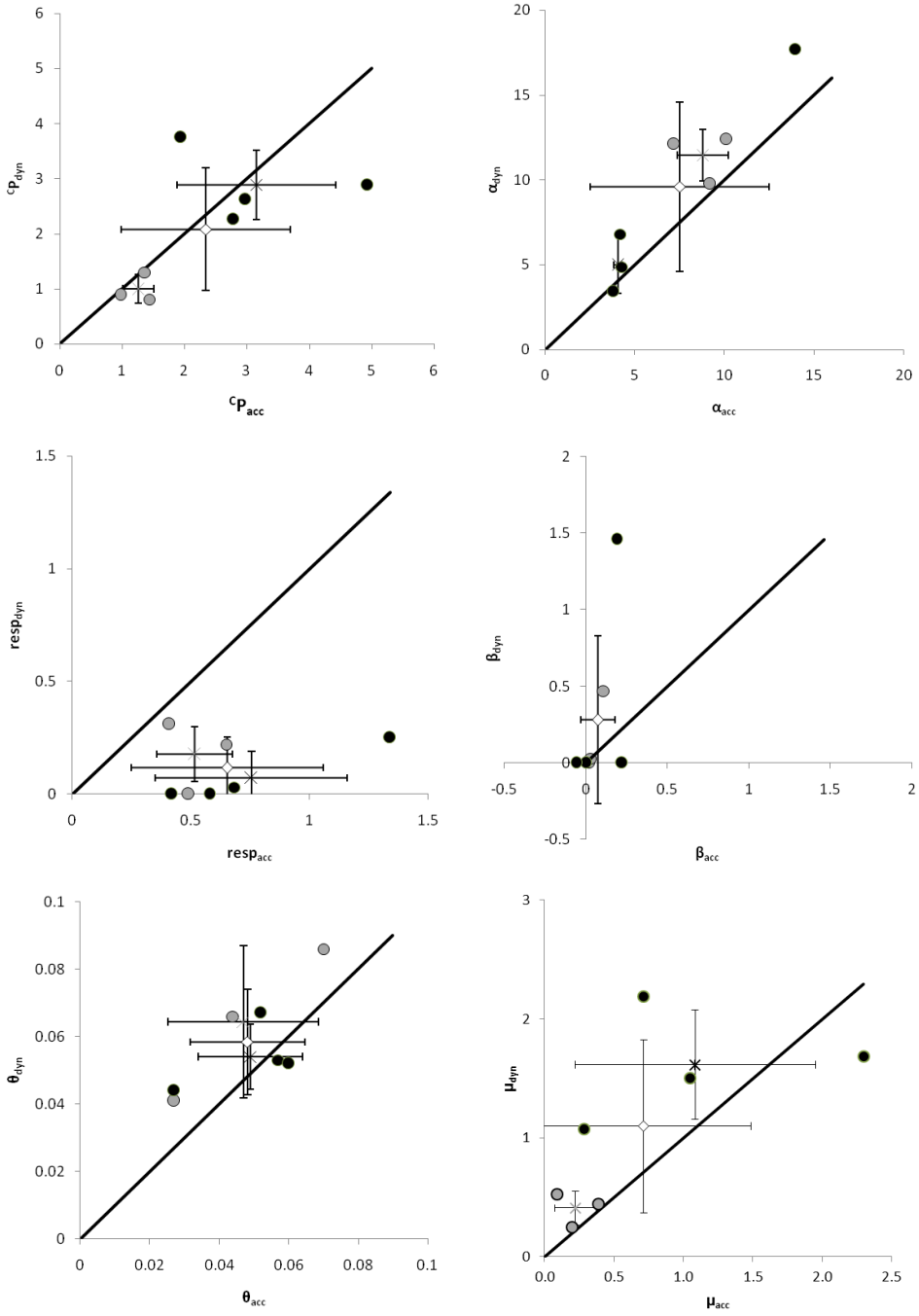

Figure 2. 3 PI parameter estimations from acclimated (acc) and dynamic (dyn) models (circles). black: Picoeukaryotes, grey: Picoprokaryotes, crosses: Mean of the group, diamonds: Mean of both groups, μ represents μmax, θ represents θmax. Lines are 1:1.

2.4.5. Light dependent growth response curves

Figure 2. 4 shows measured growth rates from different species and estimated growth rates by the dynamic photosynthesis light response model. It simulates the acclimated chlorophyll *a* to carbon ratio and photosynthesis rate to calculate the maximum growth rate.

Growth rates of all picophytoplankton species increase with increasing light intensity until they reach their maximum at light saturation (I_{Opt}). Beyond this point, light inhibition may cause a decline in growth rate. Picoeukaryotes show significantly ($p < 0.05$) higher measured maximum growth rates (1.2 – 2 d^{-1}) at observed saturated light levels in incubations between 120 and 500 µmol photons m^{-2} s^{-1}) than picoprokaryotes (0.3-0.6 d^{-1} between 64 and 330 µmol photons m^{-2} s^{-1}). We find light inhibition in both groups. *Synechococcus* and the low light *Prochlorococcus* experience the steepest decline in growth rate at high light levels. The low light *Prochlorococcus* ecotype grows at the narrowest light intensity range and is light inhibited at the lowest light level in this experiment of only 147 µmol photons m^{-2} s^{-1}.

On average, the dynamic model is able to estimate light dependent growth rates well as an independent variable, when the higher weighting parameter for growth rate measurements is introduced (Figure 2. 4A). However, for several species there is a negative bias in the model at low light intensities and a positive bias at high light (Figure 2. 4B). This indicates that the photoinhibition of growth tends to be underestimated. This is found in agreement with the fact that in most cases β^{chl} calculated by the dynamic model (Table 2. 3) is lower than that calculated from the acclimated model (Table 2. 2) and thus that growth rates tend to be more light inhibited than instantaneous photosynthesis rates.

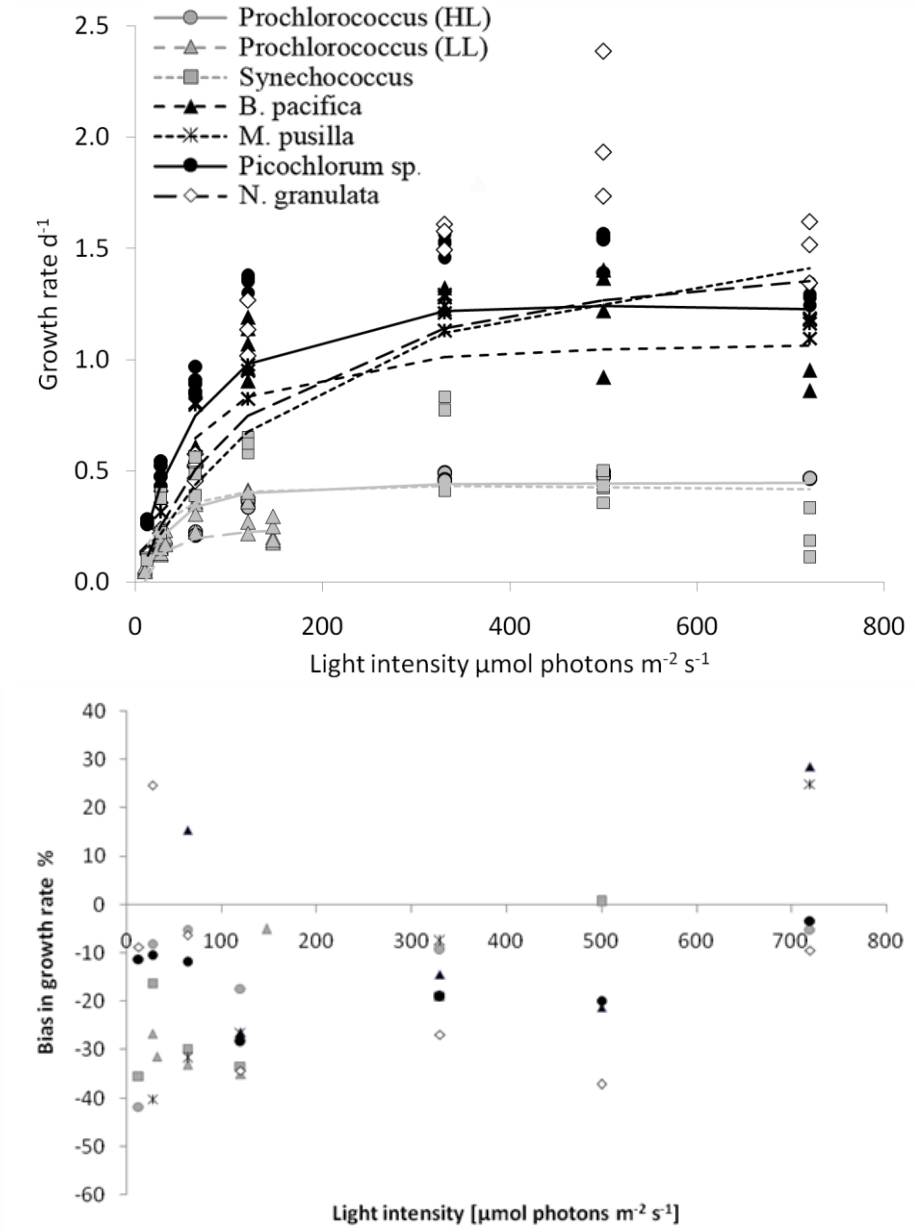

Figure 2. 4 Light dependent growth rates of picophytoplankton. Symbols: laboratory data, lines: dynamic model fit and bias between the dynamic model fit and measured growth rates in %

Figure 2. 5 and Table 2. 4 show measured and modelled maximum growth rates using photosynthesis parameter values from the acclimated and dynamic photosynthesis model in Equation 2. 2. Picoprokaryotes achieve measured maximum growth rates of 0.48 ± 0.15 and picoeukaryotes of 1.51 ± 0.36 d^{-1}. Maximum growth rates increase with cell size (Figure 2. 5).

The dynamic model parameters are able to represent μ_{max} better with a lower bias (24%) compared to the photosynthetic parameters estimated from the acclimated model (59%). The increasing trend of growth rate with cell size is significant in measurements (p =

0.001) and estimates from the dynamic model (p = 0.003). The better representation in the dynamic model compared to the acclimated model may be a consequence of the inclusion of growth rate measurements in the estimation of P_m^C and resp. The acclimated model tends to underestimate growth rates which may be due to the overestimation of respiration rates. Direct growth rate measurements are more accurate than estimates from photosynthesis response curves. However, growth rates were only measured at specific light intensities and may deviate slightly from the true maximum growth rate. Still, there is a significant difference ($p < 0.05$) in the measured μ_{max} between the two picophytoplankton groups which is also reflected in the dynamic model.

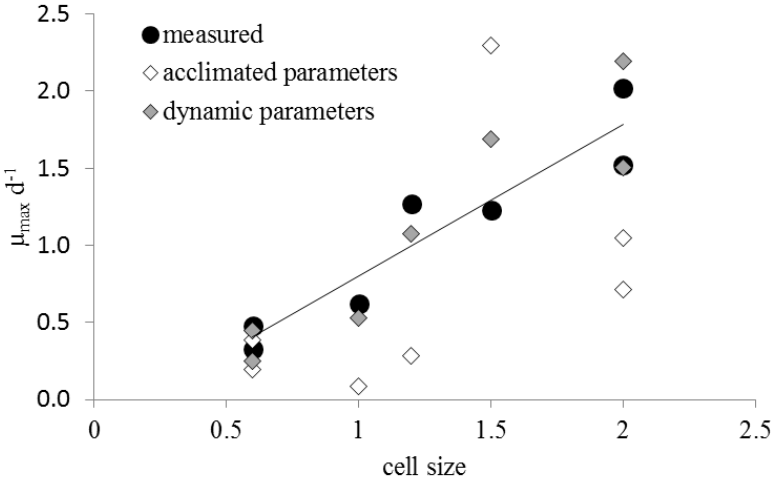

Figure 2. 5 Measured maximum growth rates (black circles) and estimated growth rates from photosynthesis and respiration measurements depending on cell size : acclimated model parameters (white diamonds), dynamic model parameters (grey diamonds). Line: linear regression through measured growth rates.

2.4.6. Light intensity at saturated and optimum photosynthesis

Light intensities at which photosynthesis is saturated (Table 2. 4) were estimated from Equation 2. 4 using photosynthetic parameters from both models (Table 2. 2 and Table 2. 3). There is a general increase in maximum growth rate with light saturation in both models for picophytoplankton (Figure 2. 6), which is significant ($p = 0.02$) if using parameters from the dynamic model. There is also a significant difference in I_k between the groups in both ($p < 0.05$) models.

Light saturation occurs at lower light levels and lower growth rates for picoprokaryotes (19 - 65 µmol photons m^{-2} s^{-1}) than for picoeukaryotes (170 - 367 µmol photons m^{-2} s^{-1}) (Table 2. 5, Figure 2. 2) and is substantially higher in *Micromonas pusilla* (2046 µmol photons m^{-2} s^{-1}) in the acclimated model. *Bolidomonas pacifica* was regarded as an outlier in the estimation of photosynthetic parameters due to less data input. If β^{chl} was included in the estimation of I_{opt} (Equation 2.3) in the acclimated model, picoprokaryotes had optima in the range of 260 - 386 µmol photons m^{-2} s^{-1} and both picoeukaryotes with positive β^{chl} values at 747 µmol photons $m^{-2}s^{-1}$ for *Picochlorum sp.* and in the indefinite range for *Micromonas pusilla* (5928 µmol photons m^{-2} s^{-1}).

The dynamic model shows generally lower I_k, because P_m^{chl} tends to be lower (data not shown) and α^{Chl} (Figure 2. 3) tends to be higher. For the species with the highest β^{chl}, the low light *Prochlorococcus* ecotype had an optimum at 114 µmol photons m^{-2} s^{-1}, *Synechococcus* at 140 µmol photons m^{-2} s^{-1} and *Picochlorum sp.* at 293 µmol photons m^{-2} s^{-1}. It would be 6 times higher for the high light *Prochlorococcus* ecotype compared to the low light strain, because β^{chl} is very low and goes towards indefinite for the other species (> 2460 µmol photons m^{-2} s^{-1}).

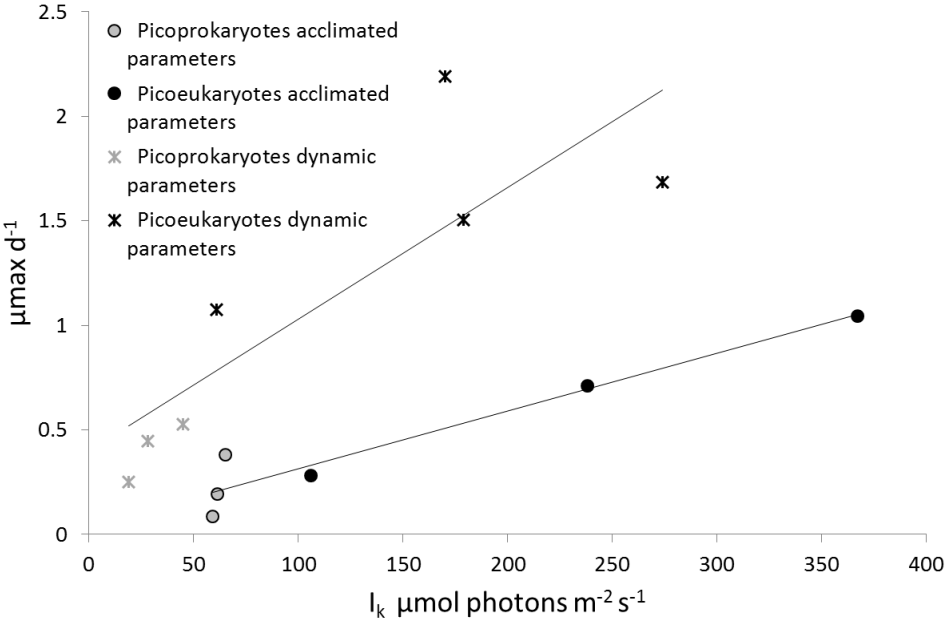

Figure 2. 6 Maximum growth rate at light saturation calculated from acclimated (circles) and dynamic (crosses) model parameters. grey: picoprokaryotes, black: picoeukaryotes, The acclimated model result for *Micromonas pusilla* is excluded.

Table 2. 4 Parameters derived from model parameter estimates, measured and modelled maximum growth rates (μ_{max}), Light intensities at growth saturation (I_k and I_{opt}) chlorophyll *a* to carbon ratios at optimum light intensities, and chlorophyll specific maximum rates of photosynthesis corrected for respiration (P_m^{chl} – resp) for comparison with literature values.

	Measured		Acclimated model					Dynamic model				
Species	size	μ_{max}	I_k	I_{opt}	θ_{Opt}	μ_{max}	P_m^{chl}- resp	I_k	I_{opt}	θ_{Opt}	μ_{max}	P_m^{chl}- resp
	µm	d^{-1}	µmol photons m^{-2} s^{-1}	µmol photons m^{-2} s^{-1}	g C g^{-1} Chl	d^{-1}	mg C h^{-1} (mg Chl a)$^{-1}$	µmol photons m^{-2} s^{-1}	µmol photons m^{-2} s^{-1}	g C g^{-1} Chl	d^{-1}	mg C h^{-1} (mg Chl a)$^{-1}$
Prochlorococcus (HL)	0.6	0.48 (±0.03)	65	384	0.034	0.38	2.01	28	660	0.045	0.45	1.58
Prochlorococcus (LL)	0.6	0.33 (±0.07)	61	357	0.027	0.19	2.09	19	114	0.040	0.25	1.04
Synechococcus	1	0.62 (±0.03)	59	258	0.021	0.09	1.68	45	140	0.024	0.53	2.74
Bolidomonas pacifica	1.2	1.27 (±0.07)	106	-	0.022	0.28	4.71	61	2462	0.024	1.08	5.93
Micromonas pusilla	1.5	1.23 (±0.06)	2046	5929	0.007	2.30	42.0	274	9129	0.036	1.69	5.77
Picochlorum sp.	2	1.52 (±0.05)	238	747	0.022	0.71	4.8	170	293	0.038	2.19	7.09
Nannochloropsis granulata	2	2.02 (±0.14)	367	-	0.022	1.05	7.28	179	4963	0.035	1.51	5.26

2.4.7. Chlorophyll to carbon ratios

Chlorophyll *a* to carbon ratios decline reciprocally with increasing light intensity in both picophytoplankton groups from 0.043 ± 0.016 g Chl g^{-1} C at 13 µmol photons m^{-2} s^{-1} to 0.014 ± 0.004 g Chl g^{-1} C at the highest measured light intensity of 720 µmol photons m^{-2} s^{-1} (Figure 2. 7). Maximum chlorophyll to carbon ratios calculated by linear regression of $\frac{1}{\theta}$ versus I give 0.03 – 0.07 g Chl g^{-1} C for picoprokaryotes with *Synechococcus* having the lowest concentration of chlorophyll. The same range of values was found for picoeukaryotes (Table 2. 2). Consequently there is no statistically significant difference in θ_{max} (0.058 ± 0.016 g Chl g^{-1} C) between the two groups.

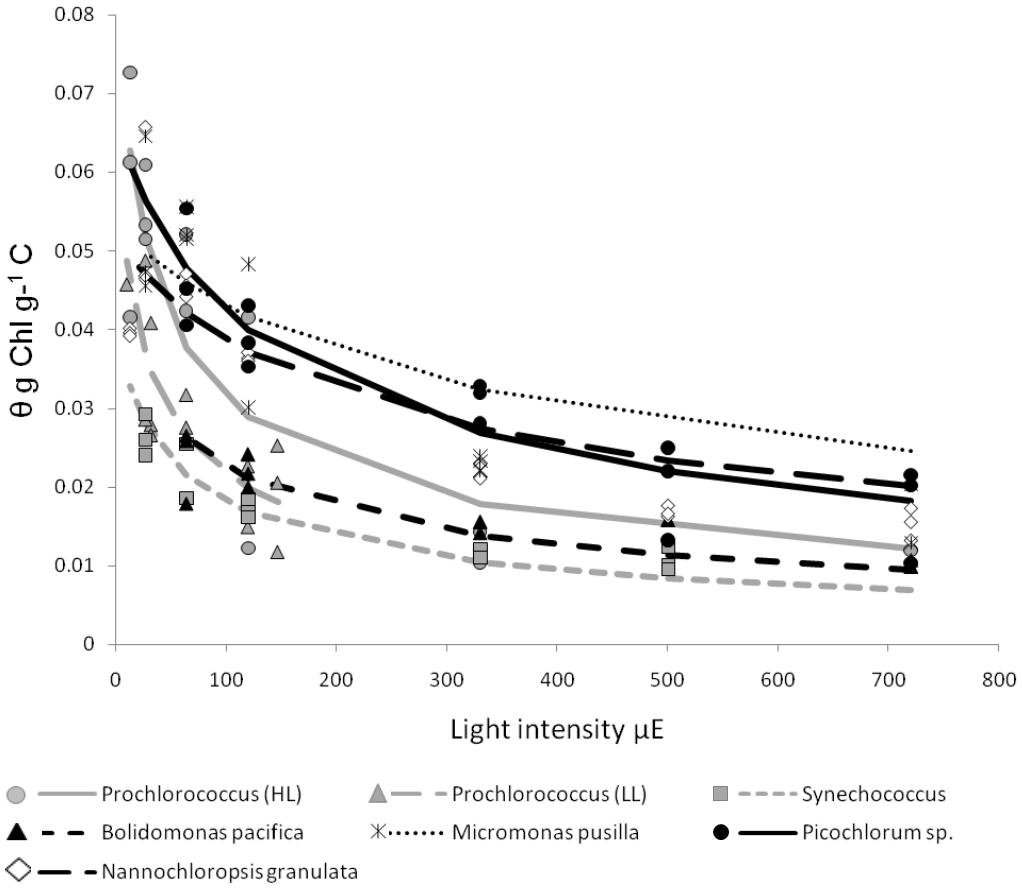

Figure 2. 7 Light dependent chlorophyll: carbon ratio (g g^{-1}) in acclimated cultures. points: measured, lines: estimated by the dynamic model.

In the acclimated model we normalized photosynthesis rate to measured chlorophyll to carbon ratios within the different acclimations to estimate the other model parameters. The dynamic photosynthesis model estimated θ itself. Those estimates for each culture are indicated by the lines in Figure 2. 7. They all match the measured values well. Only

for *Micromonas pusilla* the curve was not steep enough to reach maximum and minimum values. This can be explained by a low contribution of θ to the total RSS. An increase of this fraction led to an increase in $\theta_{max}/\theta_{min}$ in this species.

2.5. Discussion

2.5.1. Photosynthetic parameters

The instantaneous response of photosynthesis to light was approached by two different methods. They agree well considering P^C_m, α^{chl} and θ_{max} but give differing results for respiration and β^{chl} and therefore also for the optimum light intensity and μ_{max}. The acclimated model has a lower RSS relative to the photosynthesis measurements (29) compared to the dynamic model for which RSS are 33 times higher (955). This is a consequence of the high relative uncertainty in the photosynthesis measurements which is better described if each curve is calculated individually only to match carbon specific rates of photosynthesis at a measured chlorophyll to carbon ratio. The dynamic model fits one parameter set to all curves, also considering growth rates and chlorophyll to carbon ratios. In the end this method causes a bigger error in the estimation of the photosynthesis rates, but allows to consider conditions of photoacclimation in the field while the first model needs conditions of balanced growth and measured values of θ. This is needed for translating observational chlorophyll concentrations into phytoplankton biomass and/or primary production. Therefore it is necessary to continuously improve and validate these types of models with laboratory data.

The photosynthetic response of picophytoplankton has been investigated in several studies in a variety of units (Partensky et al. 1993; Moore & Chisholm 1999; Shimada et al. 1996; Glover et al. 1987). These results have been summarised for picoprokaryotes and picoeukaryotes by (Veldhuis et al. 2005). Unfortunately, those studies report maximum photosynthesis rates in mg C h^{-1} (mg Chl *a*)$^{-1}$ and do not separate it from respiration rate. Hence, for a direct comparison, P_m^{Chl} - respiration is shown in the same units.

They find an increase in P_m^{Chl} with cell size with 1.18 - 5.58 mg C h^{-1} (mg Chl *a*)$^{-1}$ in picoprokaryotes, which is comparable to results in both the acclimated and the dynamic model. For picoeukaryotes values between 0.8 - 10.2 mg C h^{-1} (mg Chl *a*)$^{-1}$ were reported.

In the acclimated model P_m^{Chl} has comparable values, with the exception of *Micromonas pusilla*. In the dynamic model all species fit into the range as found in literature.

The initial slope of the photosynthesis versus light curve, also described as the photosynthetic efficiency (α^{chl}), was found between 0.50 - 38.89 g C m^2 (mol photons g Chl)$^{-1}$ consistent with our findings.

In contrast to those studies, we find that there are significant differences in P_m^C and α^{chl} concerning the two picophytoplankton groups, both if parameter values are fit to individual photosynthesis versus irradiance curves, and the dynamic model shows support for a separation of the two groups as well ($p = 0.05$).

A light inhibition index is widely used to describe the light intensity at which photoinhibition occurs (P_m^{Chl} / β^{chl}). The reported range is very wide between 86 - 922 µmol photons m^{-2} s^{-1} for picoprokaryotes and 448 - 548 µmol photons m^{-2} s^{-1} for the two picoeukaryotic species investigated by Glover et al. (1987). All estimates from the acclimated model are above these values (> 4500 µmol photons m^{-2} s^{-1}) and indicate that β^{chl} may be underestimated in the model. This is supported by a slight underestimation of photosynthesis rates close to light saturation by 13 - 26 % on average with a good agreement at high light intensities (Table 2. 6). However photoinhibition was not strongly reflected in most instantaneous photosynthesis measurements.

In turn the dynamic model gives more realistic values for the 2 species with the highest β^{chl}, with a light inhibition index of 945 µmol photons m^{-2} s^{-1} for *Synechococcus sp* and 785 µmol photons m^{-2} s^{-1} for *Picochlorum sp*., but has 28 % and 187 % higher RSS in these 2 species respectively compared to the other model. This is a consequence of photosynthesis rates being substantially overestimated close to optimum light intensity by up to 350 % in *Synechococcus sp.* and 665 % in *Picochlorum sp*. and therefore β^{chl} seems to have been overestimated in these species (Table 2. 6).

Light saturation (I_k) was reported for several strains in the previously mentioned studies, ranging between 11.7 - 130 µmol photons m^{-2} s^{-1} in picoprokaryotes, which agrees with our findings in both models. For picoeukaryotes higher values (143 - 267 µmol photons m^{-2} s^{-1}) were previously obtained. In the acclimated model, this is in agreement with estimates for *Picochlorum sp.*, one species has an even higher saturated light intensity and *Micromonas pusilla* approaches infinity. Only photosynthesis in *Bolidomonas pacifica* was saturated at a lower light intensity in both models. In turn, all estimates for the other three picoeukaryotes in the dynamic model are within or very close to this range.

Optimum light intensities (I_{Opt}) for picoprokaryotes ranged between 39 and 341 µmol photons m^{-2} s^{-1} in previous studies. Our findings are similar or slightly higher in the acclimated model. There is a better agreement in the dynamic model, only the high light Prochlorococcus ecotype, which was less affected by light inhibition exceeds this estimate. Glover et al. (1987) report values between 143 - 267 µmol photons m^{-2} s^{-1} for the two picoeukaryotes *Micromonas pusilla* and *Imantonia rotunda*. The estimates from the acclimated model are both above this range, only I_{opt} of *Picochlorum sp*. in the dynamic model gets close to this range as β^{chl} is higher than for the other species.

There is a better agreement of our findings with other studies regarding I_k rather than I_{Opt} in both models. The low representation of photoinhibition in photosynthesis measurements and consequently in the models suggests that I_k is a better measure than I_{Opt} for estimating the light intensity at which photosynthesis reaches its maximum in the investigated species.

2.5.2. Growth rates

The maximum growth rates obtained for *Prochlorococcus* in these experiments are in the range of those measured in various other studies. For example, Moore & Chisholm (1999) investigated different high light *Prochlorococcus* ecotype strains and found maximum values between 0.51 ± 0.03 and 0.83 ± 0.05 d^{-1} while we measured values up to 0.5 d^{-1}. The maximum growth rates for low light *Prochlorococcus* ecotype were found to be between 0.51 and 0.75 d^{-1} (Moore et al. 1995; Shimada et al. 1996; Reckermann & Veldhuis 1997). In this study we measured slightly lower values of up to 0.4 d^{-1} which may be explained by strain related differences. Maximum measured growth rates of *Synechococcus* also agree with data from the literature (Moore et al. 1995; Shimada et al. 1996; Timmermans et al. 2005) and are up to two times higher than those of *Prochlorococcus*. However our *Synechococcus* strain shows strong inhibition at high light levels, which is contrary to its general distribution shallower in the water column (Veldhuis et al. 2005; Buitenhuis et al. 2012). As our strain was isolated from a depth of 120m we can assume that it is a low light adapted ecotype and not representative for the whole *Synechococcus* community.

Compared to the low light *Prochlorococcus* ecotype which was light saturated at a lower light level, the high light adapted strain grew over a wider range of light intensities and

was less affected by light inhibition which is a consequence of differences in pigment composition (Veldhuis et al. 2005).

Results presented here show that picoeukaryotes have significantly higher growth rates at all light levels than picoprokaryotes, this is in agreement with previous studies (Worden et al. 2004; Morán 2007). The relationship between cell size and maximum growth rate is negatively correlated over a wide range of phytoplankton size classes (Marañón et al. 2013), but it is well established that picophytoplankton do not follow this rule. Picophytoplankton have a higher proportion of non-scalable cell components resulting in a decrease in growth rate below 2-3 µm or 50 – 100µm^3 (Raven 1998; Bec et al. 2008; Marañón et al. 2013).There are, however, field measurements which show the opposite trend for picophytoplankton in oligotrophic ocean regions (Zubkov 2014; Taniguchi et al. 2014).

The higher growth rates of picoprokaryotes in oligotrophic ocean areas are a consequence of the better adaptation of small cells to low nutrient availability (Taniguchi et al. 2014).

This is supported by the increase in growth rates of small picoeukaryotes of up to 41% after nutrient enrichment (Bec et al. 2008) and the better success of picoprokaryotes in competition for e.g. phosphorus (Zubkov et al. 2007) or organic nitrogen components (Zubkov et al. 2003) in oligotrophic ocean waters. Also iron enrichment experiments have revealed that phytoplankton communities only grow at half of their maximum growth rates due to nutrient limitation and grazing control (Landry et al. 2000; Laws 2013).

Picoprokaryotes have been shown to dominate picophytoplankton biomass in oligotrophic environments (Moore et al. 1995; Partensky et al. 1999b), but the proportion of picoeukaryotes and also the community growth rate increases with nutrient availability over a spatial and seasonal gradient (Morán 2007; Vázquez-Domínguez et al. 2013). With the dominance of picoeukaryotes, maximum community growth rates are significantly higher (Morán 2007; Vázquez-Domínguez et al. 2013).

Measurements of growth rates presented here are consistent with *in situ* growth rates of the dominant phytoplankton group in coastal areas (Vázquez-Domínguez et al. 2013).

By calculating growth rates with a dynamic model that also takes into account measurements of photosynthesis rates, we find that the slope and growth rates will be underestimated slightly over the range of light intensities that were used in our experiments (Figure 2. 4). Also, it is not able to account for the strong light inhibition in *Synechococcus sp.*. This appears because, as previously mentioned, light inhibition was not strongly reflected in most instantaneous photosynthesis measurements. This might

reflect a shortcoming in the model, which can only represent reversible light inhibition as a function of θ, but not "irreversible" damage that might be acquired over days (the time-scale of the growth rate measurements) rather than minutes (the time-scale of the photosynthesis measurements).

The dynamic model agrees better with the maximum growth rates, calculated using Equation 2. 2, which is a consequence of the inclusion of growth rate estimates in the calculation of the photosynthesis parameters. The lower and more variable respiration rates in comparison to the acclimated model may reflect the adjustment to meet the measured growth rates.

In summary, we find evidence that there are significant differences in the physiological characteristics of both groups with picoeukaryotes having lower affinities for light (α^{chl}) but higher maximum rates of photosynthesis (P_m^C), maximum growth rates (μ_{max}) and consequently higher light intensities at which photosynthesis is saturated I_k.

The relationship of maximum growth rate and cell size found in this study (Figure 2. 5) can only be applied to this group because of its small size (Raven 1998; Veldhuis et al. 2005). Investigating the impact of cell size on maximum growth rates for phytoplankton in general will give an inverse trend (Chisholm 1992). The mechanism behind this decrease in growth rate with decreasing cells size is thought to be the increased fraction of non-scalable cell compounds which leads to a decrease in growth rate (Raven 1998) and is reflected in significant differences in P_m^C and μ_{max} between picoprokaryotes and picoeukaryotes, However the small package effect leads to an increased efficiency in light acquisition (Raven 1998) which is reflected in a higher α^{chl} in picoprokaryotes. This leads to lower light saturation levels in the smaller group, but also to higher damage at high light intensities and is reflected in the relatively strong light inhibition in *Synechococcus sp*. in this study and the low light intensity range at which the low light *Prochlorococcus* strain grew.

Altogether, the higher growth and photosynthesis rates over a wider range of light intensities give picoeukaryotes an advantage over the smaller group and explain their higher global contribution to picophytoplankton biomass of 49 - 68 % (Buitenhuis et al. 2012). However, the higher affinity to light, lower nutrient requirements and lower grazing pressure are beneficial for picoprokaryotes in the deep chlorophyll maximum and in oligotrophic ocean regions (Chen & Liu 2010).

Most studies which were conducted on picophytoplankton were biased towards picoprokaryotes. Hence, using a parameterisation that is mainly based on the physiological response of picoprokaryotes is not representative for a picophytoplankton community and indicates that there is a special need to study this diverse group more thoroughly.

We also show that the acclimated model is able to reproduce steady state photosynthesis rates better than the dynamic model with lower RSS. However, the dynamic model is able to reproduce P_m^C and α^{chl} in a similar way as the acclimated model in a range of values that have previously been reported in other studies. Hence, also estimates of μ_{max} and I_k can be regarded as adequate in this study. The estimation of μ_{max} from the dynamic model parameters was even more accurate and showed the same significant trend with cell size as was found in measured growth rates. The only limitation was found in the representation of long term damage during acclimation to high light. Due to the low representation of photoinhibition in the instantaneous photosynthesis measurements, it was not reflected in the subsequent calculations of light dependent growth rates and lead to a bias towards lower growth rates.

2.6. Conclusion

We conclude that within the picophytoplankton group photophysiological properties of picoprokaryotes and picoeukaryotes differ significantly. For picoprokaryotes P_m^C (0.81 - 1.44 d^{-1}) and growth rates (0.48 ± 0.15 d^{-1}) are lower, but α^{chl} is higher (7.15 - 12.42 g C m^2 (mol photons g Chl)$^{-1}$ resulting in lower light saturation levels (19 - 65 µmol photons m^{-2} s^{-1}). For picoeukaryotes the corresponding values are 1.93 - 4.93 d^{-1}, 1.51 ± 0.36 d^{-1}, 3.42 - 9.81 g C m^2 (mol photons g Chl)$^{-1}$ and 170 - 367 µmol photons m^{-2} s^{-1} (classifying *Bolidomonas pacifica* as an outlier). This agrees with theoretical assumptions related to size and gives picoprokaryotes an advantage in oligotrophic, light limited environments. There are no differences in maximum chlorophyll to carbon ratios (θ_{max}) between the two groups (0.058 ± 0.016 g Chl g^{-1} C).

The dynamic model it is able to reproduce P_m^C and α^{chl} adequately. The only limitation was found in the representation of long term damage during acclimation to high light. With further improvement of this model we will be able to improve the understanding on translating chlorophyll *a* concentration into carbon biomass and primary production.

2.7. Appendix

Table 2. 5 parameter calculations from acclimated model using one parameter set for all PI curves

Species	size	P_m^C	α^{chl}	β^{chl}	respiration
	µm	d^{-1}	gC m^{-2} (mol photons g Chl)$^{-1}$	gC m^{-2} (mol photons g Chl)$^{-1}$	d^{-1}
Prochlorococcus (HL)	0.6	1.186	5.188	-0.043	0.274
Prochlorococcus (LL)	0.6	0.950	6.077	-0.059	0.642
Synechococcus	1	0.780	8.638	0.002	0.391
Bolidomonas pacifica	1.2	2.634	12.890	-0.007	1.381
Micromonas pusilla	1.5	4.487	2.340	-0.041	0.392
Picochlorum sp.	2	1.519	3.910	0.029	0.457
Nannochloropsis granulata	2	2.531	3.811	-0.114	0.744

The following graphs show the comparison of photosynthetic parameter estimates of the acclimated model for single photosynthesis light response curves compared to estimations for one parameter set that tries to fit all data.

Circles show mean values for each parameter for individual estimates at a given acclimation light intensity with its standard deviation. The black long dashed line shows the mean of all data points as used in Table 2. 2 with short dashed lines giving its area of standard deviation. The grey straight line shows the value calculated by using a single parameter set for all photosynthesis light response curves.

Prochlorococcus (HL)

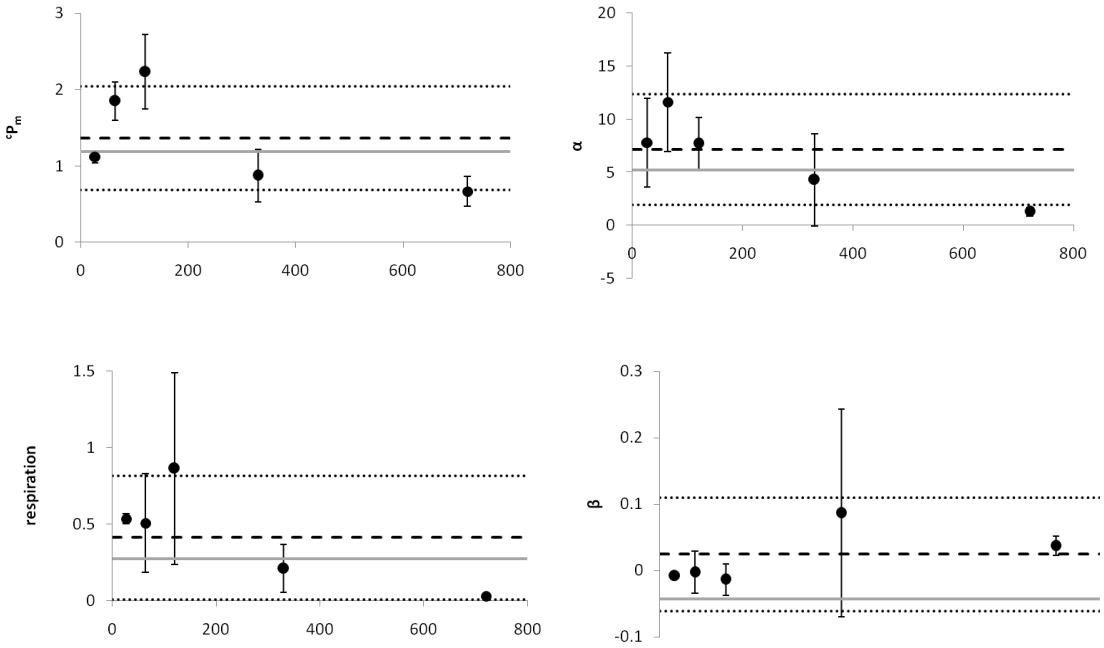

Prochlorococcus (LL)

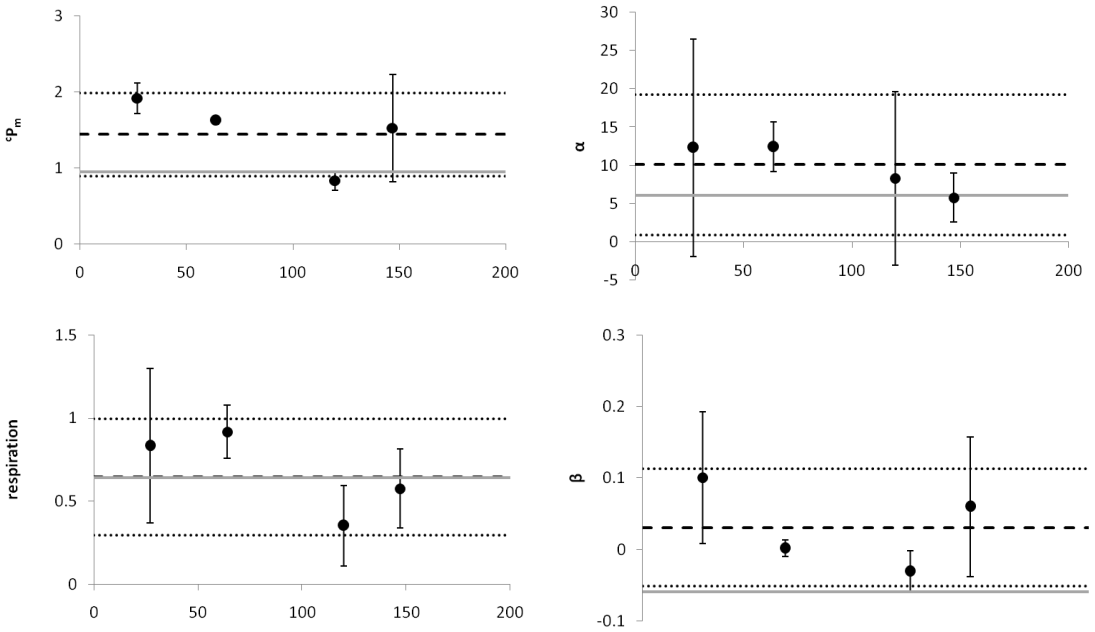

Synechococcus

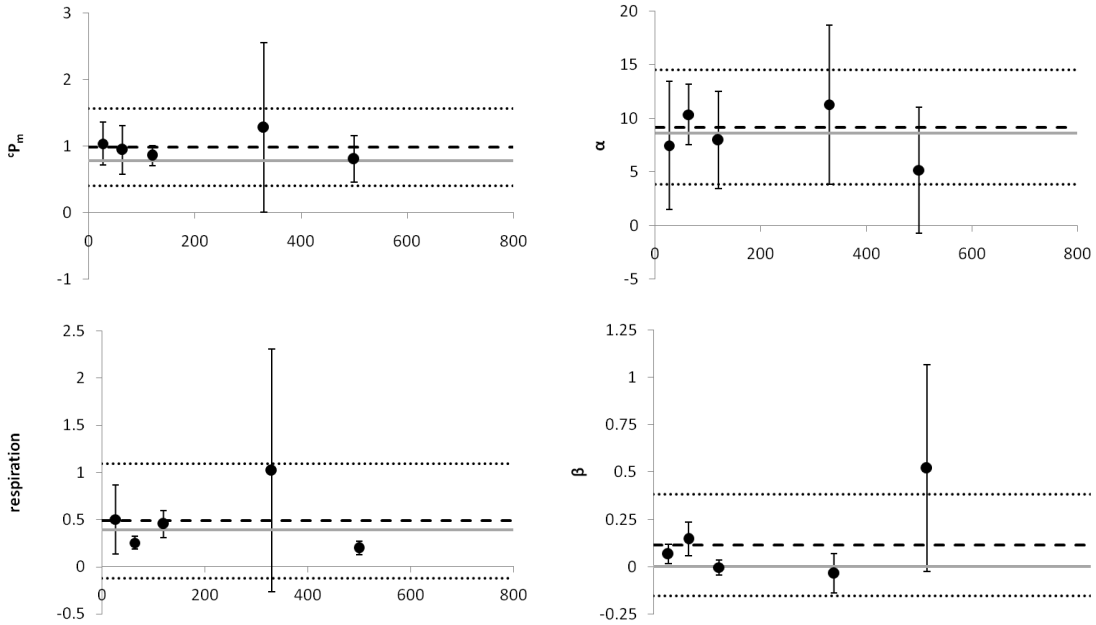

Bolidomonas pacifica

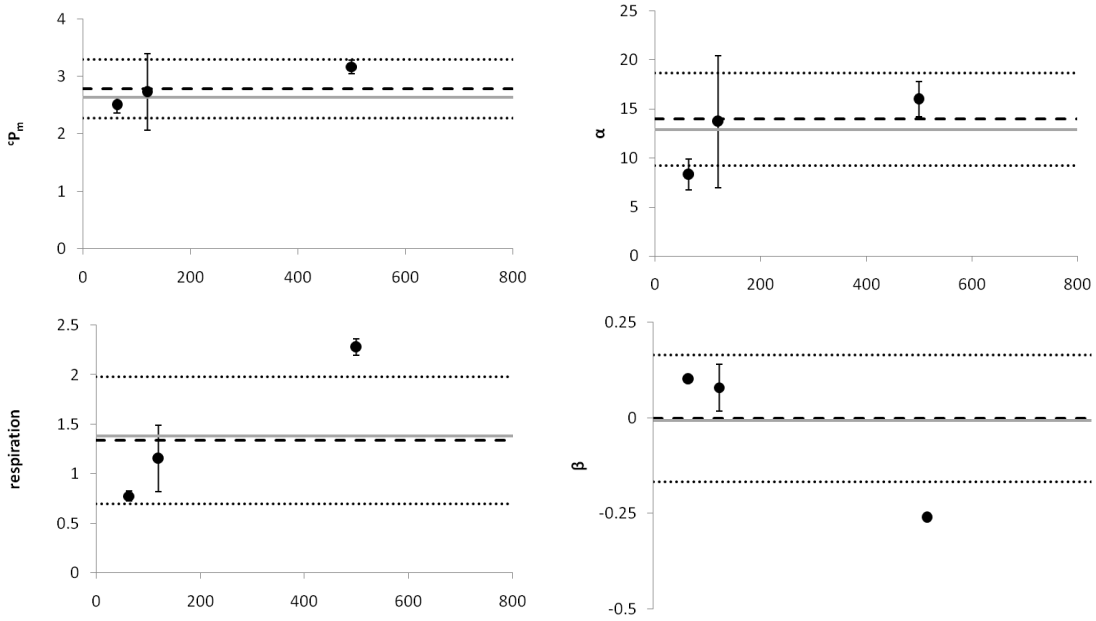

Micromonas pusilla

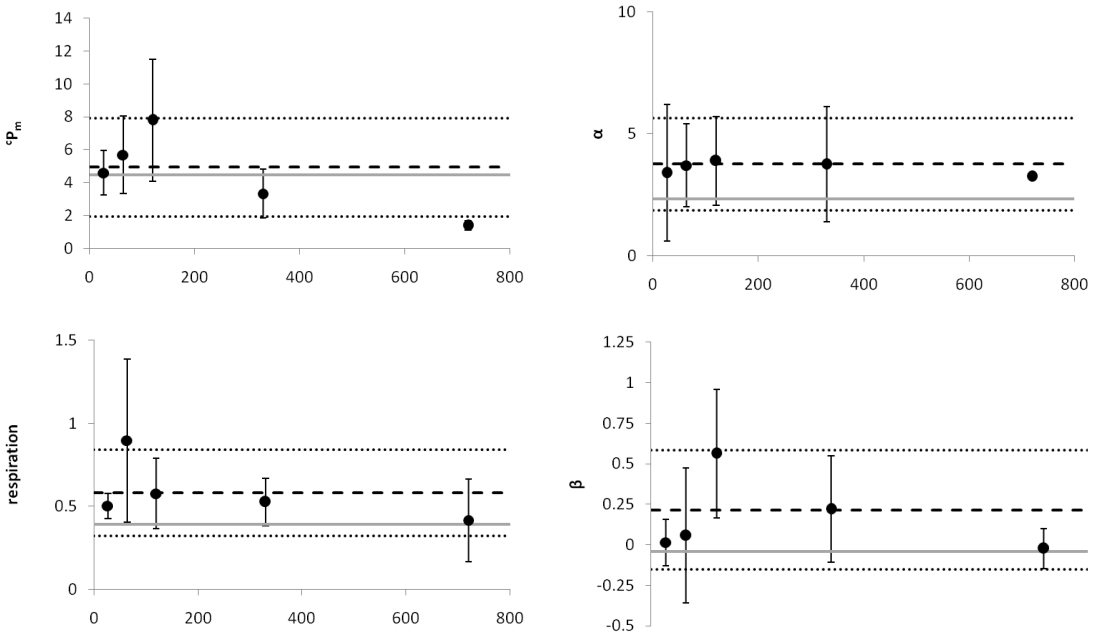

Picochlorum sp.

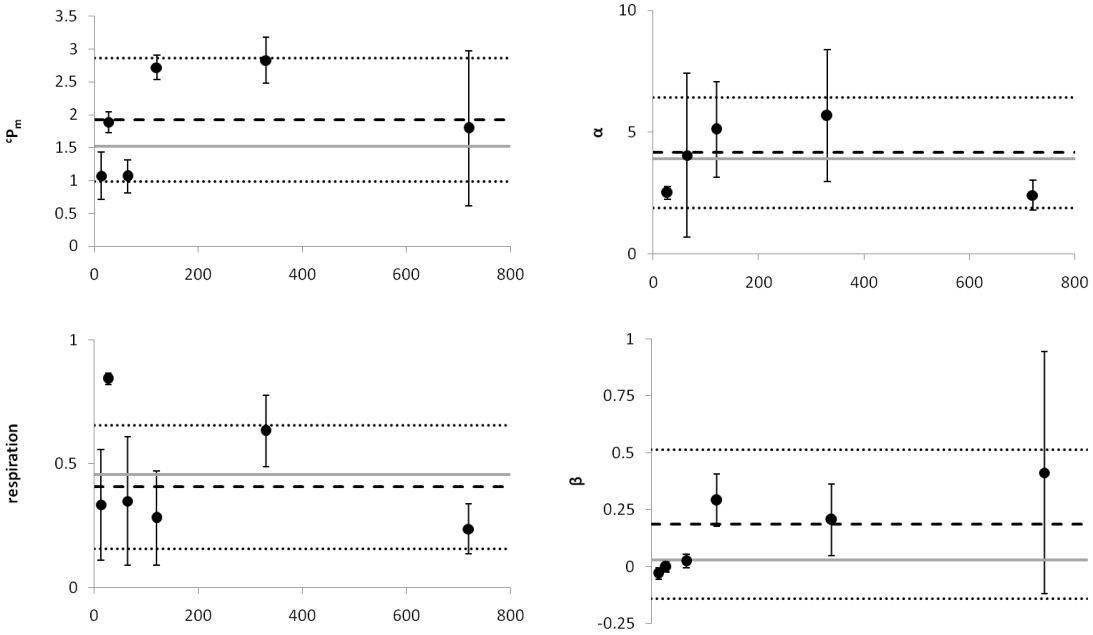

Nannochloropsis granulata

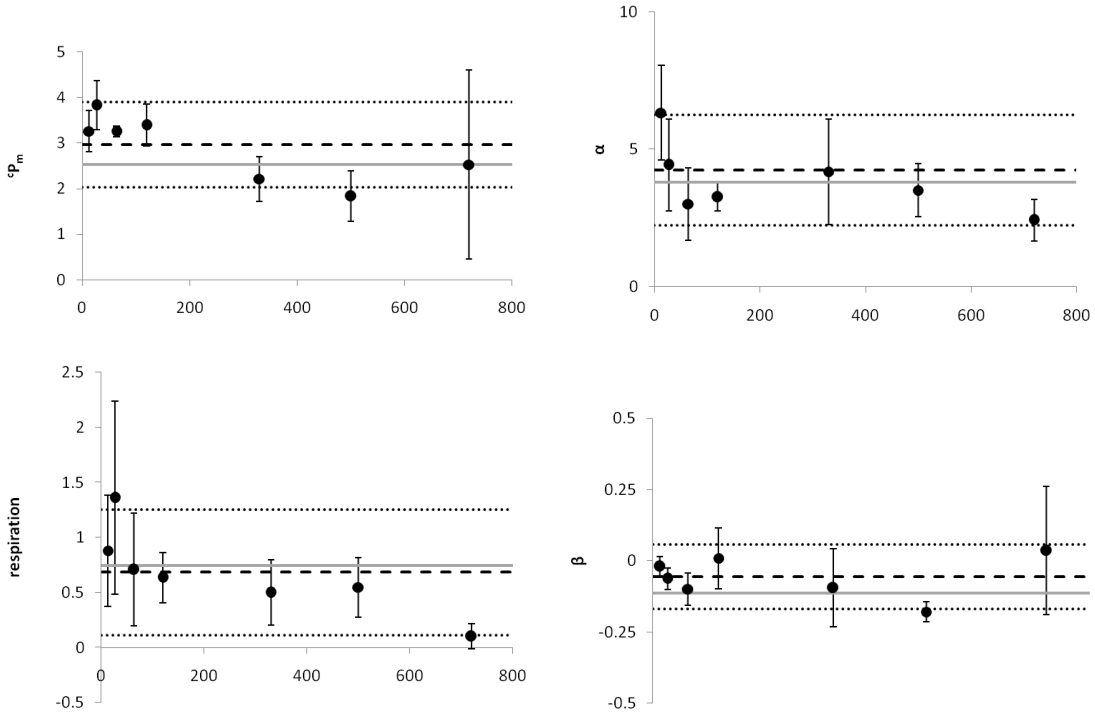

Figure 2. 8 PI curve parameters for individual species and acclimation light intensities.

Table 2. 6 Bias between acclimated and dynamic model fit and photosynthesis measurements

	Prochlorococcus (HL)	*Prochlorococcus (LL)*	*Synechococcus*	*Bolidomonas pacifica*	*Micromonas pusilla*	*Picochlorum sp.*	*Nannochloropsis granulata*
acclimated model							
0	-25.4	-5.0	-11.8	-12.2	-33.9	-12.1	-23.9
2	29.3	24.1	9.0	18.7	-40.0	4.8	8.9
25	-28.6	111.8	35.8	38.8	-0.4	2.9	28.9
65	-7.5	-82.2	59.9	8.0	-41.9	-17.8	-8.5
150	-1.7	-29.7	11.3	-44.8	-85.8	-28.0	-5.3
315	19.2	13.2	-1.3	25.0	10.5	-2.9	22.2
600	-18.3	-6.4	1.7	-3.3	-5.5	22.7	-8.3
1300	-2.5	-0.6	8.9	-5.7	0.3	-7.3	-6.2
2000	4.8	2.4	-2.2	4.5	0.4	5.1	1.3
dynamic model							
0	-8.8	-16.5	-100.0	-80.7	-18.2	-100.0	-93.5
2	-47.0	-32.8	-105.4	-79.4	-22.8	-108.5	-93.2
25	-165.1	10.3	-216.8	-357.2	11.2	-420.8	-100.8
65	153.0	12.1	214.8	-39.1	71.8	104.2	-109.2
150	14.3	24.7	348.4	93.7	-26.4	665.5	178.2
315	-23.2	12.2	242.1	159.9	-71.1	296.8	78.9
600	10.1	6.4	123.4	48.4	-12.2	163.0	-22.5
1300	11.2	1.4	77.1	43.0	11.5	68.5	-4.1
2000	19.2	-3.6	2.8	69.0	18.3	16.3	22.1

3. THE INFLUENCE OF TEMPERATURE ON THE PHYSIOLOGY OF PICOPHYTOPLANKTON

3.1. Abstract

This study focuses on the physiological response of 9 marine picophytoplankton strains in the size range of 0.6 - 3 µm to temperature. Growth rates and chlorophyll *a* to carbon ratios were investigated in laboratory experiments at temperatures between -0.5°C and 33°C. Eppley (1972) made two assumptions about the physiological response to temperature: 1) the response of single species can be best described by an optimum function, and 2) the mean community growth is better explained by an exponential fit. We statistically test and confirm these assumptions. Picoeukaryotes differ significantly from picoprokaryotes in terms of optimum growth rate, which is 0.47 ± 0.17 for prokaryotes and 1.05 ± 0.47 d^{-1} for eukaryotes. Their mean optimum growth temperature is 23.3 ± 2.7°C with no significant difference between the groups. The temperature tolerance range is higher for picoeukaryotes, which grew at temperatures between 2.8 and 32.4°C. *Prochlorococcus* grew between 16.3 °C and 25.3°C, *Synechococcus* grew between 13.7°C and 27°C. This is consistent with their biogeographical distribution. Chlorophyll *a* to carbon ratios increase linearly with increasing temperature but in some species drop above the optimum temperature. Applying a 99th quantile regression, the maximum picophytoplankton community growth is lower than the curve estimated by Eppley, but has a higher Q_{10} value of 2.3. For picoprokaryotes the Q_{10} value is even higher (4.9). The increase of ocean temperature due to climate change will be beneficial for picophytoplankton not only because of the indirect effect through nutrient depletion but also because of a higher Q_{10} compared to other phytoplankton groups. It will also have a stronger effect on picoprokaryotes and may shift their distribution because of their narrow temperature tolerance range.

3.2. Introduction

Temperature affects the biogeographical distribution of different phytoplankton groups or even ecotypes of single species by setting limits on growth, but also by influencing the dynamics of the water column and the availability of nutrients and light (Eppley 1972; Behrenfeld et al. 2006; Johnson et al. 2006).

Eppley (1972) used data of approximately 130 species to review the influence of temperature on phytoplankton between 2°C and 40°C to calculate the maximum growth rate of the phytoplankton community. He suggested that the temperature response of single species follows an optimum function, while their maxima increase with increasing optimum temperature following an exponential curve. Even though neither of these two assumptions was statistically verified, he created a fundamental new aproach to this problem and a base for discussion. A recent study that uses the larger Liverpool phytoplankton database and includes statistical analysis using 99^{th} quantile regression has shown the estimated Q_{10} value to be appropriate, but that phytoplankton growth rate tends to be higher (Bissinger et al. 2008). However, they did not test the appropriateness of other formulations. Montagnes et al. (2003) showed that for most individual species a linear function fits better than an exponential function, but they did not consider an optimum function, nor did they test the whole phytoplankton population.

Eppley's generalized equation of phytoplankton growth (Equation 3. 6) is widely used in ecosystem models (Bissinger et al. 2008). However, due to the variability in the physiological response of different phytoplankton groups to environmental conditions, plankton functional type models need to use individual temperature parameters to estimate their direct effects (Le Quéré et al. 2005).

Eppley (1972) also mentioned the importance of temperature dependence of the chlorophyll *a* to carbon ratio (θ) that affects photosynthesis rate. He explains the high variabilty in the data by variations in cell size and pigmentation.

Later it was confirmed that the chlorophyll *a* to carbon ratio decreases with decreasing temperature due to low temperature chlorosis. It has also been shown that this effect can be amplified by exposure to high light levels. Further, it was suggested that this decrease can also be linked to the increase in lipids to maintain membrane fluidity or slower metabolic reactions (Geider 1987). Picophytoplankton account for 26 – 56% of the global phytoplankton biomass (Buitenhuis et al. 2013) with a substantial contribution in the warmer subtropical oligotrophic areas, decreasing polewards. In contrast, diatoms and

coccolithophores can be found globally in different ecological niches, with high abundances in higher latitudes (Partensky, J., et al. 1999; Agawin et al. 2000; Buitenhuis et al. 2012). Picophytoplankton thus play a significant role in the carbon cycle.

With the extension of the subtropical gyres as a consequence of global warming, it is assumed that they will gain more importance (Morán et al. 2010). Field studies are able to link biomass to temperature, but temperature was found to be strongly correlated with nutrient concentration, and it is not fully understood whether temperature itself or the associated indirect effect on nutrient depletion in these regions will be more influential on the composition of the phytoplankton community (Agawin et al. 2000; Finkel et al. 2010). Consequently, laboratory studies with individual groups are important to separate these two variables to estimate the direct effect on growth rates and improve the parameterisation of those models (Chen et al. 2014; Finkel et al. 2010).

Most data is available on the picoprokaryotes, *Prochlorococcus* and *Synechococcus*, but less information has been gathered on picoeukaryotes (Moore et al. 1995; Johnson et al. 2006; Zinser et al. 2007; Kulk et al. 2012; Chen et al. 2014).

Thus, the first aim of this study is to investigate whether picoeukaryotes differ significantly from picoprokaryotes in terms of physiological parameterization in specific temperature environments. For this temperature dependent growth rates, carbon and chlorophyll quotas will be measured.

The second aim is to statistically test Eppley's assumptions, and whether they can be applied to picophytoplankton.

Eppley's assumptions:

a) The temperature dependent maximum growth rates of single phytoplankton species follow an optimum function.

b) The temperature dependent maximum growth rates of a phytoplankton community approach an exponential function.

To uncover these trends, linear, exponential, and optimum functions are first applied to growth rates of individual species and second to growth rates of the entire community. In this way it is tested which function describes the mean trend in growth rates best. If the exponential function shows to be adequate to represent the temperature dependent trend

in community growth a 99th quantile regression will be applied to data of both picophytoplankton groups. The obtained Q_{10} value by this method will then be quantitatively compared to Eppley's estimate which represents the absolute maximum community growth rate.

3.3. Material and Methods

3.3.1. Cultures

Picophytoplankton, including 3 prokaryotic and 6 eukaryotic strains, were obtained from the Roscoff culture collection (Vaulot et al. 2004) (Table 3. 1). They include *Synechococcus* (RCC 30) a high light (HL) and a low light (LL) ecotype of *Prochlorococcus* (RCC 296 and 162) as well as the picoeukaryotes *Bolidomonas pacifica* (RCC 212), *Micromonas pusilla* (RCC 1677), *Picochlorum sp*. (RCC 289), *Nannochloropsis granulata* (RCC 438),*Imantonia rotunda* (361) and *Phaeomonas sp.* (RCC 503). They were isolated between 2.5° S and 49° N in the Pacific and Atlantic Oceans as well as the Mediterranean and the North Sea (Figure 3. 1, Table 3. 1).

Figure 3. 1 Map of locations of isolation of culture strains. Numbers indicate individual RCC numbers

Table 3. 1Species information: Roscoff culture collection number (RCC), size and location of isolation

Species	RCC	Size [µm]	Location of isolation	Isolation depth [m]
Prochlorococcus (HL)	296	0.6	8° 32.5'N, 136° 31.8'E	150
Prochlorococcus (LL)	162	0.6	38° 59'N, 40° 33' W	10
Synechococcus	30	1	26° 18' N, 63° 26'W	120
Bolidomonas pacifica	212	1.2	2° 30'N, 150° 0 W	15
Micromonas pusilla	1677	1.5	54° 24'N, 4° 3'E	10
Picochlorum sp.	289	2	7° 0'S, 150° 0'W	15
Nannochloropsis granulata	438	2	41° 40'N, 2° 48'E	0
Imantonia rotunda	361	2.5	48° 45'N, 3° 57'W	0
Phaomonas sp.	503	3	41° 40'N, 2° 48'E	0

3.3.2. Experimental setup

The experiment was conducted in 55ml culture tubes (Pyrex Brand 9826) in a temperature gradient bar (Buitenhuis, in prep., Figure 3. 2). They were placed in 13 positions, across a temperature gradient between -0.5°C and 33°C. The light cycle was set to 14 hours of light per day and the intensity was 291 ± 18 µmol photons m^{-2} s^{-1} provided by an individual LED under each tube (Winger WEPW1-S1 1W, 95 Lumen, white). It was decreased to 81 ± 5 photons m^{-2} s^{-1} for the low light *Prochlorococcus* ecotype. Artificial seawater medium (ESAW) (Berges et al. 2001) with ammonium (882 µM $(NH_4)_2SO_4$) as the single nitrogen source and selenium (10 nM Na_2SeO_3) was used. Light intensities within the cells of the temperature gradient bar were measured with a Radiometer (Biospherical Instruments Inc. QSL-2101). Cultures were acclimated to each temperature for at least 4 divisions to reach balanced growth. In vivo fluorescence was measured daily using a Turner Design Fluorometer (10 AU). Growth rates were calculated during the exponential growth phase by taking the logarithm of the in vivo fluorescence values and applying a linear regression through at least three consecutive measurements.

Figure 3. 2 Temperature gradient bar with the insulated cover removed, photo by Sian Foch-Gatrell.

3.3.3. Sampling

All cultures were sampled for Chlorophyll *a* and particulate organic carbon (POC) and nitrogen (PON) content. POC/PON samples were collected on precombusted 13 mm GF/F filters for all species. *Prochlorococcus* cells were too small to remain on the filters, but preliminary tests showed that no cells passed through if a layer of 3 filters was used. For chlorophyll *a* and POP analyses samples were collected on precombusted 25 mm GF/F filters, while *Prochlorococcus* was sampled on 25 mm polycarbonate filters (0.2µm). Between 5 and 20 ml were filtered, depending on the cell density, and rinsed with Milli-Q water. All filters were frozen immediately after sampling in liquid nitrogen and stored at -80°C until analyses.PON and POP results are presented in chapter 4. Cell numbers were measured by flow cytometry (BD Biosciences FACSCalibur, flow cytometer). Flow rate was calibrated using the method by Marie et al. (2005).

3.3.4. Elemental analysis

POC samples were dried at 40°C for 24 hours, placed into precombusted tin capsules and analysed with an elemental analyser (Exeter Analytical, CE-440 Elemental Analyser), which was calibrated with acetanilide (Exeter Analytical). Results were corrected for blank filters. For POP analysis and the results of PON and POP see the nutrient chapter.

3.3.5. Chlorophyll *a* analysis

Chlorophyll *a* samples were extracted in 10 ml acetone (Fisher Scientific, 99.8+ %) in 15ml centrifuge tubes and disintegrated by shaking and vortexing. Tubes were wrapped in aluminium foil and stored at 4°C for 24 hours. For analysis samples were centrifuged and the supernatant was analysed in a Fluorescence Spectrometer (PerkinElmer LS 45 Luminescence Spectrometer). After reading a sample 3 drops of 8% HCl were added into the cuvette to measure the background signal. The concentration of the calibration standard (SIGMA product No C5753) was obtained prior to analyses (Parson et al. 1984).

3.3.6. Calculations

A linear, an exponential and an optimum function (Schoemann et al. 2005) (Equation 3. 1- Equation 3. 3) were used to fit the data as suggested by Buitenhuis et al. (2008). Where possible, the parameters and their standard errors were estimated using Mystat 12 (Systat software). It was not possible to estimate the parameters for the optimum fit to all data obtained in this study using the Mystat software. For that reason the solver function in Excel 2007 was used to estimate the 3 parameters, minimizing the sum of squares between the model and the data. The equation was solved 15 times with varying starting values and it was found that there was only a minor variability in the residual sum of squares (< 0.03%) and the parameters. That way one parameter was fixed in Mystat to calculate the missing parameters with the corresponding standard errors. The relative quality of the fits was compared using the Akaike's Information Criterion (AIC, Equation 3. 4 and Equation 3. 5, (Burnham & Anderson 1998).

The absolute value of this measure is not of relevance. The best solution is given by the model with the lowest AIC value. If the difference between the lowest and the second lowest value is less than 2, the second solution is also appropriate. The data was also compared to Eppley's equation (Equation 3. 6).

Equation 3. 1

linear: $\mu_{max} = \mu_{max,0°C} + \text{slope x } T$

Equation 3. 2

exponential: $\mu_{max} = \mu_{max,0°C} \times Q_{10}^{\frac{T}{10}}$

Equation 3. 3

optimum: $\mu_{max} = \mu_{Opt} \times \exp\left(-\frac{(T-T_{Opt})^2}{\Delta T^2}\right)$

Equation 3. 4

Akaike's Information Criterion $AIC = n_{obs} log(\sigma^2) + 2n_{param}$

Equation 3. 5

Standard Error $\sigma^2 = \frac{1}{(n_{obs} - n_{param})} \times \sum(\mu_{obs} - \mu_{fit})^2$

Eppley equation converted into [d^{-1}] (Bissinger et al. 2008):

Equation 3. 6

$$\mu = 0.59 * 1.89^{(T/10)}$$

Following Bissinger et al. (2008), the upper 99% quantile was estimated and compared to Eppley's curve. A linear quantile regression through the logarithmically transformed data was applied to get estimates of the standard error. The Software R version 3.1.0 (http://www.r-project.org) with the software package quantreg was used.

3.4. Results

3.4.1. Temperature dependent growth rates

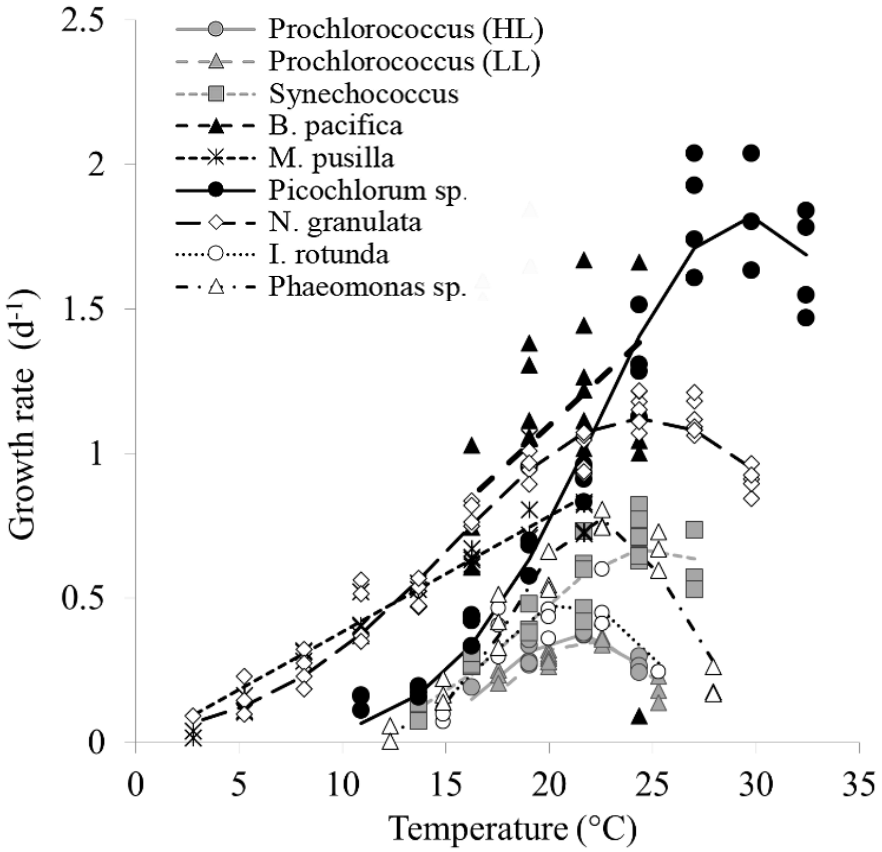

Figure 3. 3 Temperature dependent growth rates of picophytoplankton, lines indicate best fit chosen by AIC. Grey symbols: picoprokaryotes, black and white symbols: picoeukaryotes

Growth rates of picophytoplankton increase with increasing temperature until they reach a maximum (μ_{Opt}) at their optimum temperature (T_{Opt}). With further increase, rates decrease (Figure 3. 3, Figure 3. 6).

Picoprokaryotes grow at a narrower temperature range than picoeukaryotes (Figure 3. 3 and Table 3. 2). Both *Prochlorococcus* ecotypes grow at temperatures between 16.3 and 25.3°C (0. 14 - 0.44 d^{-1}), and *Synechococcus* between 13.7 and 27 °C with growth rates ranging from 0.07 to 0.82 d^{-1}. Picoeukaryotes grow at temperatures between 2.8 and 32.4°C with growth rates ranging from 0.005 to 2.04 d^{-1}. *Picochlorum sp.* (RCC 289) reaches the highest growth rates of all strains tested in this experiment. *Micromonas pusilla* (RCC 1677) and *Nannochloropsis granulata* (RCC 438) grow at the widest temperature range.

3.4.2. Changes in chlorophyll to carbon ratios related to temperature

Chlorophyll *a*: carbon ratio (θ) increases with temperature between 0.004 and 0.037 g Chl g^{-1} C (linear regression, $p < 0.05$, $R^2 = 0.417$, Figure 3. 4) within the picophytoplankton group and can be described by Equation 3. 7.

The relationship between θ and temperature was also significant on a species level, unless a species grew only over a narrow temperature range (both *Prochlorococcus sp.* ecotypes and *Imantonia rotunda*), or there was a high variability in the data over a low range of chlorophyll : carbon ratios (*Micromonas pusilla*).

Some strains show a drop in θ after reaching the optimum (Figure 3. 5) as measured for both *Prochlorococcus* ecotypes, *Picochlorum sp*. and *Nannochloropsis granulata. Prochlorococcus sp.* has generally high levels of Chlorophyll, while *Synechococcus sp.* is at the lower edge of the range of the data.

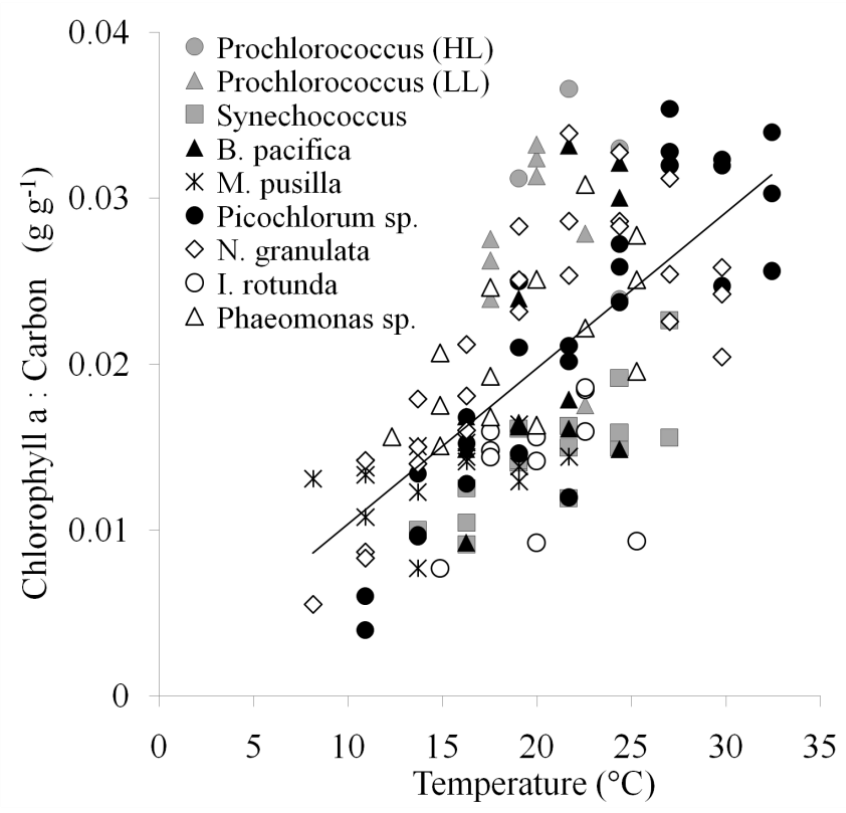

Figure 3. 4 Chlorophyll to carbon ratios as a function of temperature. Picoprokaryote symbols as in Fig. 3.3, black circles: picoeukaryotes

Equation 3. 7

$$\theta = 9.38 * 10^{-4} T + 1.01 * 10^{-3}$$

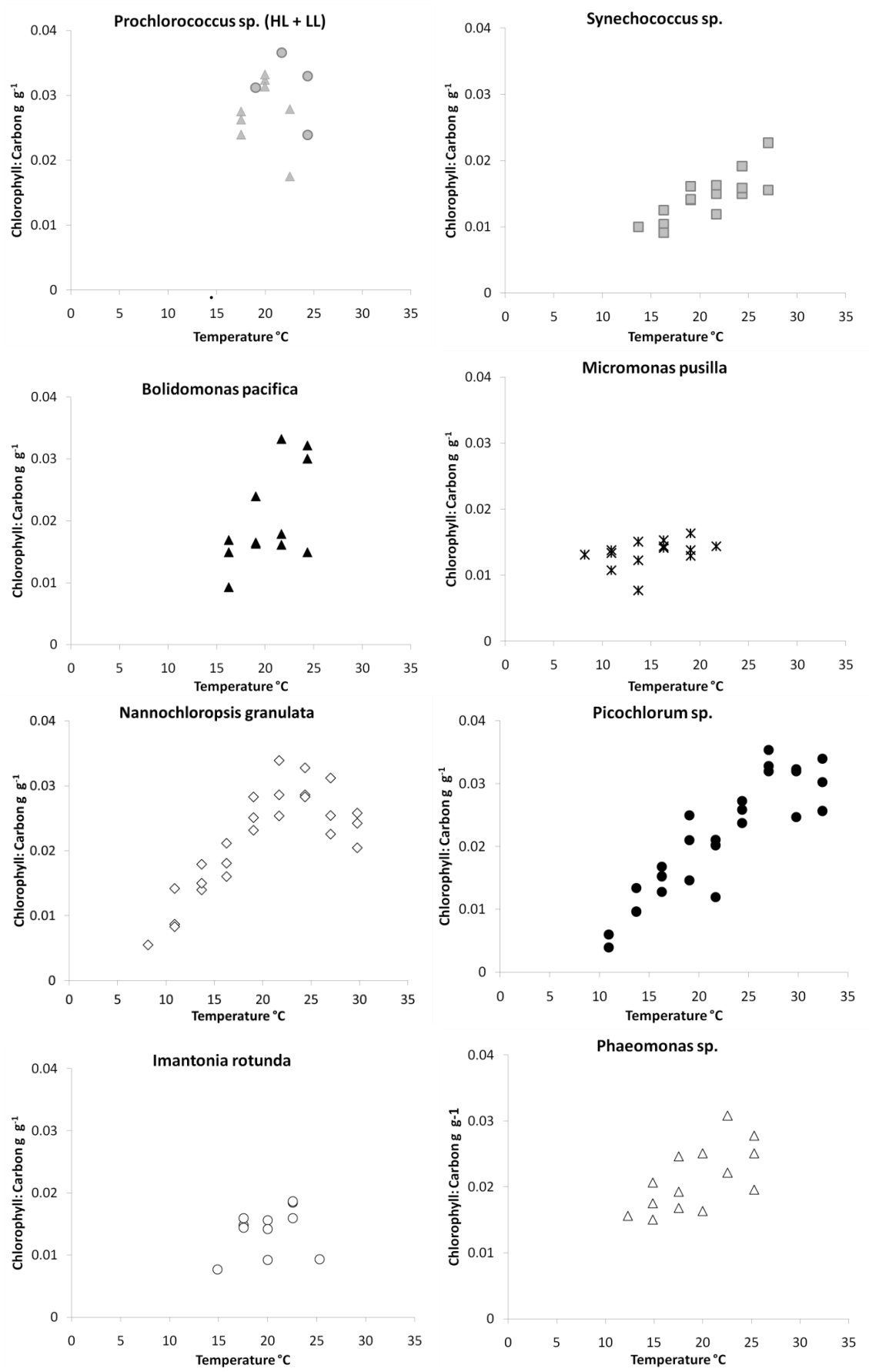

Figure 3. 5 Chlorophyll to carbon ratios as a function of temperature for individual strains.

3.4.3. Linear, exponential and optimum fits to temperature dependent growth rates.

Three equations (Equation 3. 1 - Equation 3. 3) were fit to the data of each culture, each group and to picophytoplankton as a whole community to uncover the general trends in growth rate as a function of temperature. The solutions and the corresponding AIC values are summarized in Table 3. 2 and Table 3. 3). The best AIC values are indicated in green, the second best also acceptable solutions in yellow. Those parameters are representative for the estimation of the mean maximum species specific or community growth.

The optimum function was the best or an acceptable solution for all individual species and also an acceptable solution for the groups of picoprokaryotes and picoeukaryotes. *Micromonas pusilla* (RCC 1677) didn't show a drop of growth rate above optimum temperature, because it didn't grow at all at the next higher temperature above the optimum temperature. Therefore the linear solution gave the best fit.

Bolidomonas pacifica (RCC 212) grew at only 4 temperatures, which was not enough to see significant differences between the fits. The same applies to picoprokaryotes as a group. For picoeukaryotes the linear and optimum solutions were almost equally good. Investigating all species together as a common group of picophytoplankton, the best fit was achieved by the exponential model fit. Plots of all equations for individual strains can be found in Figure 3. 9 and Figure 3. 10.

The mean optimum growth temperature (T_{Opt}) is 23.3 ± 2.7°C with no significant difference ($p > 0.05$, Wilcoxon-Mann-Whitney-Test) between prokaryotes and eukaryotes. The optimum growth rate (μ_{Opt}) varies significantly ($p < 0.05$, Wilcoxon-Mann-Whitney-Test) between the groups with 0.47 ± 0.17 for prokaryotes and 1.05 ± 0.47 d^{-1} for eukaryotes. Their mean optimum growth rate is 0.86 ± 0.48 d^{-1} (n = 9).

The Q_{10} value from the exponential fit through each group representing the general trend or mean maximum growth rate is slightly higher and the intercept of the growth curve is much lower for picoprokaryotes than for picoeukaryotes. Optimum growth rates of single species increase with optimum temperatures (Figure 3. 6). The linear solution gives the lowest AIC value (-5.41), the exponential solution is also acceptable (-5.3) and the optimum function has to be dismissed (-2.68).

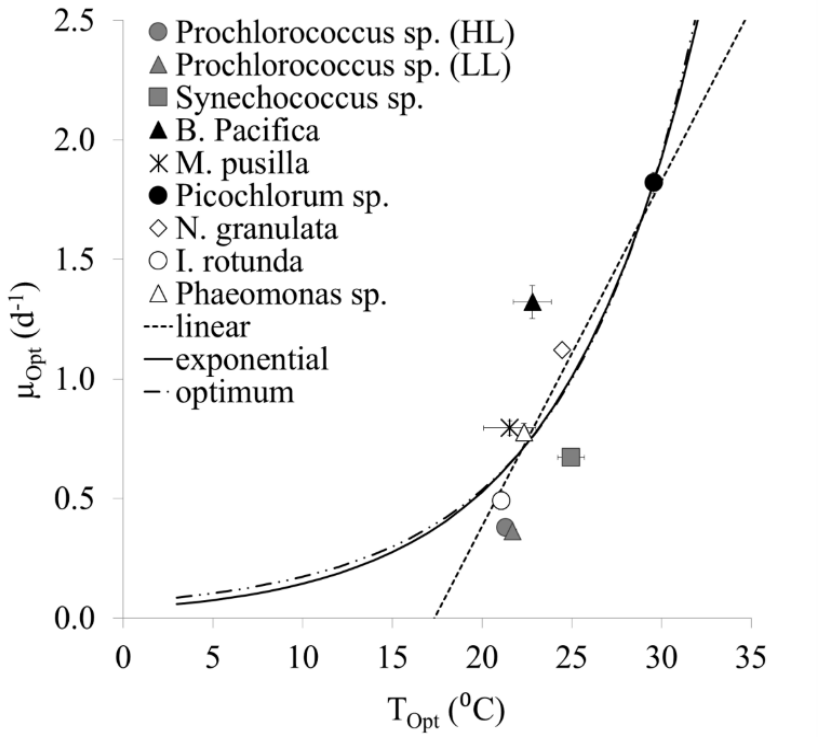

Figure 3. 6 Optimum growth rates at optimum temperatures for single species.

Table 3. 2Parameterisations of the linear, exponential and optimum fits through mean temperature dependent maximum growth rates for each species, groups and all data including measured minimum (T_{min})and maximum (T_{max}) temperatures at which growth rate was positive, ASE=asymptotic standard error in brackets.

		Linear				Exponential				Optimum						Measured	
Culture	n	$\mu_{max,0^0C}$	ASE	Slope	ASE	$\mu_{max,0^0C}$	ASE	Q_{10}	ASE	μ_{Opt}	ASE	T_{Opt}	ASE_t	ΔT	ASE	T_{min}	T_{max}
Prochlorococcus sp.(HL)	16	0.30	(0.15)	0.001	(0.007)	0.30	(0.15)	1.02	(0.23)	0.378	(0.01)	21.3	(0.2)	5.3	(0.4)	16.3	24.4
Prochlorococcus sp.(LL)	19	0.35	(0.17)	-0.003	(0.008)	0.35	(0.20)	0.92	(0.25)	0.362	(0.02)	21.7	(0.2)	4.8	(0.5)	17.5	25.3
Synechococcus sp.	24	-0.38	(0.13)	0.042	(0.006)	0.10	(0.04)	2.08	(0.31)	0.672	(0.03)	25.0	(0.7)	8.6	(1.1)	13.7	27.0
Bolidomonaspacifica	18	-0.22	(0.44)	0.066	(0.021)	0.38	(0.16)	1.70	(0.33)	1.322	(0.07)	22.8	(1.1)	8.3	(2.1)	16.3	24.4
Micromonaspusilla	29	-0.02	(0.06)	0.040	(0.003)	0.21	(0.03)	1.92	(0.16)	0.795	(0.03)	21.5	(1.5)	12.9	(1.7)	2.8	21.7
Picochlorum sp.	35	-0.90	(0.16)	0.087	(0.006)	0.22	(0.05)	1.96	(0.17)	1.821	(0.04)	29.6	(0.4)	10.3	(0.6)	10.9	32.4
Nannochloropsisgranulata	50	0.19	(0.08)	0.033	(0.004)	0.43	(0.06)	1.39	(0.07)	1.122	(0.02)	24.5	(0.3)	13.0	(0.5)	2.8	29.8
Imantonia rotunda	13	-0.12	(0.24)	0.024	(0.012)	0.13	(0.10)	1.67	(0.59)	0.491	(0.04)	21.1	(0.5)	5.5	(0.7)	14.9	25.3
Phaeomonas sp.	20	0.17	(0.26)	0.013	(0.012)	0.29	(0.18)	1.22	(0.33)	0.776	(0.04)	22.3	(0.2)	5.5	(0.3)	12.3	27.9
Picoprokaryotes	59	-0.23	(0.14)	0.029	(0.006)	0.08	(0.03)	2.02	(0.36)	0.509	(0.08)	27.7	(5.0)	12.7	(5.6)	13.7	27.0
Picoeukaryotes	165	-0.28	(0.10)	0.054	(0.005)	0.23	(0.03)	1.83	(0.11)	1.514	(0.28)	37.7	(6.8)	21.8	(5.2)	2.8	32.4
All	224	-0.35	(0.10)	0.050	(0.005)	0.14	(0.02)	2.09	(0.14)	33.925*	(1.1)	125.5*	(0.4)	52.7*	(0.2)	2.8	32.4

Table 3. 3 AIC values based on Standard deviation obtained from parameterization in Table 3.2

Culture	Lin	Exp	Opt
Prochlorococcus sp.(HL)	-33.62	-33.66	-42.71
Prochlorococcus sp.(LL)	-37.74	-37.76	-43.57
Synechococcus sp.	-42.85	-39.18	-44.89
Bolidomonaspacifica	-19.25	-18.73	-18.63
Micromonaspusilla	-59.43	-49.91	-58.86
Picochlorum sp.	-42.54	-32.16	-52.7
Nannochloropsisgranulata	-74.73	-64.1	-107.91
Imantonia rotunda	-18.46	-17.74	-21.96
Phaeomonas sp.	-20.33	-19.83	-37.31
Picoprokaryotes	-95.1	-94.3	-94.02
Picoeukaryotes	-162.62	-158.92	-161.22
All	-200.77	-205.71	-203.31

*solved in Excel

3.4.4. Comparison with Eppley

Figure 3. 7 shows the picophytoplankton growth rates gained in this study compared to Eppley's curve (black line, converted into d^{-1}). The growth rates of picophytoplankton are generally lower than his curve. The dotted line indicates the exponential curve through the mean picophytoplankton maximum growth rates using the parameterisation in Table 3. 2 which was used to uncover the main trend in the data. It was included for completeness.

An exponential 99th quantile regression (dashed black line) was applied to all picophytoplankton data (μ_{pic}) to estimate the absolute maximum community growth rate following Eppley's example. Another exponential 99th quantile regression was also applied to picoprokaryotic data (μ_{pro}) (grey dashed line). The regression coefficients for the linear 99th quantile of the log-transformed growth rates are shown in Table 3. 4.

Table 3. 4 Linear quantile regression (99th) coefficients and standard errors

	Intercept	Standard Error	Slope	Standard error
Picoprokaryotes	-3.774	0.076	0.160	0.004
ALL	-1.496	0.237	0.084	0.013

The exponential conversion of the coefficients obtained from the linear quantile regression to the log-transformed data equates to the 99th exponential curve for picophytoplankton in Equation 3. 8.

Equation 3. 8

$$\mu_{pic} = 0.22 \times 2.3^{\frac{T}{10}}$$

For picoprokaryotes the 99th exponential curve is described by (Equation 3. 9).

Equation 3. 9

$$\mu_{pro} = 0.023 \times 4.9^{\frac{T}{10}}$$

The log transformed slope represents the Q_{10} which is the temperature coefficient for the absolute maximum growth rate of the investigated group following the example by Eppley.

μ_{pic} approaches the measured data well and is shifted towards lower growth rates compared to Eppley's curve (Figure 3.7). The obtained temperature coefficients (Q_{10}) (Equation 3.8 and 3.9) indicate a higher sensitivity of picoprokaryotes (4.9) compared to picoeukaryotes (2.3) which is reflected in their steeper slope. Also generally lower maximum growth rates at all temperatures lead to a lower intercept. As an alternative means of showing the community maximum growth rate the exponential fit through the species specific optima only, as shown in Figure 3. 6 is included in Figure 3. 7 (grey dotted line). This fit is lower than the 99th quantile regression.

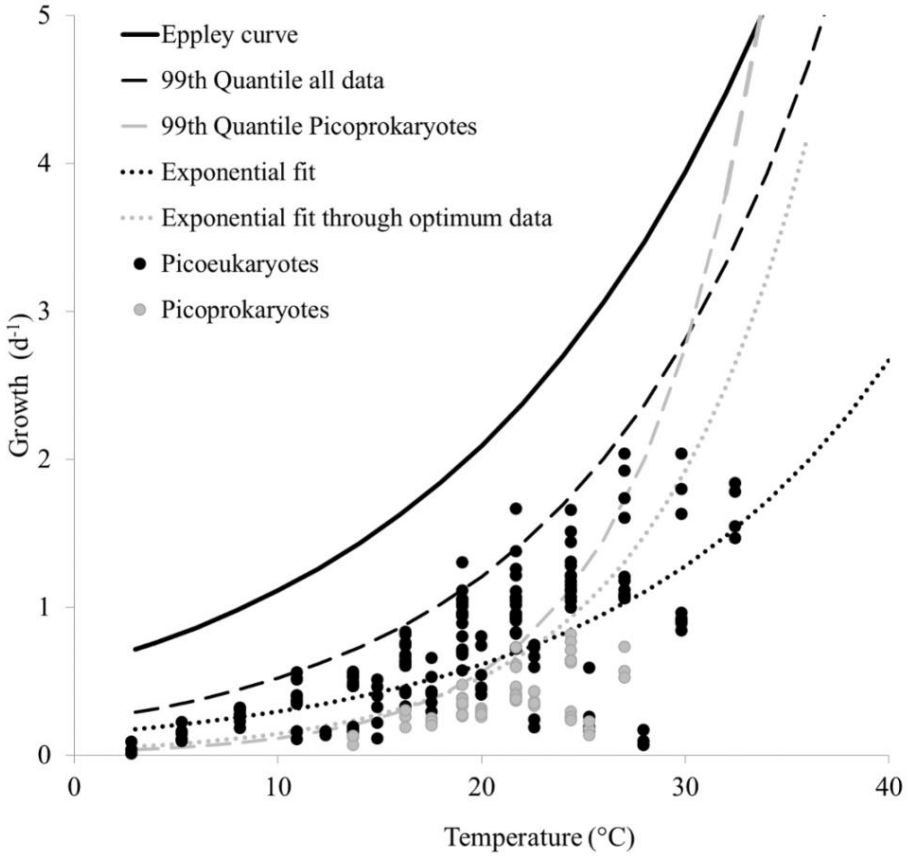

Figure 3. 7 Temperature dependent growth rates of picophytoplankton species (dots) measured in this study compared to Eppley's curve (black line), exponential solution from Equation 3. 2through our data (black dotted line), exponential fit through calculated optima only (grey dotted line), 99th quantile regressions to all (black dashed line) and picoprokaryote data (grey dashed line).

There is no evidence for a relationship between T_{opt} and either latitude or cell size (linear regression, ANOVA: $p > 0.05$,Figure 3. 8) even though the highest T_{opt} was achieved by *Picochlorum sp.*, isolated close to the equator.

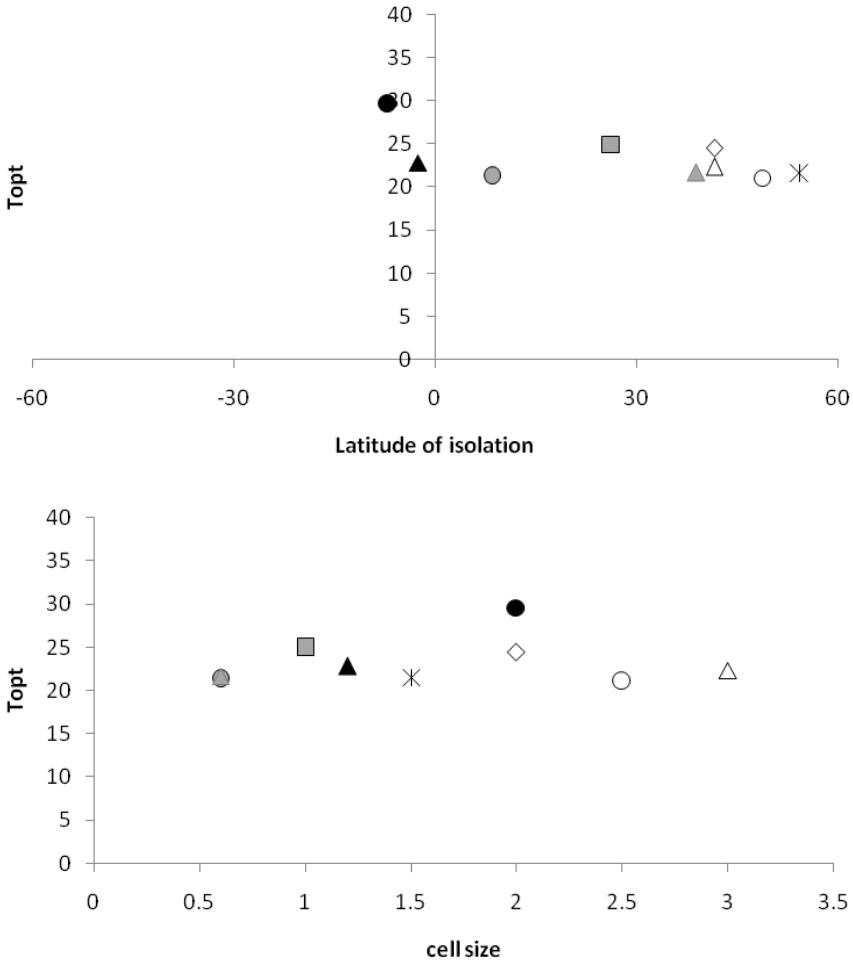

Figure 3. 8 Optimum temperature of the species as a function of the latitude of isolation (top) and cell size (below)

3.5. Discussion

3.5.1.1. Eppley's hypothesis a)

The maximum temperature dependent growth rates of single phytoplankton species follow an optimum function

The results show strong evidence that temperature dependent maximum growth rates of single picophytoplankton species follow an optimum function. For all species this function gives the lowest AIC value unless there was not sufficient data. In the case of *Bolidomonas pacifica* the lack of sufficient data was a combination of a small temperature range of growth with poor reproducibility of growth rates measurements at the two highest temperatures, while in the case of Micromonas *pusilla* missing data above the optimum temperature led to a linear relationship (Figure 3. 10). Even for these two species, the optimum function gives an acceptable fit. This is consistent with Eppley's assumption. Therefore, it can be concluded that for individual species using optimum growth rates, optimum temperatures and temperature tolerance ranges are the best way to describe the relationship of maximum growth rate and temperature.

There are a few laboratory studies which investigate the impact of temperature on growth of picoprokaryotes. Moore et al. (1995) report an optimum temperature of 24°C for two different *Prochlorococcus marinus* ecotypes (MED4 (HL) and SS120 (LL)).

These values are slightly higher than the estimates from the optimum fits in this study. A possible reason could be, that they do not apply an optimum model fit to their results. T_{opt} is only decribed as the temperature the highest growth rate was achieved at. For both, the high light and low light *Prochlorococcus* strains in this study the highest growth rates were lower, but the next higher tested temperatures were 24.4°C and 25.3°C for the low light strain. As laboratory measurements can only be conducted at specific temperatures, the maximum growth rate may lie between them.

However, differences in optima may also be caused by the natural variability between different strains. A different potential source of variance could also be the change of photophysiological properties with temperature. While light harvesting compounds increase with increasing temperature, photoprotective compounds decrease and may shift the optimum temperature with light intensity (Geider 1987). Based on the results of light experiments (Chapter 2) it can be assured that both ecotypes in this study were grown at light saturated conditions. Also the lower light level (90 µmol photons m^{-2} s^{-1}) used by

Moore et al. (1995) agrees with light saturation, which they reported for their high light *Prochlorococcus* ecotype. Consequently the influence by this factor can be excluded.

Johnson et al. (2006) investigated the geographical distribution of different *Prochlorococcus* ecotypes and found that different ecotypes occupy different niches correlated to temperature. They further cultured two high light ecotype strains (MED4 and MIT9312) and found an optimum temperature of 25°C, but differences in maximum growth rates and temperature tolerance ranges in agreement with field observations. Again, their study did not use an optimum function, but derived this value from observations.

Another field study found peak abundances of eMED4 (HL), the low light ecotype that was also used in this study eNATL2A (= RCC 162, LL), and eMIT9313 (LL) at 19°C. The other strain eMIT9312 (HL) peaked at 25 - 28°C, at a temperature at which the first three strains would be strongly inhibited (Zinser et al. 2007). Johnson et al. (2006) found eNATL2A at temperatures between 15 and 23°C.

Even if the highest abundances of MED4 were achieved at 19°C in the field, its optimum temperature was also higher in the laboratory study by Moore et al. 1995 (24°C).

This shows that peak abundances are not found at optimum temperatures in the field as there are fluctuations in local temperature, and growth decreases strongly above optimum temperature.

Consequently, their distribution and peak abundance is not only controlled by their optimum temperature, but also by temperature tolerance ranges and absolute maximum growth rates. This is also in agreement with the result, that there is no influence of latitude of isolation on the optimum temperature of picophytoplankton investigated in this study. However it is always difficult to compare field observations to laboratory data because of the influence of other factors such as light, nutrients, water column stratification or community structure (Johnson et al. 2006; Bouman et al. 2011).

In summary, previous studies found optima for *Prochlorococcus* between 24 and 28°C. Both *Prochlorococcus* stains in this study had lower optima, which may be a consequence of applying an optimum function to data, rather than reporting the temperature at which maximum growth was achieved. Strong inhibition was reported above 28°C (Moore et al. 1995), which is comparable to the upper temperature tolerance limit found in this study. The lower temperature limit is also consistent with the findings of Kulk et al. (2012) who show that *Prochlorococcus* is only able to grow at temperatures below 16°C if light levels are very low (25 μmol photons m^{-2} s^{-1}). However MED4, also grew at even lower

temperatures of 12.5°C at its optimum light in the laboratory study by Moore et al. (1995).

For *Synechococcus* optimum temperatures were found between 18°C and 28°C with different strains growing over a wide range of temperatures (Moore et al. 1995; Mackey et al. 2013; Malinsky-Rushansky et al. 2002). While Moore et al. (1995) didn't detect any growth below 15°C, Malinsky-Rushansky et al. (2002) successfully conducted experiments at 14°C. An early field study found *Synechococcus* between 6°C and 30°C, though (Waterbury et al. 1986). The strain investigated in this study has an optimum and a temperature tolerance range which is comparable to those results.

Chen et al. (2014) reviewed available information about optimum temperatures of three eukaryotic species between 20-25°C with *Micromonas pusilla* having an optimum at 20°C close to our estimate. They also show that there is no difference in optimum temperature between picophytoplankton and bigger phytoplankton groups, concluding that this is not the main controlling factor for the bigger success of picophytoplankton in warmer ocean areas.

There is also no significant difference in optimum temperature between picoprokaryotes and picoeukaryotes (Wilcoxon-Mann-Whitney-Test , $p > 0.05$) nor is there a relationship between T_{opt} and size in this study (linear regression, $p > 0.05$). However, Chen et al. (2014) admit that this could also be attributed to the lack of data for cold water species, a caveat that applies to our data as well: all species were isolated equatorward of 49°.

Still, picoeukaryotes grow over a wider temperature range than picoprokaryotes, which is in agreement with field observations. While picoprokaryotes favour (sub-)tropical ocean waters, picoeukaryotes dominate picophytoplankton biomass in colder waters (Buitenhuis et al. 2012).

To investigate the response of the entire phytoplankton community to temperature it is necessary to gather more laboratory data especially for picoeukaryotes and cold water species.

3.5.2. Eppley's hypothesis b)

Community growth follows an exponential function

Eppley (1972) was a pioneer in formulating an exponential relationship between temperature and phytoplankton community growth. The findings in this study give statistical support for Eppley's assumption that the best fit to the mean community growth rate and consequently the general trend of the growth rates related to temperature is exponential. Even though the AIC of the optimum fit gets close to the threshold (ΔAIC = 2.4), there is more support for the exponential fit.

To test if the absolute maximum community growth follows this relationship, fits through μ_{Opt} versus T_{opt} only were compared. The linear fit has a better relative quality but the exponential relationship is also reasonable. All three curves are very close over the range of T_{opt} values, but the linear function deviates from the others at lower temperatures. More data of cultures with optima at lower temperatures would need to be included to distinguish better between the fits. Eppley calculated a Q_{10} value of 1.89 for a phytoplankton community which has also been confirmed by Bissinger et al. (2008). The temperature coefficient which can also be described as the factor for growth rate increase with temperature estimated from the 99th quantile regression (μ_{pic}) in our study was found to be higher for picophytoplankton than for the whole phytoplankton community in these other studies. This agrees with the findings by Chen et al. (2014) who found a higher temperature coefficient for picophytoplankton compared to larger species. However, Eppley also notes that other field studies found higher values in the range between 2.1 and 2.3.

The Q_{10} value obtained from the 99th quantile regression for picoprokaryotes (μ_{pro}) is more than twice as high as for picoeukaryotes . This fact was previously reported by Kulk et al. (2012) who found values between 3.6 and 4.4 for *Prochlorococcus* and much lower values (1.7 - 2) for two picoeukaryotes.

The downward shift of the curve obtained for the picophytoplankton community (Figure 3. 7) compared to Eppley's curve can be explained by the generally lower growth rates compared to those of other phytoplankton groups, e.g. diatoms (Furnas 1990). Eppley's study contained various groups of faster growing phytoplankton and a substantial number of diatoms (43%). However, Bissinger et al. (2008) showed that a higher proportion of diatoms (68%) would not affect the fit. It is unclear how high the proportion of

picophytoplankton was in this database. Because of their substantially lower growth rates at low temperatures and the much higher Q_{10} it is important to investigate the physiological parameters of different phytoplankton groups separately. The maximum community growth could then be determined based on the physiological characteristics of the community composition in the concerned environment.

3.5.3. Influence of temperature on chlorophyll to carbon ratios

Phytoplankton acclimate to prevailing environmental conditions by changes in cell composition. Chlorophyll *a* to carbon ratio is an important variable for measuring biomass and primary production and varies between different phytoplankton groups, e.g. diatoms have higher chlorophyll *a* ratios compared to picophytoplankton (Geider et al. 1997). With increasing temperature chlorophyll *a* concentration increases in relation to carbon (Eppley 1972; Geider 1987). The results in this study basically agree with this assumption showing a linear increase with temperature on a phytoplankton community level, but may also indicate a drop above the optimum temperature for some strains. This reduction in photosynthetic machinery at supraoptimal temperatures is comparable to the effect caused by photoinhibition at high light levels (see light chapter).

3.5.4. Implications for the geographical distribution of picophytoplankton

If picophytoplankton is treated as a single plankton functional type in biogeochemical ocean models, the assumption is that it can be represented with a common set of physiological traits. There is some support for this assumption, as both groups are adapted to low nutrient conditions because of their high nutrient uptake efficiency (Raven 1998). They also have a relatively high light use efficiency (see chapter 1), which are both advantages over other phytoplankton groups and could explain their better success in oligotrophic and deep mixed water-columns.

However, the distribution of picoprokaryotes and picoeukaryotes in the natural environment is inversely related (Buitenhuis et al. 2012) and correlated with nitrogen concentration and depth of the euphotic layer in an inverse way (Bouman et al. 2011). There is no evidence in our study that optimum temperature influences their geographical

distribution, also it does not differ significantly between groups. A more important factor is the temperature tolerance range.

A recent study on the realized ecological niches of a variety of plankton functional types, including both picoprokaryotes was conducted by applying a statistical species distribution model (Brun et al. in press) to observational data from the MAREDAT database (Buitenhuis et al. 2013). They found that next to mixed layer depth and light, also temperature is an important predictor for the realized ecological niche space of all plankton functional types. Also, the quartile temperature range of the realized niche of *Prochlorococcus* (16 - 25°C) matches with the findings in our laboratory study. Unfortunately, they were not yet able to specifically separate the realized ecological niche of picophytoplankton due to the lack of available data on a broader range of species.

It has been previously shown that picoprokaryotes grow over a very narrow range of temperatures which restricts their growth to warmer waters. In turn, some picoeukaryotes are able to grow in colder environments. Hence they dominate the picophytoplankton biomass at latitudes above 40° (Buitenhuis et al. 2012). This once again highlights the importance to investigate the direct impact of temperature on a variety of phytoplankton species to define their fundamental ecological niches and separate temperature and nutrient components, which are strongly correlated in the determination of realized ecological niches from *in situ* samples. In addition, fundamental ecological niches are required for the formulation of dynamic green ocean models (Le Quéré et al. 2005), which aim to represent realized ecological niches as emergent properties.

With climate change picophytoplankton will gain more importance due to the indirect effect on water column stratification and lower nutrient availability (Morán et al. 2010). The results in this study also provide evidence for an advantage because of a direct effect as a consequence of a higher Q_{10} value compared to other phytoplankton groups. While coccolithophores e.g. have a lower Q_{10} of 1.7 (Buitenhuis et al. 2008), and average phytoplankton have a Q_{10} of 1.89 (Eppley 1972), picophytoplankton show a stronger increase in growth rate with temperature. Even though picoprokaryotes may show a strong increase in biomass in specific regions due to their extremely high Q_{10} value, they are restricted by a narrower temperature tolerance range. It is therefore assumed that they will be shifted to higher latitudes or depth, while picoeukaryotes will be able to increase their contribution to phytoplankton biomass over a wider temperature range.

3.6. Conclusion

We find substantial support that the influence of temperature on growth rates of single picophytoplankton species can be best described by an optimum function as suggested by Eppley (1972).

Mean community growth is better explained by an exponential fit, as also suggested by Eppley. When applying a 99th quantile regression for the absolute maximum community growth, the Q_{10} value is higher than Eppley's estimate, consistent with previous findings. Picoprokaryotes have a Q_{10} value which is more than twice as high as the value estimated for picoeukaryotes.

Picoprokaryotes differ significantly from picoeukaryotes in terms of optimum growth rate, while there is no difference in mean optimum temperature. There is also no correlation of optimum temperature and latitude of isolation. Therefore, it is important to not only consider optimum temperature and maximum growth rate, but also temperature tolerance ranges when defining their geographical distribution. Hence, especially when modelling primary production in subtropical oligotrophic ocean areas, where their contribution to total biomass is substantial, it is necessary to consider the influence of the physiological traits of this small phytoplankton component.

Another important parameter in biogeochemical models is the temperature dependence of the chlorophyll *a* to carbon ratio, which increases with increasing temperature. This study shows that there may also be a drop above the optimum temperature.

It can further be assumed that the increase of ocean temperature due to climate change will be beneficial for picophytoplankton not only because of the indirect effect through nutrient depletion as suggested in other studies but also because of a higher Q_{10} compared to other phytoplankton groups. It will also have a stronger effect on picoprokaryotes and may shift their distribution because of their narrow temperature tolerance range.

3.7. Appendix

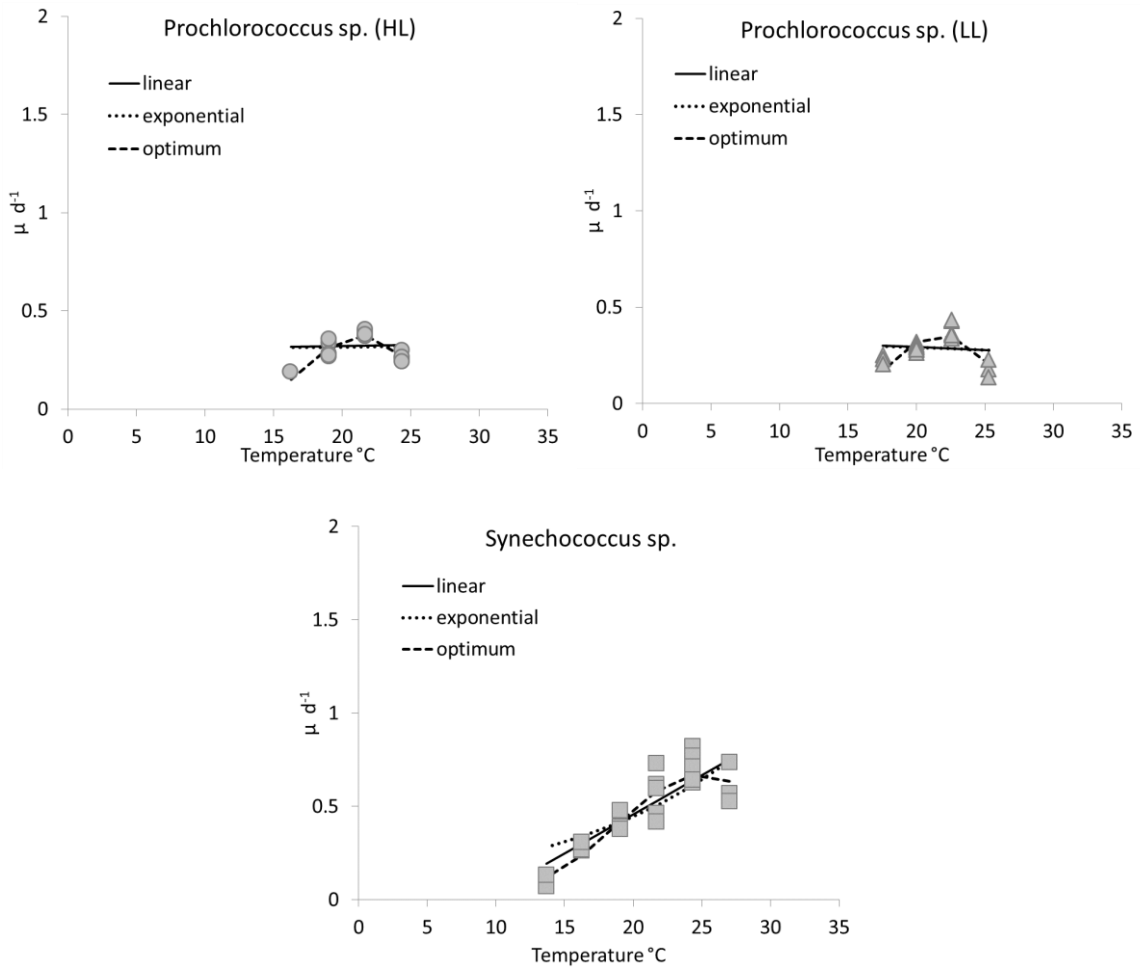

Figure 3. 9 Linear, exponential and optimum growth curve fits to picoprokaryotes including a high light (HL) and a low light (LL) adapted Prochlorococcus strain and a Synechococcus strain.

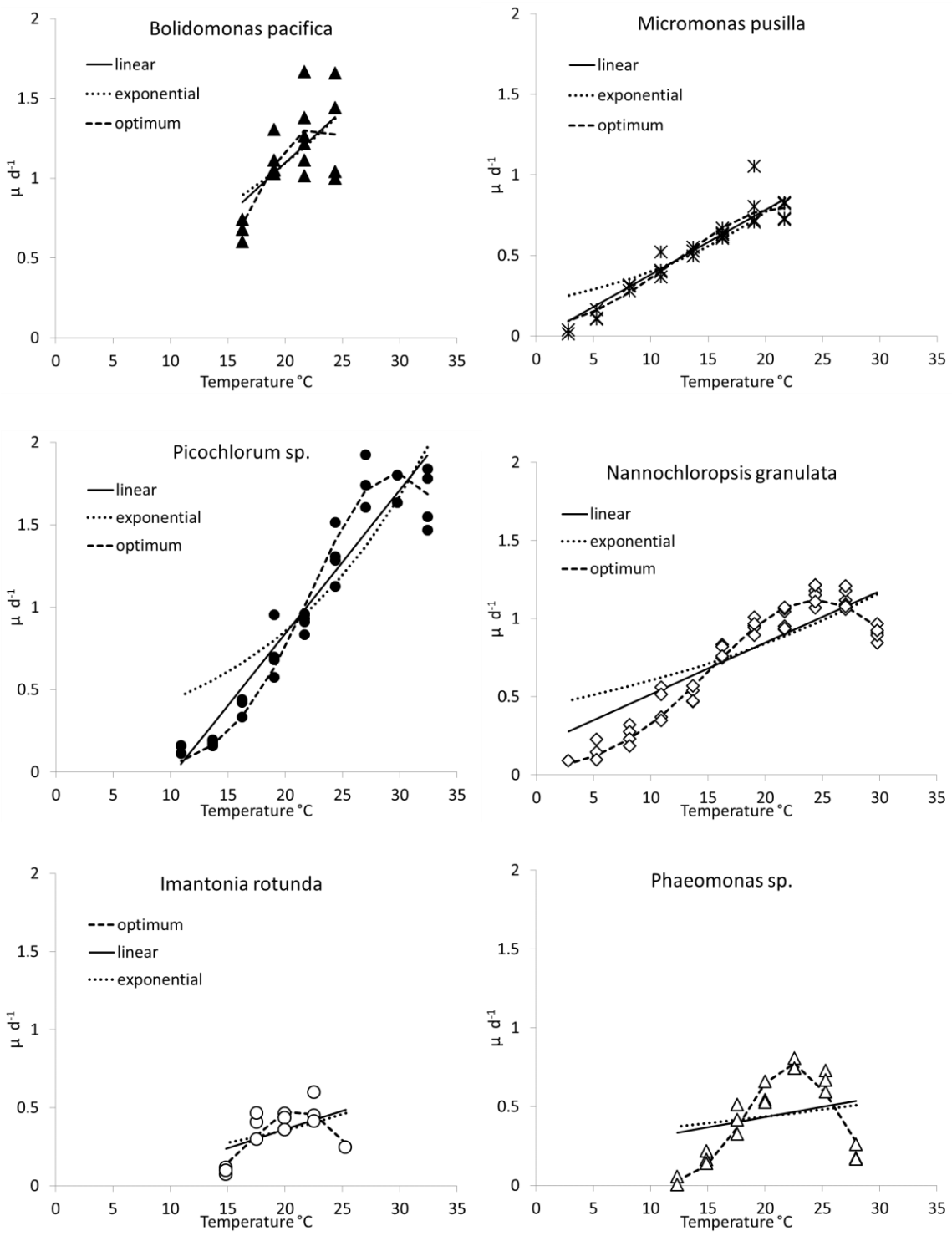

Figure 3. 10 Linear, exponential and optimum growth curve fits to 6 picoeukaryotes.

4. LIGHT AND TEMPERATURE INDUCED VARIABILITY OF THE ELEMENTAL COMPOSITION OF PICOPHYTOPLANKTON AND THEIR MINIMUM REQUIREMENTS BASED ON NUTRIENT LIMITATION EXPERIMENTS.

4.1. Abstract

This study investigates the variability of the nutrient stoichiometry within prokaryotic and eukaryotic picophytoplankton under temperature (9 strains), light (6 strains) and nitrogen and phosphorus (4 species) limited conditions. Picoprokaryotes and picoeukaryotes have similar mean C: N (5.9 ± 0.5 and 6.2 ± 1.1 respectively) but significantly different N: P ratios (13.4 ± 4.1 and 9.6 ± 3.3 respectively) under nutrient saturated conditions, which reflects the lower phosphorus demand of picoprokaryotes. With increasing temperature and decreasing light intensity C: N decreases within the picophytoplankton, and with increasing temperature N: P increases. In general, under nutrient saturated conditions, nitrogen and phosphorus are taken up in excess, causing a significant deviation from the Redfield ratio (79: 13: 1 in picoprokaryotes and 60: 10: 1 in picoeukaryotes). Nitrogen limitation leads to an increase in C: N ratios by 15 − 42 % in all three picoeukaryotes, and a decrease in N: P in *Micromonas pusilla* and *Nannochloropsis granulata*. Phosphorus limitation is reflected in an increase in C: P ratios by 37 − 65% close to the Redfield ratio. The Chlorophyll *a*: carbon ratio is significantly lower under both nitrogen (-50 − -82%) and phosphorus (-62 − -91%) limitations compared to nutrient saturated conditions. The half-saturation constants for nitrogen found in this study for *Picochlorum sp*, (0.19 ± 0.23 µmol L^{-1}) and *Micromonas pusilla* (0.07 ± 0.05 µmol L^{-1}) agree with previous estimates, but is substantially lower for *Nannochloropsis granulata* (0.01 ± 0.02 µmol L^{-1}). It is higher for *Prochlorococcus sp*., which suggests that it was not nitrogen limited under the given experimental conditions.

4.2. Introduction

Redfield investigated the elemental composition of particulate matter and seawater in 1934 and found a general relationship in nutrient stoichiometry between the samples. A general average ratio was later defined as the Redfield ratio of 106C: 16N: 1P (Redfield 1958) and used to describe the elemental stoichiometry of phytoplankton cells.

While this relationship has been widely used to explore how different biogeochemical cycles are coupled in the ocean, it is well known that phytoplankton cells acclimate to environmental conditions by changes of the proportions of specific organic components such as e.g. carbon and nitrogen rich proteins and pigments, or phosphorus rich RNA and phospholipids in order to maximise growth rate or reduce damage through e.g. photoinhibition. Further, they take up nutrients in excess of their minimum requirements under nutrient saturated conditions. This is mostly reflected by generally lower N:P ratios, while C:N ratios remain close to the Redfield ratio (Geider & La Roche 2002). These deviations are important enough that they can be seen as large-scale differences across different ocean regions and seasons (Bertilsson et al. 2003), and the N: P ratio is commonly used as a transition value to define nutrient limited regions (Geider & La Roche 2002).

Recently, efforts have been made to represent variable elemental stoichiometries and their drivers and consequences in global biogeochemical models (Tagliabue et al. 2011; Toseland et al. 2013), but not enough experimental data is available to constrain the models (Tagliabue et al. 2011).

Picophytoplankton make up 26 – 56% of the accounted for global phytoplankton biomass with a substantial contribution to total phytoplankton biomass in the subtropical oligotrophic ocean areas (Buitenhuis et al. 2013). They play a significant role as nutrient recyclers within the microbial loop, where they influence the balance between remineralisation and export production. Due to their small size this group has a very high nutrient uptake efficiency compared to other phytoplankton (Raven 1998). *Prochlorococcus* and *Synechococcus* achieve an additional advantage in nutrient poor environments by substituting phosphorus in phospholipids for sulphur and sugar (Van Mooy et al. 2006). However, *Synechococcus* also uses phycobilisomes for light harvesting, which have a higher N: C quota compared to chlorophylls (Raven 1984). Especially in these small cells pigment-protein complexes make a large contribution to

cell biomass and influence the elemental stoichiometry (Geider et al. 1996).

It is believed that global warming will cause an extension of the subtropical oligotrophic gyres leading to a higher importance of the picophytoplankton group in global biogeochemical cycles (Morán et al. 2010).

Previous studies focused on the elemental composition of cyanobacteria (e.g. Bertilsson et al. 2003; Heldal et al. 2003; Veldhuis et al. 2005; Timmermans et al. 2005), but this study aims to investigate the variability of the nutrient stoichiometry within prokaryotic and eukaryotic picophytoplankton over a broad range of temperatures and light intensities in comparison with nitrogen and phosphorus limited conditions. The benefit of this study is that the variability of the elemental composition is first investigated under nutrient saturated conditions. With this information favourable and saturated light and temperature conditions can be chosen for nutrient limitation experiments to investigate the direct impact of nutrient limitation only. Furthermore, it is possible to directly compare the nutrient stoichiometry of nitrogen or phosphorus limited cultures to the nutrient stoichiometry which was obtained under identical nutrient saturated conditions.

The results contribute to a better understanding of the flexibility in C: N: P ratios in these groups, their nutrient requirements and give an idea about their luxury nutrient uptake under nutrient saturated conditions. Further the effect of nutrient limitation on Chlorophyll to carbon ratios is addressed as chlorophyll *a* is commonly used to estimate phytoplankton biomass.

4.3. Material and Methods

4.3.1. Cultures

Picophytoplankton, including 3 prokaryotic and 6 eukaryotic strains, were obtained from the Roscoff culture collection (Vaulot et al. 2004). They include a high light (HL) and a low light (LL) ecotype strain of *Prochlorococcus sp.* (RCC 296 and 162), *Synechococcus sp.* (RCC 30) as well as the picoeukaryotes *Bolidomonas pacifica* (RCC 212), *Micromonas pusilla* (RCC 1677), *Picochlorum sp*. (RCC 289), *Nannochloropsis granulata* (RCC 438), *Imantonia rotunda* (361) and *Phaeomonas sp.* (RCC 503). They were isolated between 2.5° S and 49° N in the Pacific and Atlantic Oceans as well as the Mediterranean and the North Sea.

4.3.2. Experimental setup of nutrient saturated conditions

a) General treatment

Artificial seawater medium (ESAW) (Berges et al. 2001) with ammonium (882 µM $(NH_4)_2SO_4$) as the single nitrogen source and selenium (10 nM Na_2SeO_3) was used. The final concentration of phosphorus was 36.2 µM.
Light intensities were measured with a Radiometer (Biospherical Instruments Inc. QSL-2101). Growth rates were calculated from daily measurements during the exponential growth phase by taking the logarithm of the in vivo fluorescence values and applying a linear regression through at least three consecutive measurements. For this, aliquots of 4 ml were removed from the experimental flasks of the light experiments and measured in a Turner Design Fluorometer (10 AU). For measurements of the growth rates of the temperature samples the entire culture tube was placed in the Fluorometer.

b) Variable light conditions

The cultures were grown in conical flasks (400 ml) at up to 7 light intensities between 13 and 720 µmol photons m^{-2} s^{-1}provided by fluorescent tubes (Mitsubishi/Osram FC40ss.W/37) and dimmed by neutral density film in a 14: 10 light: dark cycle.

Experiments were conducted in a Sanyo incubator (Versatile Environmental test chamber) at a constant temperature of 22°C. Cultures were acclimated for at least 5 divisions.

c) Variable temperature conditions

The cultures were grown in 55ml culture tubes (Pyrex Brand 9826) in a temperature gradient bar (Buitenhuis, in prep.). They were placed in 13 positions across a temperature gradient between -0.5°C and 33°C. The light cycle was set to 14 hours of light per day and the intensity was 291 ± 18 µmol photons m^{-2} s^{-1} provided by an individual LED under each tube (Winger WEPW1-S1 1W, 95 Lumen, white). It was decreased to 81 ± 5 µmol photons m^{-2} s^{-1} for the low light Prochlorococcus ecotype. Cultures were acclimated to each temperature for at least 4 divisions to reach balanced growth.

4.3.3. Experimental setup of nutrient limited conditions

Nutrient limitation experiments were conducted in chemostats that were built into a Sanyo incubator as used in the light experiments. The temperature was 21°C at a light intensity of 258 ± 12 µmol photons m^{-2} s^{1}. The schematic experimental setup is shown in Figure 4. 1.

Medium flows from one of the medium bottles (1) through a peristaltic pump (Watson Marlow 323) (2). An air flow connects to the system (3). Air and medium flow into a separating funnel containing culture (4) where it is sampled by a syringe (5). The excess volume is caught in a waste bottle (6).

The ESAW medium bottles contained different nitrogen to phosphorus ratios to create nitrogen (N : P = 3 : 1 ≙ 100 µM NH_4 : 33 µM PO_4) and phosphorus (N : P = 80 : 1 ≙ 500 µM NH_4 : 6.25 µM PO_4) limitation. The ratio of the limiting nutrients was 16N: 1P to try and achieve similar biomasses in the N and P limited cultures. Separating funnels with culture volumes between 66 and 200ml depending on the species specific growth rate were used. Medium flow was measured by daily weighing of the waste bottles and adjusted to match a steady state growth rate. The cell density was measured daily by flow cytometry to ensure stable conditions. For this 0.5 – 1 ml volume were removed with a

syringe. Cultures were acclimated until cell density reached a steady state for 3 consecutive days (at least 10 dilutions) before cell composition and nutrient concentration samples were taken.

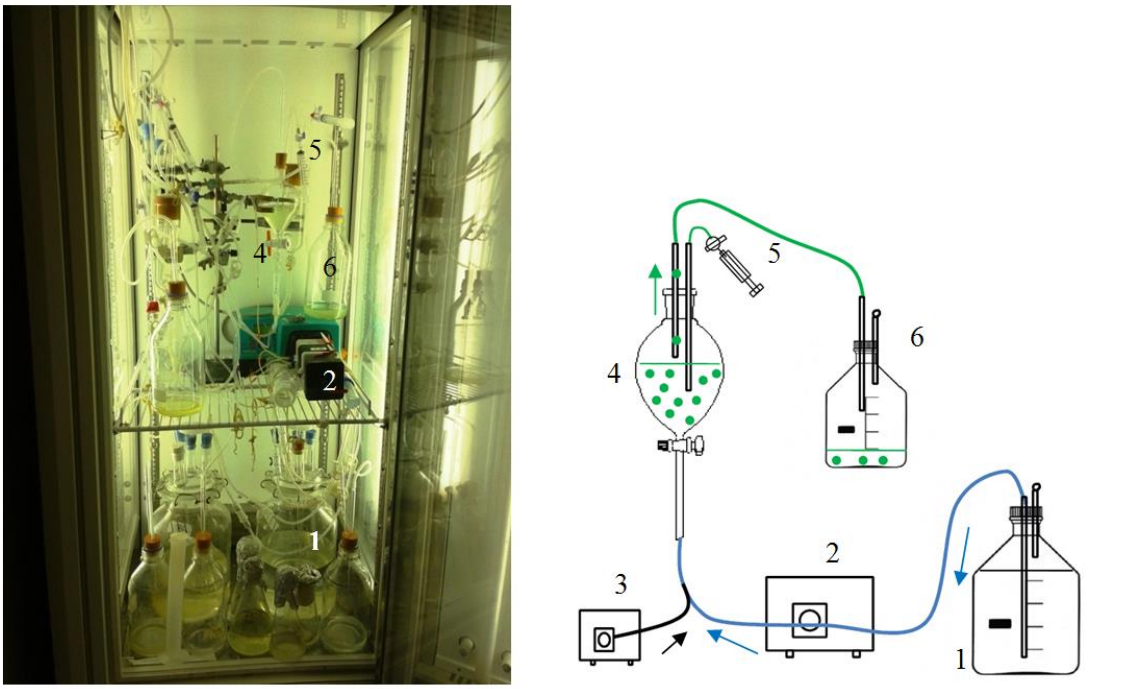

Figure 4. 1Experimental setup of the nutrient limitation experiment. left: Photo of the experiment with 3 cultures growing at 2 limitations each, right: schematic view of medium, air and culture fluxes for one incubation: 1 medium bottle, 2 medium pump, 3 air pump, 4 separating funnel containing culture, 5 sampling syringe, 6 waste bottle.

Dilution rates (Table 4. 1) were adjusted to 70% of the maximum growth rate of *Prochlorococcus sp.*, to approximately 50% for *Micromonas pusilla, Nannochloropsis granulata* and the phosphorus limited *Picochlorum sp.*, and 13% for the nitrogen limited *Picochlorum sp.* culture.

Table 4. 1 Dilution rates (d^{-1}) in the nutrient limitation experiments

	Nitrogen limitation dilution rate	Phosphorus limitation dilution rate
Prochlorococcus sp. (HL)	0.28 ± 0.11	0.28 ± 0.13
Micromonas pusilla	0.4 ± 0.08	0.47 ± 0.21
Picochlorum sp.	0.16 ± 0.03	0.5 ± 0.03
Nannochloropsis granulata	0.66 ± 0.07	0.71 ± 0.27

4.3.4. Cell components

All cultures were sampled for Chlorophyll *a*, particulate organic carbon (POC), nitrogen PON) and phosphorus (POP) quota after acclimation.

Precombusted 13mm GF/F filters were used for POC/PON sampling for all species. *Prochlorococcus* cells were too small to remain on the filters, but preliminary tests showed that no cells passed through if a layer of 3 filters was used.

For chlorophyll *a* and POP analyses samples were collected on precombusted 25 mm GF/F filters, while *Prochlorococcus sp.* was sampled on 25 mm polycarbonate filters (0.2µm). Between 5 and 20 ml were filtered, depending on the cell density, and rinsed with Milli-Q water. All filters were frozen immediately after sampling in liquid nitrogen and stored at -80°C until analyses. Cell numbers were measured by flow cytometry (BD Biosciences FACSCalibur, flow cytometer). Flow rate was calibrated using the method by Marie et al. (2005) .

The filtrate from cultures which were grown under nutrient limitation was kept for analysis of the nutrient concentrations in the medium. Part of the filtrate was re-filtered, and the Milli-Q rinsed filter was used as a blank for the particulate samples.

4.3.4.1. Carbon and nitrogen analysis

POC/PON samples were dried at 40°C for 24 hours, placed into precombusted tin capsules and analysed with an elemental analyser (Exeter Analytical, CE-440 Elemental Analyser), which was calibrated with acetanilide (Exeter Analytical). Results were corrected for blank filters. Ammonium in filtrates was analysed by the method of Krom (1980) (Perkin Elmer Lambda 25 UV/VIS Spectrometer). Samples > 80 µmol NH_4^+ L^{-1} were diluted with nutrient free medium to fit into the calibration range.

4.3.4.2. Phosphorus analysis

Particulate organic phosphorus was digested by persulfate chemical wet oxidation (Suzumura 2008) and phosphate was analysed using the colorimetric method (Strickland & Parson 1972). Dried filters were placed into 18 ml of 3% persulfate solution (Potassium

persulfate, Sigma Aldrich, ≥ 99.0%) and autoclaved for 30 minutes at 120°C. After cooling for 24 hours 18 ml of Milli-Q water and 3.6 ml of mixed reagents were added and absorbance was measured at 885 nm within 2 hours (Perkin Elmer Lambda 25 UV/VIS Spectrometer). Phosphate in filtrates was analysed the same way by the colorimetric method.

Phosphorus samples from filtrates with concentrations above 20 µmol L^{-1} needed to be diluted to fit into the calibration range. This affected all filtrates from nitrogen limitation experiments. Initial tests using nutrient free medium as the dilutant showed an intense colour reaction. Consequently Milli-Q water was used for a 10-fold dilution.

4.3.4.3. Chlorophyll a analysis

Chlorophyll *a* samples were extracted in 10 ml of Acetone (Fisher Scientific, ≥ 99.8%) in 15 ml centrifuge tubes and disintegrated by shaking and vortexing. Tubes were wrapped in aluminium foil and stored at 4°C for 24 hours. For analysis samples were centrifuged and the supernatant was analysed in a Fluorescence Spectrometer (PerkinElmer LS 45 Luminescence Spectrometer). After reading a sample 3 drops of 8% HCl were added into the cuvette to measure the background signal. The concentration of the calibration standard (Sigma Aldrich, product No C5753) was obtained prior to analyses (Parson et al. 1984).

4.3.4.4. Statistics and calculations

To compare distributions of elemental quotas or ratios between experiments and groups data was tested for normality (Kolmogorow-Smirnow-Test). With $p < 0.05$ a non parametric test (Mann-Whitney U test) was used. Trends were determined by linear regression analysis and p-values were obtained by ANOVA. All statistical analyses were conducted with the software Mystat, version 12.

Half-saturation constants were obtained for individual measurements of remaining nutrient concentration in the chemostat medium and the relative growth rate, which was obtained in the previous 3 - 4 days before sampling using equation 22 in (Morel 1987). Averages and standard deviations of the pairs are shown. The relative growth rate is defined as the dilution rate /growth rate under similar nutrient saturated conditions (i.e. as the fraction of the maximum growth rate).

4.4. Results

4.4.1. Nutrient saturated conditions

4.4.1.1. Elemental quotas and trends

Regarding the entire range of quotas of the cell components within both light (Table 4. 12 - Table 4. 15, Appendix) and temperature experiments (Table 4. 16 - Table 4. 19, Appendix), we find that the carbon quota in *Prochlorococcus sp.* ranges between 0.06 and 0.24 pg cell^{-1}. It is higher in *Synechococcus sp.* (0.21 - 1.57 pg cell^{-1}) and highest in picoeukaryotes. In that group cells up to a size of 2 µm have carbon quota between 0.8 and 3.9 pg cell^{-1}, the two bigger picoeukaryotes that were only investigated in the temperature experiment have a carbon quota between 2.5 and 8.4 pg cell^{-1}.

Nitrogen quota in *Prochlorococcus* range between 0.012 and 0.047 pg cell^{-1}, in *Synechococcus sp.* between 0.045 and 0.317 pg cell^{-1}, in the smaller picoeukaryotes between 0.141 and 0.751 pg cell^{-1} and in the two larger between 0.522 and 1.87 pg cell^{-1}.

Phosphorus quota in *Prochlorococcus sp.* range between 0.002 and 0.008 pg cell^{-1}, in *Synechococcus sp.* between 0.007 and 0.069 pg cell^{-1}, in the smaller picoeukaryotes between 0.026 and 0.286 pg cell^{-1} and in the larger picoeukaryotes between 0.08 and 0.413 pg cell^{-1}. There is an increasing trend in all elements with cell size. Only *Bolidomonas pacifica* deviates from this relationship.

Mean species specific ranges of elemental quotas are similar in both light and temperature experiments (Figure 4. 2 and Table 4. 20, Appendix). We only find statistically significant differences in *Synechococcus sp.* concerning all three elements (Table 4. 2). There are significant differences in nitrogen in *Micromonas pusilla* and in phosphorus in *Bolidomonas pacifica*, *Picochlorum sp.* and *Nannochloropsis granulata*. Mean nutrient quotas in picoprokaryotes do not vary significantly between the experiments, only phosphorus varies significantly in picoeukaryotes.

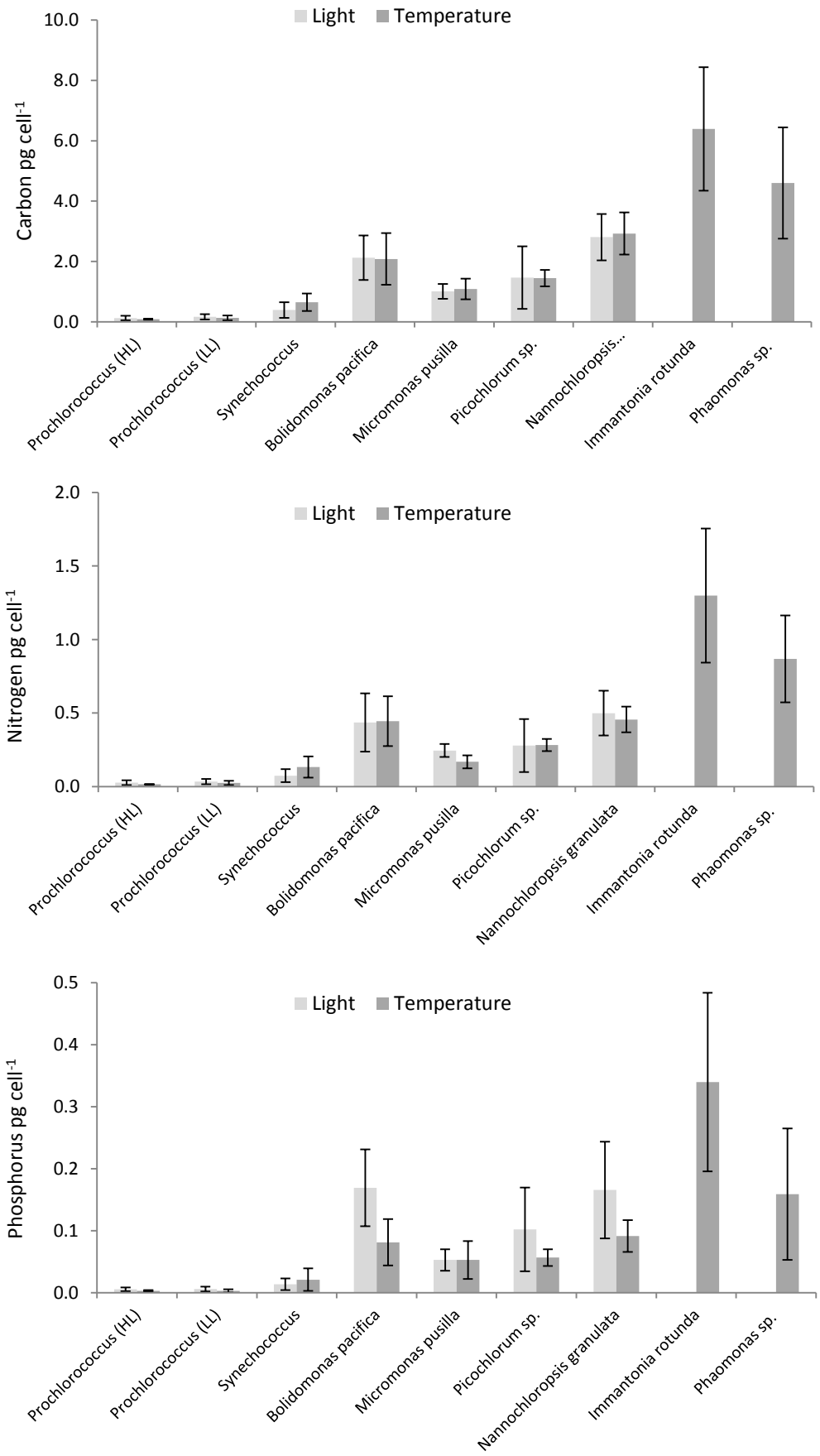

Figure 4. 2 Carbon, nitrogen and phosphorus quota [pg cell^{-1}] in picophytoplankton species obtained from light and temperature experiments. Bars: means, whiskers: Standard deviations

Table 4. 2 Statistical comparison of species specific carbon, nitrogen and phosphorus quota [pg cell^{-1}] between the light and temperature experiments, p values from Mann Whitney U test, significant differences in bold.

Species	RCC	Carbon	Nitrogen	Phosphorus
Prochlorococcus (HL)	269	0.428	0.133	0.182
Prochlorococcus (LL)	162	0.435	0.248	0.076
Synechococcus sp.	30	**0.011**	**0.001**	**0.030**
Bolidomonas pacifica	212	0.797	0.877	< **0.001**
Micromonas pusilla	1677	0.520	< **0.001**	0.679
Picochlorum sp.	289	0.063	0.083	**0.010**
Nannochloropsis granulata	438	0.361	0.451	< **0.001**
Prokaryotes	-	0.200	0.055	0.300
Eukaryotes	-	0.383	0.699	< **0.001**
All	-	**0.006**	**0.021**	0.543

The picophytoplankton community shows a significant increase in carbon quota with increasing light intensity above 64 µmol photons m^{-2} s^{-1}. However, highest values are reached at the lowest light intensities (Table 4.12, Appendix).

On a species level trends vary, both *Prochlorococcus* strains, *Picochlorum sp.* and *Nannochloropsis granulata* have highest carbon quota at low light. In contrast, *Synechococcus sp.* and *Bolidomonas pacifica* have highest quota at the highest light intensities (Table 4.12, Appendix).

Nitrogen quota increase significantly in cells of *Synechococcus sp.* and *Bolidomonas pacifica* with increasing light level (Table 4.13, Appendix). An increase is also noticeable but not significant in *Picochlorum sp*.. Phosphorus is increased in *Synechococcus sp.* in higher light (Table 4.14, Appendix), while there is an opposite trend in *Picochlorum* sp. and *Nannochloropsis granulata.*

There is no general relationship between carbon quota and temperature in the picophytoplankton community (Table 4.16, Appendix). Still, there is a decrease with increasing temperature in cells of *Picochlorum sp., Nannochloropsis granulata* and *Phaeomonas sp.,* but an increase in the low light *Prochlorococcus sp.* ecotype. Also the high light *Prochlorococcus sp.* ecotype has higher carbon quota at higher temperatures. The same trend applies to nitrogen and phosphorus in these species (Tables 4.17 and 4.18, Appendix).

4.4.1.2. Nutrient stoichiometry

Under nutrient saturated conditions phytoplankton cells take up nutrients in excess of their minimum requirement. However, acclimation to specific light and temperature regimes causes variations in their elemental ratios.

Light and temperature induced changes in C: N and N: P and Chlorophyll *a* : C ratios are investigated in Figure 4. 3 and Figure 4. 4. Specific growth rates were discussed in the previous chapters.

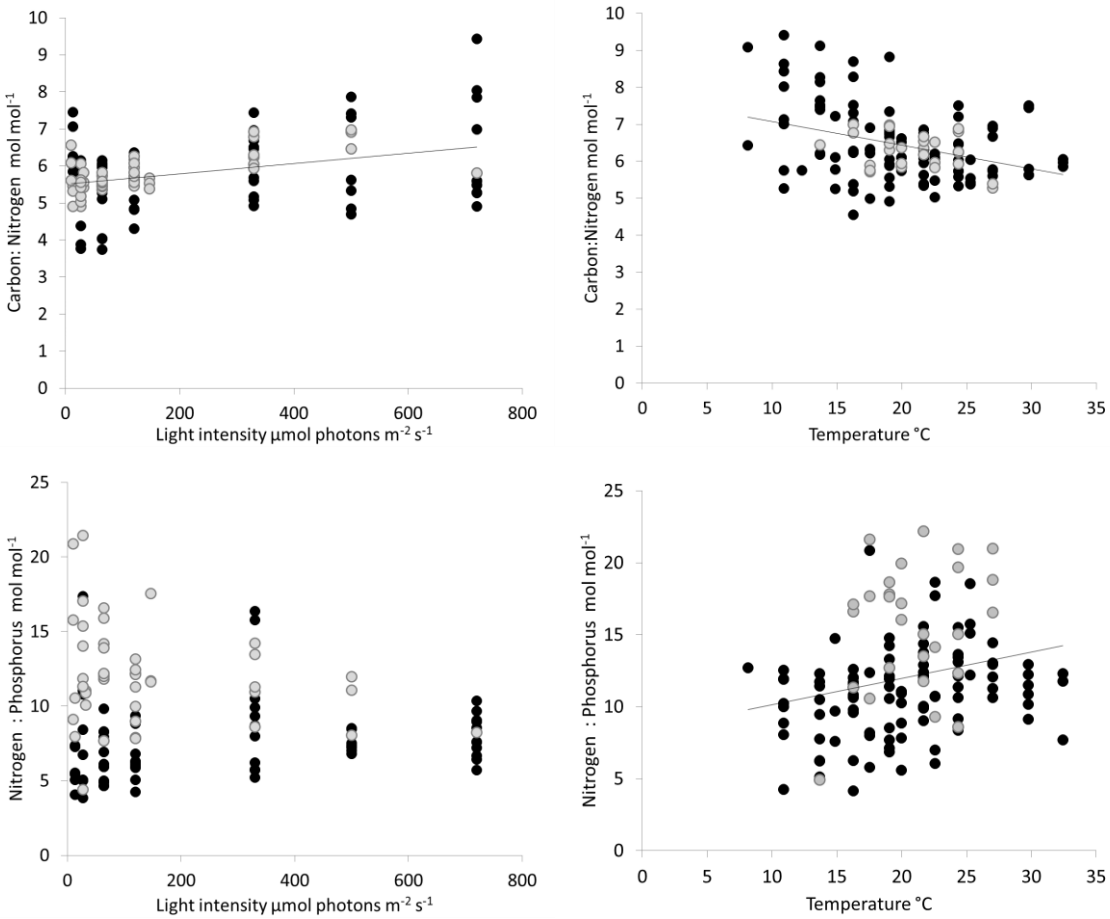

Figure 4. 3 Nutrient stoichiometry from light (left) and temperature (right) experiments: C: N (top) and N: P (bottom) ratios in mol mol^{-1}, grey: picoprokaryotes, black: picoeukaryotes

4.4.1.3. Carbon : Nitrogen

The C: N ratio increases significantly ($p < 0.05$) with increasing light intensity and decreasing temperature (Figure 4. 3). This also applies for the single groups, only

picoprokaryotes do not show a significant increase in C: N ratio with decreasing temperatures.

Species specific changes in C: N ratio with light and temperature are shown in Figure 4. 8 and Figure 4. 9 in the Appendix. There is a significant increase in C: N with light intensity for *Synechococcus sp.*.For *Prochlorococcus sp.* a significant increase is only seen between 27 and 120 µmol photons m^{-2} $s^{-1}$for the low light ecotype and between 27 and 330 µmol photons m^{-2} s^{-1} for the high light ecotype. The increasing trend is also significant for *Nannochloropsis granulata* and *Micromonas pusilla*. No significant trends were found for *Bolidomonas pacifica* or *Picochlorum sp.*. C: N ratios decrease significantly with increasing temperature in *Synechococcus sp.*, *Nannochloropsis granulata*, *Picochlorum* (between 13 and 30°C) and *Phaeomonas sp.* (between 15 and 25°C). All mean values from the light experiment (Table 4. 3) and most values from the temperature experiment (Table 4. 4) are below the Redfield ratio and show that there is luxury uptake of nitrogen.

The mean C: N ratio show slightly lower mean values of both groups (5.8 ± 0.9) in the light experiment compared to the temperature experiment (6.4 ± 0.9). The whole range for C: N ratios estimated in both experiments is 3.7 to 9.4. However, when data from both experiments is used, C: N is similar for picoprokaryotes (5.9 ± 0.5) and picoeukaryotes (6.2 ± 1.1).

The 3 species in the temperature experiments which have the highest C: N include the two picoeukaryotes which grew at the lowest temperatures.

Table 4. 3 Species, group and community specific mean, minimum and maximum C: N ratios from light experiments

Species	RCC	n	Mean C:N	STD	Min	Max
Prochlorococcus (HL)	296	14	5.5	(0.4)	4.9	6.2
Prochlorococcus (LL)	162	19	5.7	(0.3)	5.4	6.6
Synechococcus sp.	30	15	6.1	(0.6)	5.0	7.0
Bolidomonas pacifica	212	14	5.3	(0.6)	4.7	6.5
Micromonas pusilla	1677	14	4.8	(0.9)	3.7	6.5
Picochlorum sp.	289	21	6.1	(1.0)	5.2	9.4
Nannochloropsis granulata	438	20	6.6	(0.7)	5.8	8.0
Picorokaryotes	-	48	5.8	(0.5)	4.9	7.0
Picoeukaryotes	-	69	5.8	(1.1)	3.7	9.4
All	-	117	5.8	(0.9)	3.7	9.4

Table 4. 4 Species, group and community specific mean, minimum and maximum C: N ratios from temperature experiments

Species	RCC	n	Mean C:N	STD	Min	Max
Prochlorococcus (HL)	296	4	6.7	(0.2)	6.5	6.9
Prochlorococcus (LL)	162	9	6.0	(0.3)	5.7	6.5
Synechococcus sp.	30	14	6.3	(0.5)	5.3	7.0
Bolidomonas pacifica	212	12	5.5	(0.5)	4.5	6.5
Micromonas pusilla	1677	14	7.5	(1.0)	5.9	9.1
Picochlorum sp.	289	26	6.0	(0.4)	5.3	7.5
Nannochloropsis granulata	438	25	7.5	(0.8)	6.5	9.4
Imantonia rotunda	361	11	5.8	(0.4)	5.0	6.2
Phaeomonas sp.	503	16	6.1	(0.6)	5.0	7.2
Picoprokaryotes	-	27	6.3	(0.5)	5.3	7.0
Picoeukaryotes	-	104	6.5	(1.0)	4.5	9.4
All	-	131	6.4	(0.9)	4.5	9.4

4.4.1.4. Nitrogen : Phosphorus

No general trend for N: P with light was observed on a community level. It increases significantly ($p < 0.05$) in picoeukaryotes with increasing light level up to 330 µmol photons $m^{-2}s^{-1}$, but in contrast declines in picoprokaryotes (Figure 4. 3, $p < 0.05$). Regarding the influence of temperature, there is a significant ($p < 0.05$) increase in N: P on a community level (Figure 4. 3). In picoeukaryotes, it appears to increase below 25°C ($p = 0.003$) and to decrease above 25°C ($p = 0.025$), which is close to the average optimum temperature of 24°C, but there is no significant relationship with growth rate. Picoprokaryotes don't show any trend ($p = 0.210$).

On a species level all picoprokaryotes show decreasing N: P ratios with increasing light, excluding the lowest light level in the high light *Prochlorococcus* ecotype (Figure 4. 10). However, the regression analysis only confirmed a significant decrease for *Synechococcus sp.*. There is a significant increase in N: P with light in the three picoeukaryotes *Picochlorum sp.*, *Nannochloropsis granulata* and *Bolidomonas pacifica*.

N: P increases significantly with increasing temperature only in *Synechococcus sp.*, *Phaeomonas sp.* and *Nannochloropsis granulata*, which is the only species that shows a drop at the highest temperature (Figure 4. 11).

The mean N: P ratio is significantly higher in picoprokaryotes (12.1 ± 3.4) than in picoeukaryotes (7.6 ± 2.7) in the light experiments ($p < 0.001$, Table 4. 5) and it is also significantly higher in picoprokaryotes (15.7 ± 4.3) than in picoeukaryotes (11 ± 3.1) in the temperature experiment ($p < 0.001$, Table 4. 6). Combined, the N: P ratio is also

significantly higher in picoprokaryotes (13.4 ± 4.1) than in picoeukaryotes (9.6 ± 3.3, $p < 0.001$). The range of measured N: P ratios is 3.9 – 22.2.

Table 4. 5 Species, group and community specific mean, minimum and maximum N: P ratios from light experiments

Species	RCC	N	Mean N:P	STD	Min	Max
Prochlorococcus (HL)	296	13	9.5	(2.3)	4.4	12.2
Prochlorococcus (LL)	162	18	13.6	(3.8)	7.8	21.5
Synechococcus sp.	30	14	12.6	(2.2)	8.1	16.6
Bolidomonas pacifica	212	14	6.4	(1.6)	4.3	9.7
Micromonas pusilla	1677	14	11.1	(3.2)	8.3	17.4
Picochlorum sp.	289	21	7.4	(1.3)	3.9	8.4
Nannochloropsis granulata	438	20	7.3	(1.7)	5.0	10.5
Picoprokaryotes	-	45	12.1	(3.4)	4.4	21.5
Picoeukaryotes	-	83	7.6	(2.7)	3.9	17.4
All	-	128	9.4	(3.7)	3.9	21.5

Table 4. 6 Species, group and community specific mean, minimum and maximum N: P ratios from temperature experiments

Species	RCC	n	Mean N:P	STD	Min	Max
Prochlorococcus (HL)	296	4	11.4	(1.9)	8.6	12.7
Prochlorococcus (LL)	162	8	15.8	(4.3)	9.3	21.6
Synechococcus sp.	30	16	16.7	(4.2)	4.9	22.2
Bolidomonas pacifica	212	11	11.8	(2.4)	8.4	15.6
Micromonas pusilla	1677	14	8.6	(3.7)	4.2	14.4
Picochlorum sp.	289	26	11.3	(1.7)	7.7	14.8
Nannochloropsis granulata	438	24	11.3	(1.7)	7.7	14.4
Imantonia rotunda	361	11	9.2	(3.1)	5.6	14.7
Phaeomonas sp.	503	14	13.1	(4.5)	7.6	20.8
Prokaryotes	-	28	15.7	(4.3)	4.9	22.2
Eukaryotes	-	100	11.0	(3.1)	4.2	20.8
All	-	128	12.0	(3.9)	4.2	22.2

4.4.1.5. Carbon: Nitrogen :Phosphorus

Table 4. 7 Cell stoichiometry as a mean from nutrient saturated experiments, standard deviation in brackets

Species	Light experiment	Temperature experiment	Mean from both experiments
	C:N:P	C:N:P	C:N:P
Prochlorococcus (HL)	55 (16) : 9 (2) : 1	76 (11) : 11 (2) : 1	60 (17) : 10 (2) : 1
Prochlorococcus (LL)	77 (22) : 14 (4) : 1	94 (24) : 16 (4) : 1	82 (23) : 14 (4) : 1
Synechococcus sp.	76 (12) : 13 (2) : 1	101 (30) : 17 (4) : 1	88 (26) : 15 (4) : 1
Bolidomonas pacifica	33 (7) : 6 (2) : 1	64 (14) : 12 (2) : 1	47 (19) : 9 (3) : 1
Micromonas pusilla	54 (20) : 9 (4) : 1	62 (22) : 9 (4) : 1	58 (21) : 10 (4) : 1
Picochlorum sp.	34 (10) : 6 (1) : 1	67 (9) : 11 (2) : 1	54 (17) : 9 (3) : 1
Nannochloropsis granulata	49 (15) : 7 (2) : 1	84 (13) : 11 (2) : 1	69 (22) : 9 (3) : 1
Imantonia rotunda	-	53 (17) : 9 (3) : 1	-
Phaomonas sp.	-	83 (30) : 13 (4) : 1	-
Prokaryotes	70 (20) : 12 (3) : 1	95 (27) : 16 (4) : 1	79 (25) : 13 (4) : 1
Eukaryotes	44 (15) : 8 (3) : 1	71 (20) : 11 (3) : 1	60 (23) : 10 (3) : 1
All	54 (22) : 9 (4) : 1	76 (24) : 12 (4) : 1	66 (25) : 11 (4) : 1

Table 4. 7 summarises C: N: P ratios from both experiments. As mentioned in the previous section, there are no differences in nitrogen relative to carbon between the groups, but lower phosphorus requirements of picoprokaryotes. Picoprokaryotes have a mean C: N: P ratio of 79 ± 25 : 13 ± 4 : 1, picoukaryotes of 60 ± 23 : 10 ± 3 : 1. The picophytoplankton community nutrient ratio is 66 ± 25 : 11 ± 4 : 1.

4.4.1.6. Chlorophyll a : carbon

The light dependency of the Chlorophyll *a* to carbon ratio was investigated thoroughly in the light chapter and is included in this section for completeness (Figure 4. 4). It increases reciprocally with decreasing light due to an increase in light acquisition components within the cells and is similar in both groups at its maximum. It ranges between 0.004 and 0.073 g Chl g^{-1} C. At higher light levels picoeukaryotes show slightly higher ratios than picoprokaryotes.

Further, chlorophyll *a* to carbon ratio decreases with decreasing temperature (Figure 4. 4) due to low temperature chlorosis, but was also suggested to be linked to the increase in lipids to maintain membrane fluidity (Geider 1987). Some strains show a drop after reaching the optimum as measured for both *Prochlorococcus sp.* ecotypes, *Picochlorum*

sp. and *Nannochloropsis granulata. Prochlorococcus sp.* has generally high levels of chlorophyll *a*, while *Synechococcus sp.* is at the lower edge of the range of the data.

The range of chlorophyll *a* to carbon ratios within the temperature experiment is narrower than within the light experiments, but matches perfectly with measurements between 120 and 330 µmol photons m^{-2} s^{-1}, the light intensity at which the temperature experiments were conducted.

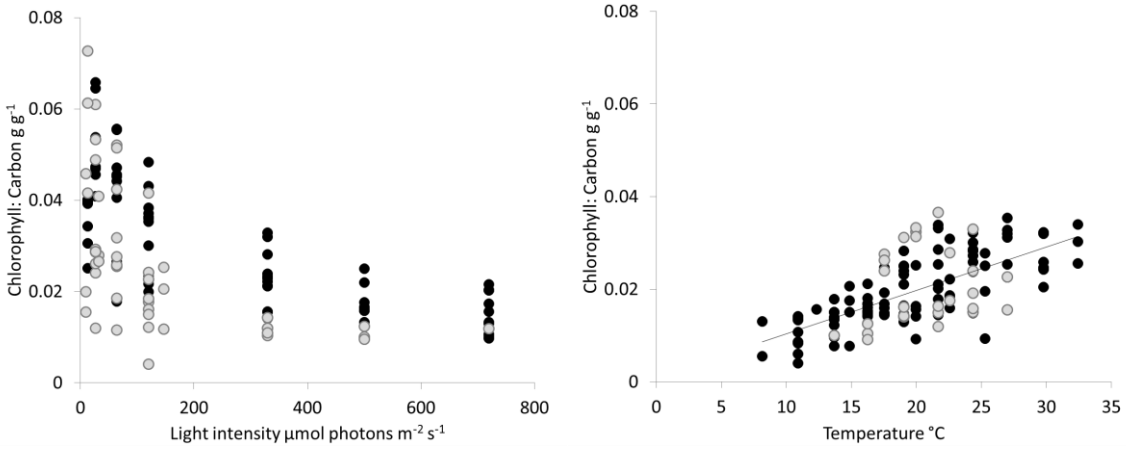

Figure 4. 4 Chlorophyll a to carbon ratios [g Chlorophyll a g^{-1} C] under nutrient saturated conditions in light (left) and temperature (right) experiments, grey: prokaryotes, black: eukaryotes

4.4.2. Nutrient limited conditions

4.4.2.1. Elemental quotas

For *Prochlorococcus sp*. the carbon and nitrogen quota under phosphorus limitation (Table 4. 8) are close to the maximum that was achieved under nutrient saturated conditions in low light. They are almost twice as high under nitrogen limitation. However, there are only two samples and one had a similar quota as the phosphorus limited sample. Phosphorus quota is similar under both limitations and twice as high as under nutrient saturation.

Picochlorum sp. has similar carbon and nitrogen quota in both limitation experiments, which are close to the mean value measured in the nutrient saturated experiments (Table 4. 20). Phosphorus quota in nitrogen limited samples is at the lower edge of the range as measured under nutrient saturation and lower under phosphorus limitation.

The values of all three elements in nitrogen limited cultures of *Micromonas pusilla* and *Nannochloropsis granulata* are within the range or close to the values obtained from nutrient saturated experiments. However, the quota in phosphorus limited cells are 10 times higher. There is no logical explanation for this, as cell numbers were low but elemental concentration within the calibration range. Still, elemental ratios in those cultures are reasonable.

Table 4. 8 Mean carbon, nitrogen and phosphorus quota from nitrogen and phosphorus limitation experiments

	Nitrogen limitation			Phosphorus limitation		
	Carbon [pg cell^{-1}]	Nitrogen [pg cell^{-1}]	Phosphorus [pg cell^{-1}]	Carbon [pg cell^{-1}]	Nitrogen [pg cell^{-1}]	Phosphorus [pg cell^{-1}]
Prochlorococcus sp. (HL)	0.43 ± 0.3	0.09 ± 0.07	0.016 ± 0.003	0.22	0.06 ± 0.04	0.014
Micromonas pusilla	2. 39 ± 0.47	0.38 ± 0.06	0.088 ± 0.015	(20.57 ± 14.91)	(4.01 ± 3.03)	(0.56 ± 0.45)
Picochlorum sp.	1.33 ± 0.21	0.23 ± 0.04	0.049 ± 0.018	1.5 ± 0.17	0.25 ± 0.02	0.03 ± 0.006
Nannochloropsis granulata	4.32 ± 0.81	0.44 ± 0.15	0.109 ± 0.023	(48.78 ± 48.19)	(9.51 ± 10.41)	(1.06 ± 0.92)

4.4.2.2. Nutrient stoichiometry

It has been shown in previous studies that in chemostat cultures cell quota have an exponential relationship with growth rate. The more the dilution rate approaches the maximum growth rate of the species, the higher the nutrient quota within the cell will rise (Goldman 1986; Morel 1987). At half of the maximum growth rate quota are still close to the minimum. Consequently, to be able to investigate the minimum requirements of both nutrients, we decreased growth rates to close to half of the maximum growth rate in *Micromonas pusilla*, *Nannochloropsis granulata* and the phosphorus limited *Picochlorum sp.*. The experiments with the nitrogen limited *Picochlorum sp.* culture were conducted with a lower dilution rate (13%) (Table 4.1) due to difficulties in the experimental set-up, but which should still allow the measurement of the minimum N requirement. *Prochlorococcus sp.* grew at 70% of its maximum growth rate.

The Redfield ratio for example is a common tool to detect the limitation by a nutrient. However, there are species specific differences. For this reason, we first compare nutrient limited data to data within the same temperature and light intensity range of both nutrients from previously described nutrient saturated experiments (Table 4. 9 and Table 4. 10).

At nutrient saturated conditions all species show significant (t-test, $p < 0.01$) deviations from the Redfield ratio with lots of luxury nutrient uptake. *Prochlorococcus sp*. has a C: N: P ratio of 67: 10: 1, *Micromonas pusilla* of 68: 11: 1, *Picochlorum sp.* of 55: 9: 1 and *Nannochloropsis granulata* of 66 : 10 : 1 (Table 4. 10).

Under nutrient limited conditions, the carbon to non limiting nutrient ratio (C: N or C: P) is within the range that was estimated under similar nutrient saturated conditions (Table 4. 9), with two exceptions, the phosphorus limited *Picochlorum sp.* and the nitrogen limited *Nannchloropsis granulata,* which have significantly lower ($p < 0.05$) ratios of the non-limiting nutrient.

Under nitrogen limited conditions N: C ratio decreases significantly in *Micromonas pusilla* by 20.4% ($p = 0.024$), in *Picochlorum sp.* by 15.5% ($p = 0.014$), and in *Nannochloropsis granulata* by 42.1% ($p = 0.009$). It increases by 9.9 % in *Prochlorococcus sp.*($p = 0.197$).

Under phosphorus limited conditions P:C ratio is reduced significantly in the two picoeukaryotes, in *Picochlorum sp.* by 65.2% ($p = 0.009$) and in *Nannochloropsis granulata* ($p = 0.009$) by 48.5%. It is reduced, though not significantly, by 31.2% in *Prochlorococcus sp.* ($p = 0.127$) and in *Micromonas pusilla* by 37.2 % ($p = 0.133$).

Prochlorococcus sp. accumulates most nitrogen and phosphorus per unit carbon of all the four investigated species under limited conditions of the specific nutrient, though its dilution rate was highest and nitrogen was not completely used up in the nitrogen limited chemostat (Figure 4. 7).

Table 4. 9 Mean carbon to nitrogen and carbon to phosphorus ratios in mol per mol within cells of different species investigated under nitrogen and phosphorus limitation and under similar nutrient saturated conditions

	Nitrogen limitation				Phosphorus limitation				Nutrient saturation at 19-22°C and 120 - 330 µmol photons m^{-2} s^{-1}			
	C:N [mol mol^{-1}]		C:P [mol mol^{-1}]		C:N [mol mol^{-1}]		C:P [mol mol^{-1}]		C:N [mol mol^{-1}]		C:P [mol mol^{-1}]	
Prochlorococcus sp. (HL)	5.7	(0.5)	68	(36)	7.2*		93*		6.4	(1.1)	67	(15)
Micromonas pusilla	7.4	(0.4)	78	(15)	6.1	(0.2)	98	(10)	6.1	(1.2)	68	(23)
Picochlorum sp.	6.8	(0.2)	74	(14)	7	(0.4)	130	(15)	5.8	(0.4)	55	(20)
Nannochloropsis granulata	11.9	(2.4)	103	(4)	7	(1.6)	137	(57)	6.7	(0.4)	66	(15)

Table 4. 10 Cell stoichiometry as a mean from nitrogen and phosphorus limitation experiments, standard deviation in brackets

Species	Nitrogen limitation	Phosphorus limitation	Nutrient saturation at 19- 22°C and 120 - 330 µmol photons m^{-2} s^{-1}
	C : N : P	C : N : P	C : N : P
Prochlorococcus sp. (HL)	68 (36) : 12 (7) : 1	93 : 13 : 1*	67 (15) : 10 (2): 1
Micromonas pusilla	78 (15) : 10 (2) : 1	98 (10) : 16 (1) : 1	68 (23) : 11 (4) : 1
Picochlorum sp.	74 (14) : 11 (2) : 1	130 (15) : 19 (3) : 1	55 (20) : 9 (3) : 1
Nannochloropsis granulata	103 (4) : 9 (2) : 1	137 (57) : 19 (6) : 1	66 (15) : 10 (2) : 1

* only one measurement

In the nitrogen limitation experiments C: N ranged between 5.7 in cells of *Prochlorococcus sp*. and 11.4 in *Nannochloropsis granulata*. *Micromonas pusilla* and *Picochlorum sp.* have values of 6.8 and 7.4. The general range of the four species under nutrient saturated conditions lies between 6.1 and 6.7 (Table 4. 9).

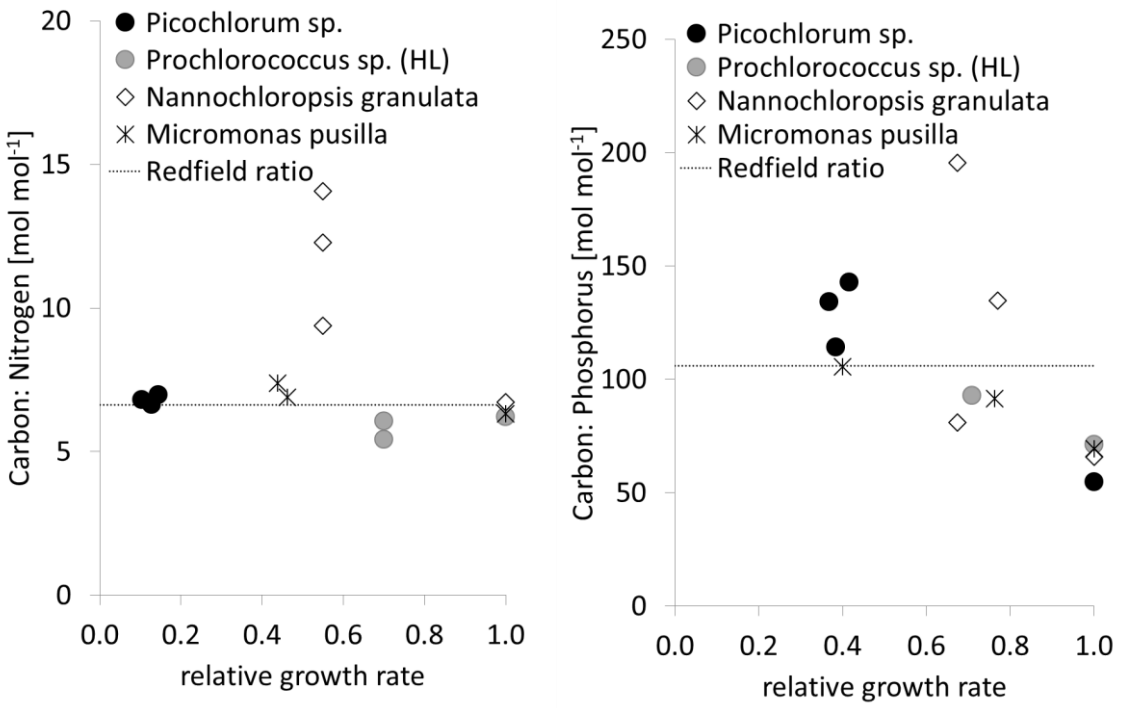

Figure 4. 5 C:N and C:P ratio as a function of relative growth rate. Grey circles: Prochlorococcus sp., crosses: Micromonas pusilla, black circles: Picochlorum sp., diamonds: Nannochloropsis granulata, dotted line: Redfield ratio

The carbon : nitrogen ratio stays constant regardless of nitrogen limitation and close to the Redfield ratio in 3 species (Figure 4.5). Only cells of *Nannochloropsis granulata* show a highly increased carbon: nitrogen ratio as a consequence of nitrogen limitation.

Even though they have the highest nitrogen quotas, their cells are not able to reach the same nitrogen levels relative to carbon as the other species. Under phosphorus limitation C: P ratios in turn are increased relative to nutrient saturated conditions (Figure 4. 5).

The same N: P range was found under nitrogen limitation as under nutrient saturated conditions, but is visibly higher under phosphorus limitation (Table 4. 10). It also exceeds the Redfield ratio in *Picochlorum sp.* and *Nannochloropsis granulata*.

4.4.2.3. Chlorophyll a : carbon ratios

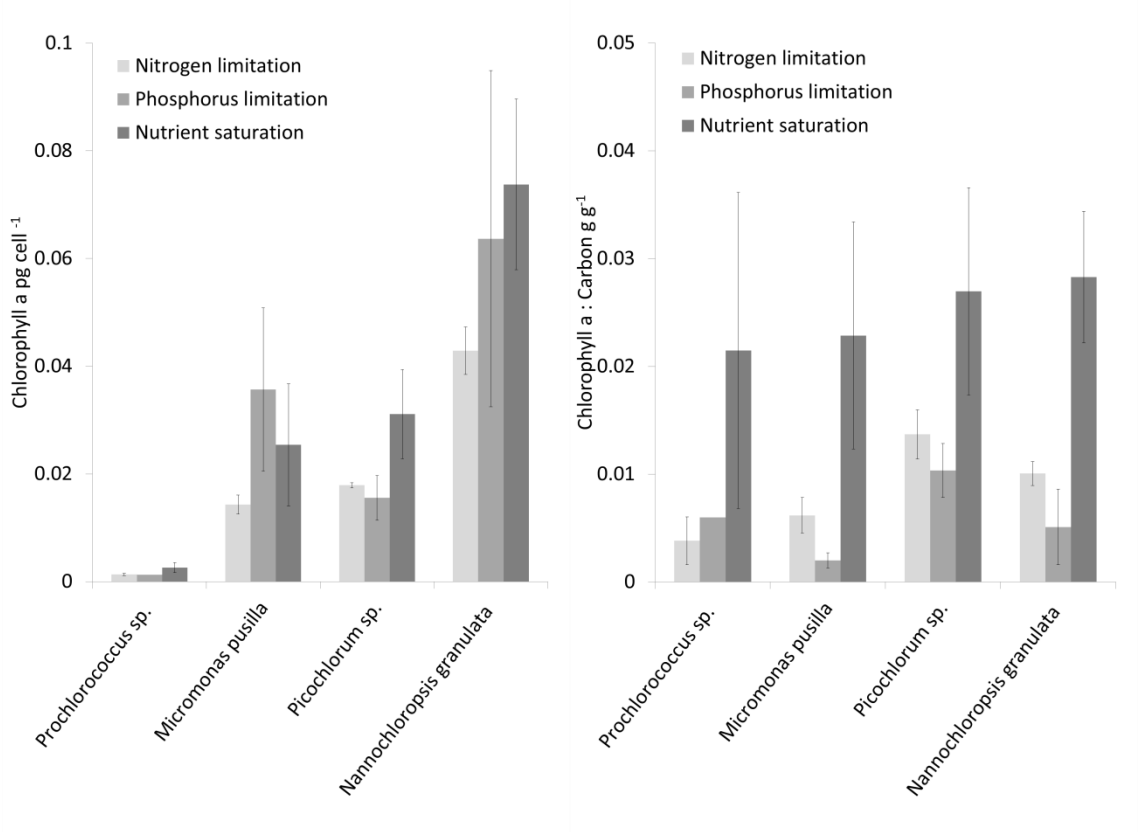

Figure 4. 6 Chlorophyll quota [pg cell^{-1}] (left) and Chlorophyll a to carbon ratios [g Chlorophyll a g^{-1} C] (right) under nitrogen (light grey), phosphorus (middle grey) limitation and nutrient saturation (dark grey), whiskers indicate standard deviation

Chlorophyll *a* quota range between 1.3 and 1.5 fmol cell^{-1} in *Prochlorococcus sp.* and 11.4 and 94.9 fmol cell^{-1} in picoeukaryotes (Figure 4. 6). The variability is higher between species than between experiments.

The Chlorophyll *a* : carbon ratio is significantly lower in all picoeukaryotes under both limitations compared to nutrient saturated conditions. It decreases in all species by 50 - 82% under nitrogen limitation and by 62 - 91% under phosphorus limitation. The mean values vary between 0.002 and 0.014g Chl *a* g^{-1} C.

Chlorophyll *a* to carbon ratios are higher under nitrogen limitation in the picoeukaryotic cells and lower in *Prochlorococcus sp.*. However data for this species was limited. The two bigger picoeukaryotes have higher values than the picoprokaryote, consistent with the results at saturated conditions at the same light level (Figure 4. 6).

4.4.2.4. Inorganic nutrient concentrations

Nitrogen was only < 0.5 µmol L^{-1} in nitrogen limitation experiments for the picoeukaryotes (Figure 4. 7, Table 4. 11), while the concentration remained higher in the *Prochlorococcus sp.* culture (10 - 80 µmol L^{-1}). In comparison, measured levels at the end of the phosphorus limitation experiments were 784 ± 95 µmol NH_4^+ L^{-1}. This is a higher concentration than was added to the initial medium. As the initial concentration in the medium was not measured, this relatively high difference is most likely attributable to the nitrogen concentration of the stock solution which was used. Additional N-sources from the other ESAW components and/or the experimental equipment cannot be excluded but their contribution would be lower. Final phosphorus concentrations were 10 ± 5.6 µmol L^{-1} under phosphorus limitation and 42.1 ± 5.4 under nitrogen limitation (Figure 4. 7). Both values are higher than the initial concentration, which may have also been caused by methodological complications in the analytical determination of dissolved phosphorus or from contaminations after sampling from experimental equipment, during sampling procedure or from the centrifuge tubes in which they were stored until analysis. Only the filtrate of the phosphorus limited *Picochlorum sp.* contained less than half of the initial concentration of phosphorus.

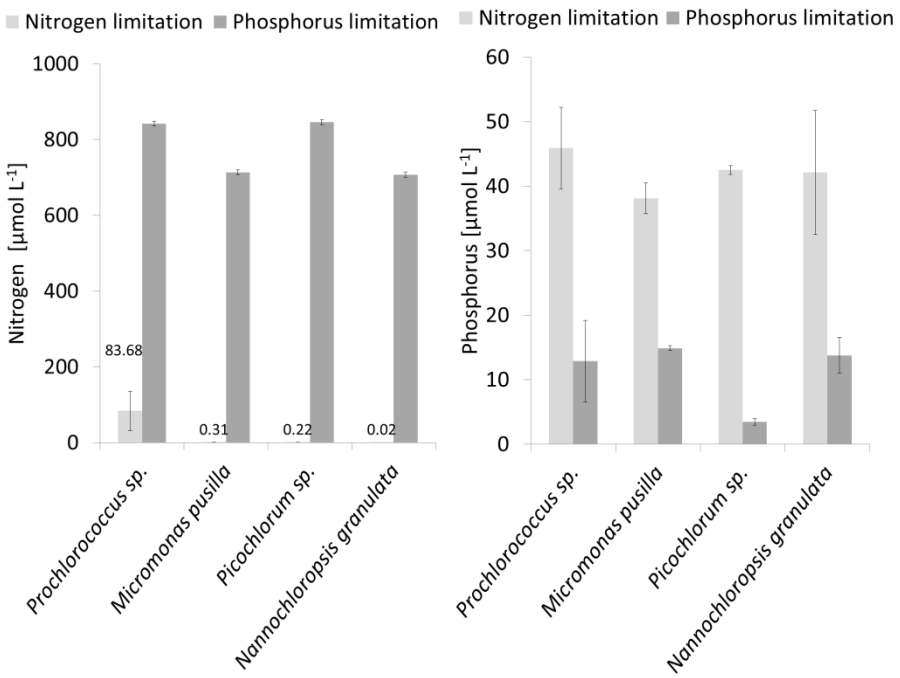

Figure 4. 7 Remaining nutrient concentrations (left: Nitrogen, right: Phosphorus) in chemostat experiments under nitrogen (light grey) and phosphorus (dark grey) limitation, whiskers indicate standard deviation

Half-saturation constants for growth ($K_{1/2}$) are shown in Table 4. 11. *Prochlorococcus sp*. has the highest $K_{1/2}$ for nitrogen with 13.97 ± 15.74 µmol L^{-1}, *Picochlorum sp.* has a lower $K_{1/2}$ of 0.19 ± 0.23 µmol L^{-1}, *Micromonas pusilla* and *Nannochloropsis granulata* have the lowest $K_{1/2}$ of 0.07 ± 0.05 and 0.01 ± 0.02 µmol L^{-1}. The $K_{1/2}$ for phosphorus in *Picochlorum sp.* is 2.21 ± 0.25 µmol L-^{1}. For the group of picoeukaryotes a $K_{1/2}$ of 0.09 ± 0.15 µmol NH_4 L^{-1} is estimated.

Unfortunately, methodological complications with dilutions of the higher concentrated filtrates lead to higher measured contents of both nutrients than were added to the initial medium. Hence, $K_{1/2}$ for phosphorus needs to be treated with caution.

Table 4. 11 Ammonium and phosphate concentrations and half saturation constants ($K_{1/2}$) in nitrogen and phosphorus limitation experiments

	Nitrogen limitation		Phosphorus limitation	
	NH_4 concentration [µmol L^{-1}]	$K_{1/2}$ [µmol L-1]	Phosphate concentration [µmol L-1]	$K_{1/2}$ [µmol L-1]
Prochlorococcus sp. (HL)	46. 6 ± 52.5	13.97 ± 15.74	-	-
Micromonas pusilla	0.12 ± 0.09	0.07 ± 0.05	-	-
Picochlorum sp.	0.22 ± 0.26	0.19 ± 0.23	3.63 ± 0.5	2.21 ± 0.25
Nannochloropsis granulata	0.02 ± 0.04	0.01 ± 0.02	-	-

4.5. Discussion

4.5.1. Cellular carbon quotas

The elemental stoichiometry is usually compared on the basis of carbon quota of the cell. Buitenhuis et al. (2012) give a summary of measurements of carbon quota of picophytoplankton in the literature. The quotas increase with cell size in agreement with our results and range between 0.016 and 0.092 pg C $cell^{-1}$ for *Prochlorococcus sp*., 0.112 and 0.6 in *Synechococcus sp.* and between 0.53 and 3.8 pg C $cell^{-1}$ for picoeukaryotes.
Our mean estimates under nutrient saturated conditions are slightly higher for *Prochlorococcus sp.*. However, some studies calculated carbon quota from different variables, while our direct measurements contain data from a broad set of environmental conditions and the average standard deviation in triplicate samples of 14.1%.
The mean carbon quota of *Synechococcus sp.* in this study agrees well with the literature. The maximum size of picophytoplankton is not clearly defined and varies between 2 and 3 µm, depending on the study. The carbon quota in the smaller picoeukaryotes up to a size of 2 µm agrees with the carbon quota summarized by Buitenhuis et al. (2012). However, the two bigger species exceed those measurements. It shows that it needs to be taken into account that picoeukaryotes are a very diverse group, so differences in species composition or sizes can cause a higher variability.

4.5.2. Trends in nutrient stoichiometry related to light and temperature

Nitrogen is a substantial component of the pigment protein complex, which is used for light acquisition, while phosphorus is required for RNA and phospholipid synthesis and consequently important for growth (Davey et al. 2008). In the light experiments C: N ratio increased with increasing light level. Cells acclimated to low light conditions show high levels of nitrogen relative to carbon as a consequence of accumulation of nitrogen rich light harvesting components. Also, carbon rich energy storage reserves are built up at saturating light levels and used up under light limited conditions (Geider et al. 1998).
This trend also results in a high N: P ratio in picoprokaryotes in low light environments. With increasing light intensity, pigments are reduced and more phosphorus is required with increasing growth rate for cell division.

In contrast, picoeukaryotes do not show this trend. Three species in this study even increased the level of nitrogen and also carbon relative to phosphorus up to an intermediate light intensity of 330 µmol photons m^2 s^{-1}. A possible explanation is the excess uptake of nitrogen in picoeukaryotes at higher light intensities as a consequence of an increased growth rate and higher flexibility of cells which allows them to store more nutrients than required. This enhanced uptake also results in an increasing fraction of nutrient acquisition components within the cell, which are rich in nitrogen in relation to phosphorus. In turn, picoprokaryotes have a higher efficiency for nutrient uptake because of their smaller size which is reflected in a lower nitrogen demand of their nutrient acquisition machinery.

The decreasing carbon to nitrogen ratio with temperature is a result of a higher nitrogen demand due to an increasing maximum growth rate with temperature. Toseland et al. (2013) predicted that N: P ratios would increase with increasing temperature in eukaryotic phytoplankton based on transcriptomic analysis, because of an enhanced, but more efficient protein synthesis that requires fewer phosphorus rich ribosomes. Here we confirm this trend with direct stoichiometry observations, as far as we're aware for the first time, in the two picoeukaryotes which grew over the widest temperature range and in the entire eukaryotic community. The positive correlation between N: P ratio and growth rate also seemed to hold above the optimum temperature, with a small but not significant drop at the highest temperatures.

4.5.3. Carbon specific nutrient quotas

Veldhuis et al. (2005) reviewed available information on cell composition of picoprokaryotes and summarized C: N ratios between 4.5 and 10. They estimated a mean value of 6.5 ± 1.3, close to the Redfield ratio. A similar range was found in our study. While values in the light experiments are slightly lower , the mean estimate for both groups in the temperature experimentis very close to the value calculated from that review. Two picoeukaryotes were investigated by Timmermans et al. (2005) with C: N ratios of 2.5 and 16.1under nutrient replete conditions. The investigated species within this study fall within the range of their values.

N: P ratios, in the same review were found between 10 and 24.6 under nutrient saturated conditions. It included only one study by Bertilsson et al. (2003), that reported a ratio of

33.5 or even 71 - 110 under phosphorus limitation. In our experiments picoprokaryotes have similar mean N: P values but a broader range (Table 4. 5 and Table 4. 6) . Picoeukaryotes have lower mean N: P ratios but decreased phosphorus quota under phosphorus limited conditions.

Veldhuis et al. (2005) also summarized C: P ratios for picoprokaryotes under nutrient saturation in the range of 64 and 166 in agreement with the mean ratios in this study (Table 4.7). Picoeukaryotes had lower values , and *Bolidomonas pacifica* reached a minimum of 23. Under phosphorus limitation the study by Bertilsson et al. (2003) found C: P to increase up to 787. *Nannochloropsis granulata* achieved the highest C: P ratio in our study under phosphorus limited condition (196), but was still far below this value. However, they calculated nutrient quotas from nutrient concentration, cell numbers and carbon quota as reported in the literature, but did not measure them directly. Another study by Heldal et al. (2003) also found higher C: N and C: P values but those were obtained by a different method, using X-ray microanalysis. It further needs to be mentioned that both studies only investigated the cell composition under specific light and temperature conditions, while we use a mean of their entire growth spectrum. Also, ecotype specific variability may contribute to differences between these studies.

Our results show that nutrient saturated picoprokaryotes and picoeukaryotes, both deviate significantly from the ratio of algal assemblages measured *in situ* by Redfield (1958), using more nitrogen and phosphorus relative to carbon. They achieve similar C: N ratios under nutrient saturated conditions. The smaller group has lower phosphorus requirements which can be attributed to the substitution of phospholipids for sulfolipids (Van Mooy et al. 2006). Also, the higher nitrogen demand of the phycobilisomes (Raven 1984) is reflected in a significantly higher N: P ratio in picoprokaryotes especially under low light.

4.5.4. Conditions of nutrient limitation compared to nutrient saturation

Timmermans et al. (2005) compared nutrient to carbon ratios of *Synechococcus sp.* and the two bigger picoeukaryotes up to 4 µm under both nutrient saturated and limited conditions. Next to the above mentioned nutrient saturated C: N ratios they calculated

C: P ratios in the range of 67 – 250 under nutrient saturated conditions and lower C: N ratios of 6.3 – 28.6 and C: P ratios of 156 – 556 under nutrient limitation.

Similar values were found for picoeukaryotes in the nitrogen limitation experiments but for phosphorus limitation only *Nannochloropsis granulata* falls into the range of previous estimates suggesting that the phosphorus limitation in this study was not as strong as in the study by Timmermans et al. (2005). However, their estimates are only based on 2 species.

We find evidence that picoeukaryotes decrease nitrogen under nitrogen limitation by 15 - 42% and phosphorus under phosphorus limitation by 37 - 65% relative to carbon which can also be defined as the amount of luxury uptake under saturated conditions. The highest reduction of nitrogen is found in *Nannochloropsis granulata* while it remains close to the Redfield ratio in the other species. *Prochlorococcus sp.* is not visibly affected by N limitation, which was probably caused by the high dilution rate and is reflected in a substantially higher half saturation constant for nitrogen compared to the three picoeukaryotes and the literature.

Timmermans et al. (2005) found half-saturation constants for ammonium between 0.68 and 5.29 µmol L^{-1} in picophytoplankton. Values for half saturation for ammonium in *Micromonas pusilla* were reported between 0.176 and 0.630 µmol L^{-1} (Cochlan & Harrison 1991). The values for the picoeukaryotes, obtained in this study are lower or similar in range.

The reduction in phosphorus quota indicates that phosphorus was limited in the experiments and that the analytical procedure caused difficulties in the calculation of the remaining phosphorus in the culture filtrates. Phosphorus limitation has an influence on all measured species with the strongest increase in C: P in *Picochlorum sp.*.

Half saturation constants for phosphorus in picophytoplankton were previously estimated between 0.0003 and 0.79 µmol L^{-1} (Timmermans et al. 2005).The $K_{1/2}$ for phosphorus in *Picochlorum sp.* is substantially higher in this study, which may be a consequence of the analytical problems in the determination of phosphorus in the medium.

4.5.5. Chlorophyll *a* : carbon

At low light levels the chlorophyll *a* to carbon ratio increases (Geider 1987) and requires more nitrogen for chlorophyll *a* synthesis. In turn, low temperatures or nutrient limited

conditions cause a decline in chlorophyll *a* quota due to chlorosis, but was also suggested to be linked to the increase in lipids to maintain membrane fluidity (Geider et al. 1998).
The clorophyll *a* : carbon ratio is significantly lower under both nitrogen (-50 − -82%) and phosphorus (-62 − -91%) limitation compared to saturated conditions. The decreased availability of nitrogen, limits its synthesis. However, it was previously shown that addition of phosphorus under limited conditions would further stimulate the synthesis of chlorophyll a per cell (Davey et al. 2008).

4.6. Conclusion

We investigated the changes in elemental stoichiometry in picophytoplankton cells under a broad range of environmental conditions to estimate the variability and full range of C: N: P ratios under given conditions. We further used their optimum light and temperature conditions to conduct nitrogen and phosphorus limitation experiments to estimate the reduction of the limiting nutrient within the cells and their half saturation constants. We show that picoprokaryotes and picoeukaryotes have similar mean C: N (5.9 ± 0.5 and 6.2 ± 1.1) but significantly different N: P ratios (13.4 ± 4.1 and 9.6 ± 3.3) under nutrient saturated conditions, which reflects the lower phosphorus demand of picoprokaryotes.
C: N increases within the groups with increasing light intensity and decreasing temperature but this trend is not significant in picoprokaryotes as their temperature tolerance range is restricted. Also, N: P increases with increasing temperature in picoeukaryotes. These changes are consistent with previously suggested physiological changes in the concentration of nitrogen rich light and nutrient acquisition components, and phosphorus rich ribosomes for protein synthesis. In addition, the substitution of phospholipids in the group of picoprokaryotes is influential.
In general, under nutrient saturated conditions, nitrogen and phosphorus are taken up in excess, causing a significant deviation from the Redfield ratio (79: 13: 1 in picoprokaryotes and 60: 10: 1 in picoeukaryotes). Nitrogen limitation leads to an increase in C: N in all three picoeukaryotes, and a decrease in N: P in *Micromonas pusilla* and *Nannochloropsis granulata*. Phosphorus limitation is reflected in increased N: P ratios, close to the Redfield ratio, compared to nutrient replete conditions, which is significant for picoeukaryotes. We show that nitrogen levels in picoeukaryotes decrease by 15 − 42%

and phosphorus by 37 − 65% under nutrient limitation compared to nutrient saturated conditions.

The Chlorophyll *a*: carbon ratio is significantly lower under both nitrogen (-50 − -82%) and phosphorus (-62 − -91%) limitations compared to saturated conditions due to a lower availability of nitrogen and lower synthesis rates when phosphorus is limited.

Two of the half-saturation constants for nitrogen found in this study agree with previous estimates. It is substantially lower for *Nannochloropsis granulata*, but a lot higher for *Prochlorococcus sp*., which suggests that it was not nitrogen limited under the given conditions.

Our findings contribute to the understanding of the variability in C: N: P ratios in different picophytoplankton species, their nutrient requirements and give an idea about excess nutrient uptake under nutrient saturated conditions. The high species specific variability and significant differences between picoprokaryotes and picoeukaryotes highlight the requirement for further studies, which investigate the elemental composition and species specific changes under nutrient limited conditions, with special focus on the latter group.

4.7. Appendix

Table 4. 12 Carbon quota [pg C cell^{-1}] under nutrient saturated conditions at different acclimation light intensities

Species	size	Acclimation light intensity [µmol photons m^{-2} s^{-1}]									
	µm	720	500	300	147	120	64	32	27	13	10
Prochlorococcus (HL)	0.6	0.15*	-	0.14 ± 0.04	-	0.07*	0.06 ± 0.02	-	0.08 ± 0.01	0.21 ± 0.12	-
Prochlorococcus (LL)	0.6	-	-	-	0.12 ± 0.04	0.10 ± 0.04	0.12 ± 0.05	0.16 ± 0.06	0.11 ± 0.07	-	0.24 ± 0.04
Synechococcus	1	-	0.81 ± 0.21	0.30 ± 0.05	-	0.37 ± 0.23	0.21 ± 0.07	-	0.26 ± 0.09	-	-
Bolidomonas pacifica	1.2	2.92 ± 1.03	1.83 ± 0.22	2.05 ± 0.59	-	1.98 ± 0.27	1.75 ± 0.88	-	-	-	-
Micromonas pusilla	1.5	1.12 ± 0.18	-	0.98 ± 0.10	-	1.28 ± 0.39	0.86 ± 0.09	-	0.84 ± 0.07	-	-
Picochlorum sp.	2	0.85 ± 0.26	1.21 ± 0.31	0.78 ± 0.22	-	1.07 ± 0.17	0.90 ± 0.30	-	1.98 ± 0.54	3.49 ± 1.22	-
Nannochloropsis granulata	2	2.91 ± 0.63	2.59 ± 0.69	2.29 ± 0.13	-	2.29 ± 0.11	2.83 ± 0.16	-	3.89 ± 1.72	3.22 ± 0.93	-

Table 4. 13 Nitrogen quota [pg C cell^{-1}] under nutrient saturated conditions at different acclimation light intensities

Species	size	Acclimation light intensity [µmol photons m^{-2} s^{-1}]									
	µm	720	500	300	147	120	64	32	27	13	10
Prochlorococcus (HL)	0.6	0.029*	-	0.028 ± 0.007	-	0.014*	0.013 ± 0.004	-	0.019 ± 0.004	0.047 ± 0.024	-
Prochlorococcus (LL)	0.6	-	-	-	0.025 ± 0.009	0.021 ± 0.009	0.026 ± 0.011	0.032 ± 0.011	0.019 ± 0.006	-	0.042 ± 0.003
Synechococcus	1	-	0.142 ± 0.037	0.054 ± 0.01	-	0.073 ± 0.044	0.045 ± 0.015	-	0.057 ± 0.023	-	-
Bolidomonas pacifica	1.2	0.646 ± 0.207	0.45 ± 0.063	0.423 ± 0.191	-	0.461 ± 0.094	0.201 ± 0.124	-	-	-	-
Micromonas pusilla	1.5	0.233 ± 0.038	-	0.196 ± 0.032	-	0.291 ± 0.048	0.254 ± 0.019		0.247 ± 0.038	-	-
Picochlorum sp.	2	0.141 ± 0.033	0.236 ± 0.091	0.168 ± 0.054	-	0.221 ± 0.031	0.177 ± 0.056	-	0.4 ± 0.123	0.605 ± 0.207	-
Nannochloropsis granulata	2	0.443 ± 0.084	0.416 ± 0.099	0.38 ± 0.032	-	0.434 ± 0.005	0.545 ± 0.037	-	0.751 ± 0.308	0.607 ± 0.164	-

Table 4. 14 Phosphorus quota [pg C cell^{-1}] under nutrient saturated conditions at different acclimation light intensities

Species	size	Acclimation light intensity [µmol photons m^{-2} s^{-1}]									
	µm	720	500	300	147	120	64	32	27	13	10
Prochlorococcus (HL)	0.6	0.008*	-	0.006 ± 0.003	-	0.003*	0.003 ± 0.002	-	0.007 ± 0.006	0.006 ± 0.003	-
Prochlorococcus (LL)	0.6	-	-	-	0.008 ± 0.007	0.006 ± 0.003	0.004 ± 0.002	0.007 ± 0.003	0.003 ± 0.002	-	0.008 ± 0.005
Synechococcus	1	-	0.029 ± 0.002	0.009 ± 0.001	-	0.014 ± 0.007	0.007 ± 0.003	-	0.007 ± 0.004	-	-
Bolidomonas pacifica	1.2	0.201 ± 0.092	0.286 ± 0.246	0.133 ± 0.028	-	0.187 ± 0.015	0.173 ± 0.103	-	-	-	-
Micromonas pusilla	1.5	0.055 ± 0.016	-	0.035 ± 0.014	-	0.065 ± 0.019	0.064 ± 0.002	-	0.045 ± 0.016	-	-
Picochlorum sp.	2	0.047 ± 0.008	0.071 ± 0.026	0.061 ± 0.027	-	0.086 ± 0.006	0.065 ±0.024	-	0.171 ± 0.077	0.214 ± 0.025	-
Nannochloropsis granulata	2	0.124 ± 0.047	0.114 ± 0.027	0.087 ± 0.005	-	0.134 ± 0.024	0.208 ± 0.046	-	0.275 ± 0.06	0.254 ± 0.08	-

Table 4. 15 Chlorophyll a quota [pg C cell^{-1}] under nutrient saturated conditions at different acclimation light intensities

Species	size	Acclimation light intensity [µmol photons m^{-2} s^{-1}]									
	µm	720	500	300	147	120	64	32	27	13	10
Prochlorococcus (HL)	0.6	0.002*	-	0.002 ± 0.00	-	0.003 ± 0.001	0.003 ± 0.00	-	0.005 ± 0.00	0.013 ± 0.01	-
Prochlorococcus (LL)	0.6	-	-	-	0.003 ± 0.001	0.003 ± 0.001	0.003 ± 0.001	0.005 ± 0.003	0.003 ± 0.002	-	0.006 ± 0.004
Synechococcus	1	-	0.009 ± 0.003	0.003 ± 0.001	-	0.007 ± 0.004	0.004 ± 0.001	-	0.007 ± 0.002	-	-
Bolidomonas pacifica	1.2	0.029 ± 0.009	0.042 ± 0.023	0.031 ± 0.01	-	0.044 ± 0.01	0.038 ± 0.01	-	-	-	-
Micromonas pusilla	1.5	0.018 ± 0.003	-	0.023 ± 0.002	-	0.04 ± 0.005	0.045 ± 003	-	0.044 ± 0.01	-	-
Picochlorum sp.	2	0.014 ± 0.003	0.025 ± 0.013	0.024 ± 0.005	-	0.041 ± 0.003	0.041 ± 0.01	-	0.077 ± 0.01	0.101 ± 0.019	-
Nannochloropsis granulata	2	0.045 ± 0.011	0.043 ± 0.011	0.05 ± 0.003	-	0.084 ± 0.004	0.129 ± 0.005	-	0.208 ± 0.045	0.128 ± 0.037	-

* only one measurement

Table 4. 16 Carbon quota [pg C cell^{-1}] under nutrient saturated conditions at different acclimation temperatures

Temparature	*Prochlorococcus (HL)*	*Prochlorococcus (LL)*	*Synechococcus*	*Bolidomonas pacifica*	*Micromonas pusilla*	*Picochlorum sp.*	*Nannochloropsis granulata*	*Imantonia rotunda*	*Phaomonas sp.*
8.1	-	-	-	-	1.09	-	4.62	-	-
10.9	-	-	-	-	1.03 ± 0.37	1.13 ± 0.06	3.49 ± 0.91	-	-
12.3	-	-	-	-	-	-	-	-	6.22
13.7	-	-	0.846	-	1.02 ± 0.35	1.57 ± 0.4	3.04 ± 0.62	-	-
14.9	-	-	-	-	-	-	-	8.4	6.69 ± 2.28
16.3	-	-	1.08 ± 1.02	2.16 ± 0.89	1.11 ± 0.43	1.83 ± 0.19	3.37 ± 0.6	-	-
17.5	-	0.071 ± 0.022	-	-	-	-	-	5.39 ± 0.74	4.9 ± 0.91
19	0.069	-	0.453 ± 0.127	1.85 ± 0.71	1.22 ± 0.52	1.53 ± 0.24	3.15 ± 0.21	-	-
20	-	0.093 ± 0.022	-	-	-	-	-	7.18 ± 3.91	5.14 ± 0.83
21.7	0.067	-	0.343 ± 0.923	1.99 ± 0.68	0.965	1.62 ± 0.1	2.79 ± 0.14	-	-
22.6	-	0.221 ± 0.055	-	-	-	-	-	5.89 ± 0.56	2.5 ± 0.73
24.4	0.103 ± 0.005	-	0.947 ± 0.117	2.33 ± 1.45	-	1.46 ± 0.13	2.58 ± 0.35	-	-
25.3	-	-	-	-	-	-	-	6.55	3.24 ± 0.7
27	-	-	1.57 ± 0.77	-	-	1.14 ± 0.15	2.19 ± 0.08	-	-
29.8	-	-	-	-	-	1.24 ± 0.14	2.24 ± 0.22	-	-
32.4	-	-	-	-	-	1.41 ± 0.1	-	-	-

Table 4. 17 Nitrogen quota [pg Ncell^{-1}] under nutrient saturated conditions at different acclimation temperatures

Temparature	*Prochlorococcus (HL)*	*Prochlorococcus (LL)*	*Synechococcus*	*Bolidomonas pacifica*	*Micromonas pusilla*	*Picochlorum sp.*	*Nannochloropsis granulata*	*Imantonia rotunda*	*Phaomonas sp.*
8.1	-	-	-	-	0.198	-	0.593	-	-
10.9	-	-	-	-	0.157 ± 0.04	0.239 ± 0.002	0.463 ± 0.091	-	-
12.3	-	-	-	-	-	-	-	-	1.26
13.7	-	-	0.153	-	0.15 ± 0.057	0.273 ± 0.037	0.441 ± 0.079	-	-
14.9	-	-	-	-	-	-	-	1.87	1.21 ± 0.32
16.3	-	-	0.229 ± 0.161	0.494 ± 0.185	0.163 ± 0.06	0.341 ± 0.037	0.541 ± 0.113	-	-
17.5	-	0.014 ± 0.005	-	-	-	-	-	1.13 ± 0.26	0.87 ± 0.12
19	0.012	-	0.079 ± 0.024	0.412 ± 0.19	0.194 ± 0.045	0.295 ± 0.02	0.527 ± 0.04	-	-
20	-	0.018 ± 0.005	-	-	-	-	-	1.43 ± 0.82	0.932 ± 0.124
21.7	0.012	-	0.064 ± 0.163	0.417 ± 0.156	0.168	0.319 ± 0.023	0.48 ± 0.021	-	-
22.6	-	0.042 ± 0.011	-	-	-	-	-	1.12 ± 0.12	0.522 ± 0.116
24.4	0.018 ± 0.001	-	0.18 ± 0.028	0.456 ± 0.236	-	0.292 ± 0.03	0.427 ± 0.064	-	
25.3	-	-	-	-	-	-	-	1.380	0.669 ± 0.104
27	-	-	0.317 ± 0.132	-	-	0.233 ± 0.028	0.374 ± 0.02	-	-
29.8	-	-	-	-	-	0.254 ± 0.031	0.349 ± 0.035	-	-
32.4	-	-	-	-	-	0.275 ± 0.022	-	-	-

Table 4. 18 Phosphorus quota [pg P cell^{-1}] under nutrient saturated conditions at different acclimation temperatures

Temparature	*Prochlorococcus (HL)*	*Prochlorococcus (LL)*	*Synechococcus*	*Bolidomonas pacifica*	*Micromonas pusilla*	*Picochlorum sp.*	*Nannochloropsis granulata*	*Imantonia rotunda*	*Phaomonas sp.*
8.1	-	-	-	-	0.035	-	0.106	-	-
10.9	-	-	-	-	0.054 ± 0.042	0.048 ± 0.004	0.103 ± 0.033	-	-
12.3	-	-	-	-	-	-	-	-	0.106
13.7	-	-	0.069	-	0.056 ± 0.02	0.061 ± 0.025	0.093 ± 0.016	-	-
14.9	-	-	-	-	-	-	-	0.280	0.258 ± 0.193
16.3	-	-	0.038 ± 0.033	0.093 ± 0.034	0.062 ± 0.05	0.07 ± 0.008	0.113 ± 0.025	-	-
17.5	-	0.002 ± 0.001	-	-	-	-	-	0.317 ± 0.128	0.174 ± 0.083
19	0.002	-	0.01 ± 0.003	0.062 ± 0.031	0.053 ± 0.027	0.053 ± 0.008	0.117 ± 0.029	-	-
20	-	0.002 ± 0	-	-	-	-	-	0.413 ± 0.243	0.209 ± 0.051
21.7	0.002	-	0.008 ± 0.025	0.079 ± 0.046	0.026	0.062 ± 0.013	0.092 ± 0.016	-	-
22.6	-	0.005 ± 0.004	-	-	-	-	-	0.338 ± 0.118	0.08 ± 0.037
24.4	0.004 ± 0.001		0.022 ± 0.008	0.091 ± 0.051	-	0.058 ± 0.006	0.073 ± 0.013	-	-
25.3	-	-	-	-	-	-	-	0.250	0.091 ± 0.022
27	-	-	0.037 ± 0.011	-	-	0.044 ± 0.002	0.063 ± 0.007	-	-
29.8	-	-	-	-	-	0.05 ± 0.008	0.072 ± 0.019	-	-
32.4	-	-	-	-	-	0.061 ± 0.021	-	-	-

Table 4. 19 Chlorophyll a quota [pg Chl a cell^{-1}] under nutrient saturated conditions at different acclimation temperatures

Temparature	*Prochlorococcus (HL)*	*Prochlorococcus (LL)*	*Synechococcus*	*Bolidomonas pacifica*	*Micromonas pusilla*	*Picochlorum sp.*	*Nannochloropsis granulata*	*Imantonia rotunda*	*Phaomonas sp.*
8.1	-	-	-	-	0.014	-	0.025	-	-
10.9	-	-	-	-	0.013 ± 0.005	0.006 ± 0.002	0.034 ± 0.003	-	-
12.3	-	-	-	-	-	-	-	-	0.097
13.7	-	-	0.008	-	0.011 ± 0.002	0.018 ± 0.008	0.047 ± 0.004	-	-
14.9	-	-	-	-	-	-	-	0.065	0.115 ± 0.022
16.3	-	-	0.011 ± 0.011	0.027 ± 0.003	0.016 ± 0.007	0.027 ± 0.001	0.061 ± 0.005	-	-
17.5	-	0.003 ± 0	-	-	-	-	-	0.081 ± 0.011	0.098 ± 0.017
19	0.002	-	0.007 ± 0.001	0.033 ± 0.007	0.017 ± 0.006	0.030 ± 0.004	0.081 ± 0.011	-	-
20	-	0.003 ± 0.001	-	-	-	-	-	0.085 ± 0.02	0.103 ± 0.008
21.7	0.002	-	0.005 ± 0.01	0.041 ± 0.01	0.014	0.029 ± 0.01	0.081 ± 0.008	-	-
22.6	-	0.004 ± 0.002	-	-	-	-	-	0.105 ± 0.018	0.06 ± 0.033
24.4	0.003 ± 0.001	-	0.016 ± 0.001	0.051 ± 0.01	-	0.037 ± 0.004	0.078 ± 0.017	-	-
25.3	-	-	-	-	-	-	-	0.061	0.079 ± 0.026
27	-	-	0.023 ± 0.011	-	-	0.038 ± 0.004	0.058 ± 0.011	-	-
29.8	-	-	-	-	-	0.036 ± 0.002	0.053 ± 0.011	-	-
32.4	-	-	-	-	-	0.042 ± 0.009	-	-	-

Table 4. 20 Species specific mean carbon, nitrogen and phosphorus quota from light (left) and temperature(right) experiments

Species	size [µm]	Carbon pg cell^{-1}	Nitrogen pg cell^{-1}	Phosphorus pg cell^{-1}
Prochlorococcus (HL)	0.6	0.125 ± 0.079	0.026 ± 0.034	0.005 ± 0.003
Prochlorococcus (LL)	0.6	0.144 ± 0.064	0.029 ± 0.012	0.005 ± 0.003
Synechococcus sp.	1	0.391 ± 0.257	0.074 ± 0.044	0.014 ± 0.009
Bolidomonas pacifica	1.2	2.217 ± 0.739	0.435 ± 0.198	0.196 ± 0.119
Micromonas pusilla	1.5	1.007 ± 0.243	0.245 ± 0.044	0.053 ± 0.017
Picochlorum sp.	2	1.469 ± 1.037	0.278 ± 0.181	0.102 ± 0.067
Nannochloropsis granulata	2	2.806 ± 0.768	0.499 ± 0.152	0.166 ± 0.078
Imantonia rotunda	2.5	-	-	-
Phaomonas sp.	3	-	-	-
Prokaryotes	0.6 - 1	0.204 ± 0.208	0.046 ± 0.035	0.009 ± 0.008
Eukaryotes	1.2 - 2	1.896 ± 1.035	0.367 ± 0.189	0.130 ± 0.093
All	0.6 - 2	1.209 ± 1.145	0.234 ± 0.215	0.082 ± 0.094

Species	size [µm]	Carbon pg cell^{-1}	Nitrogen pg cell^{-1}	Phosphorus pg cell^{-1}
Prochlorococcus (HL)	0.6	0.086 ± 0.021	0.015 ± 0.003	0.003 ± 0.001
Prochlorococcus (LL)	0.6	0.129 ± 0.077	0.025 ± 0.015	0.003 ± 0.003
Synechococcus sp.	1	0.646 ± 0.289	0.133 ± 0.073	0.028 ± 0.018
Bolidomonas pacifica	1.2	2.083 ± 0.858	0.445 ± 0.169	0.081 ± 0.037
Micromonas pusilla	1.5	1.086 ± 0.343	0.168 ± 0.44	0.053 ± 0.031
Picochlorum sp.	2	1.448 ± 0.275	0.282 ± 0.041	0.057 ± 0.013
Nannochloropsis granulata	2	2.925 ± 0.697	0.456 ± 0.088	0.091 ± 0.026
Imantonia rotunda	2.5	6.393 ± 2.05	1.299 ± 0.456	0.340 ± 0.144
Phaomonas sp.	3	4.6 ± 1.848	0.868 ± 0.295	0.159 ± 0.106
Prokaryotes	0.7 ± 0.2	0.555 ± 0.632	0.115 ± 0.126	0.017 ± 0.021
Eukaryotes	2 ± 0.7	2.836 ± 1.984	0.525 ± 0.393	0.113 ± 0.107
All	1.6 ± 0.8	2.352 ± 2.013	0.435 ± 0.391	0.093 ± 0.103

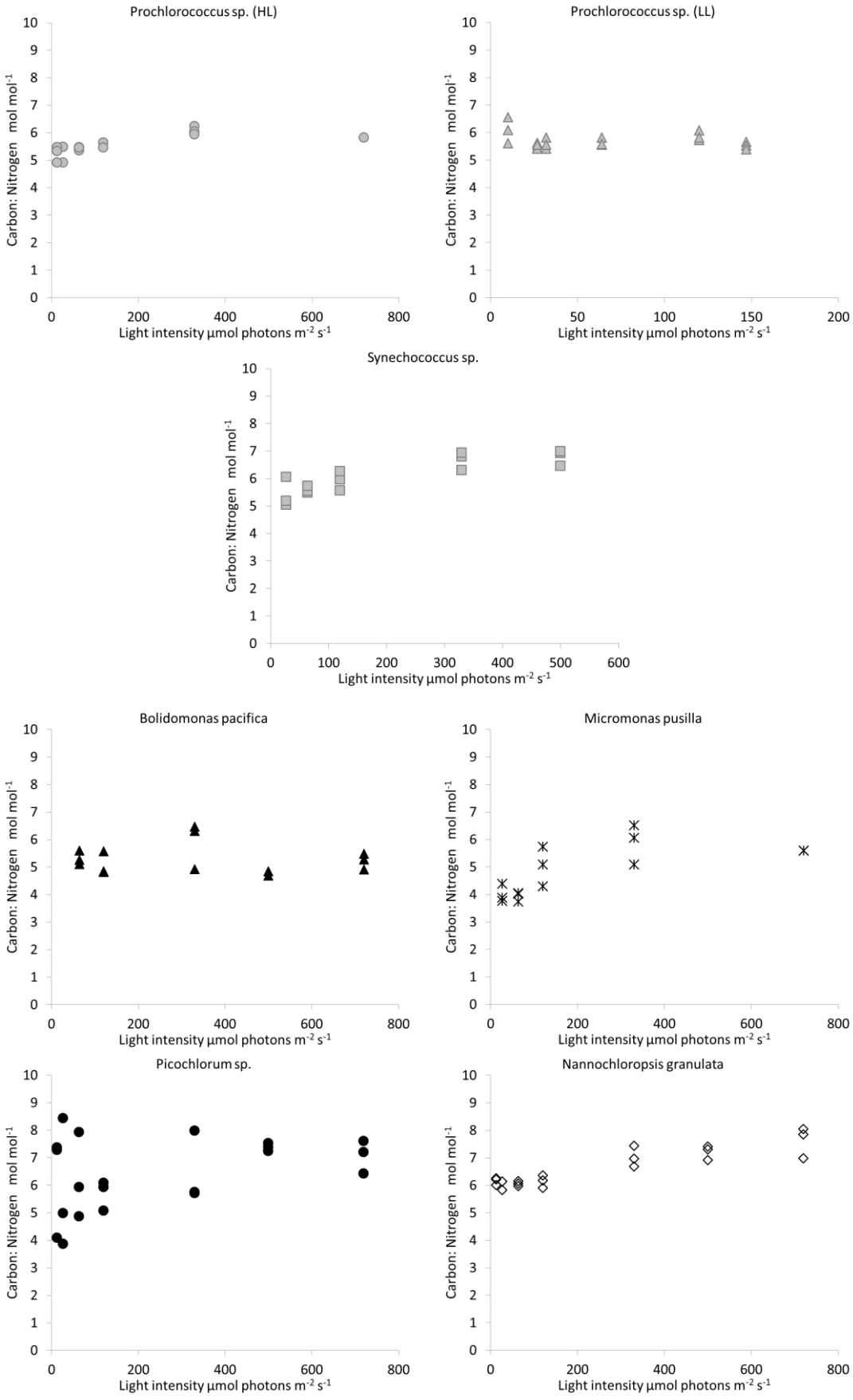

Figure 4. 8 Species specific carbon to nitrogen ratios [mol mol^{-1} cell^{-1}] depending on light intensity: top three: picoprokaryotes, below: picoeukaryotes

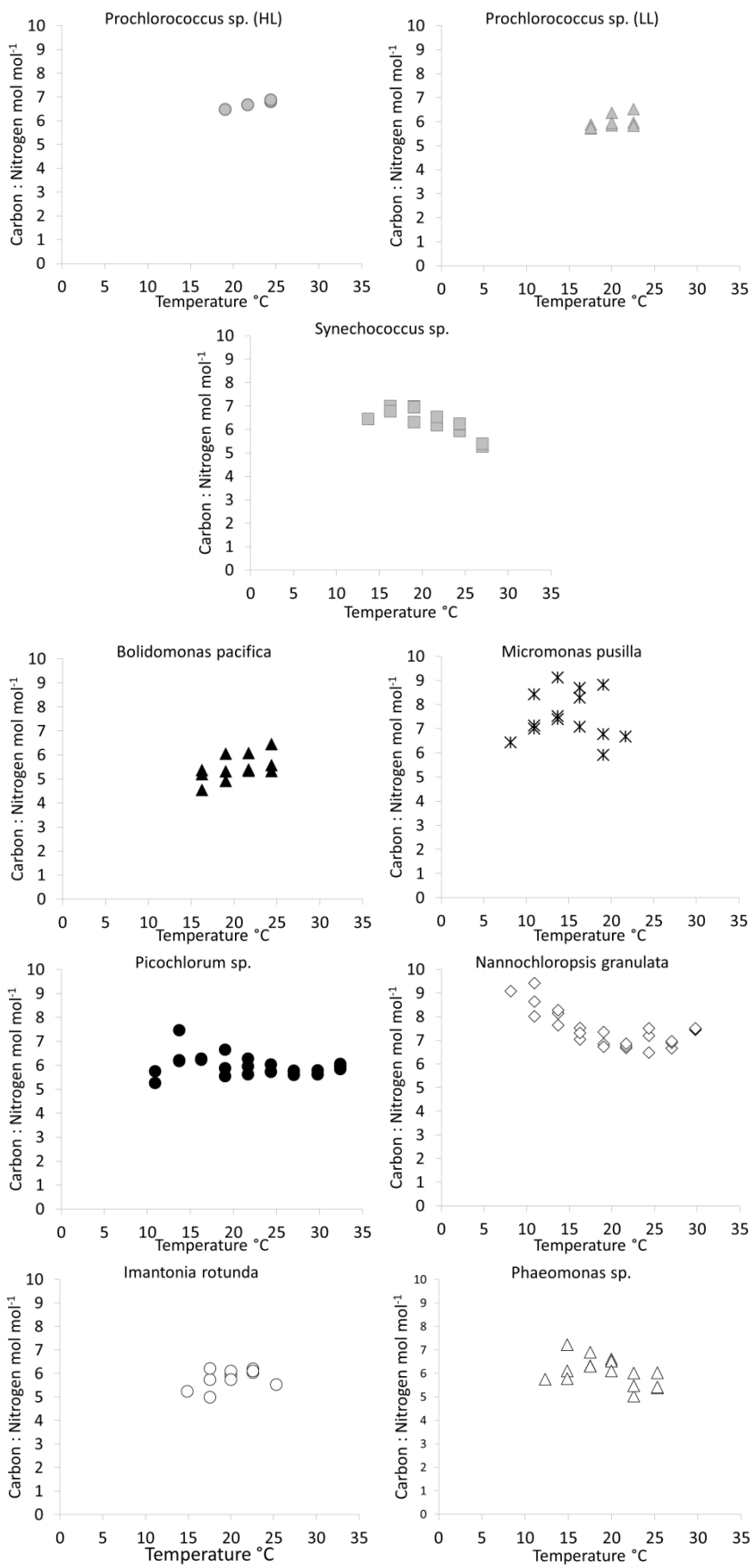

Figure 4. 9 Specific carbon to nitrogen ratios [mol mol^{-1}] depending on temperature: top three: picoprokaryotes, below: picoeukaryotes

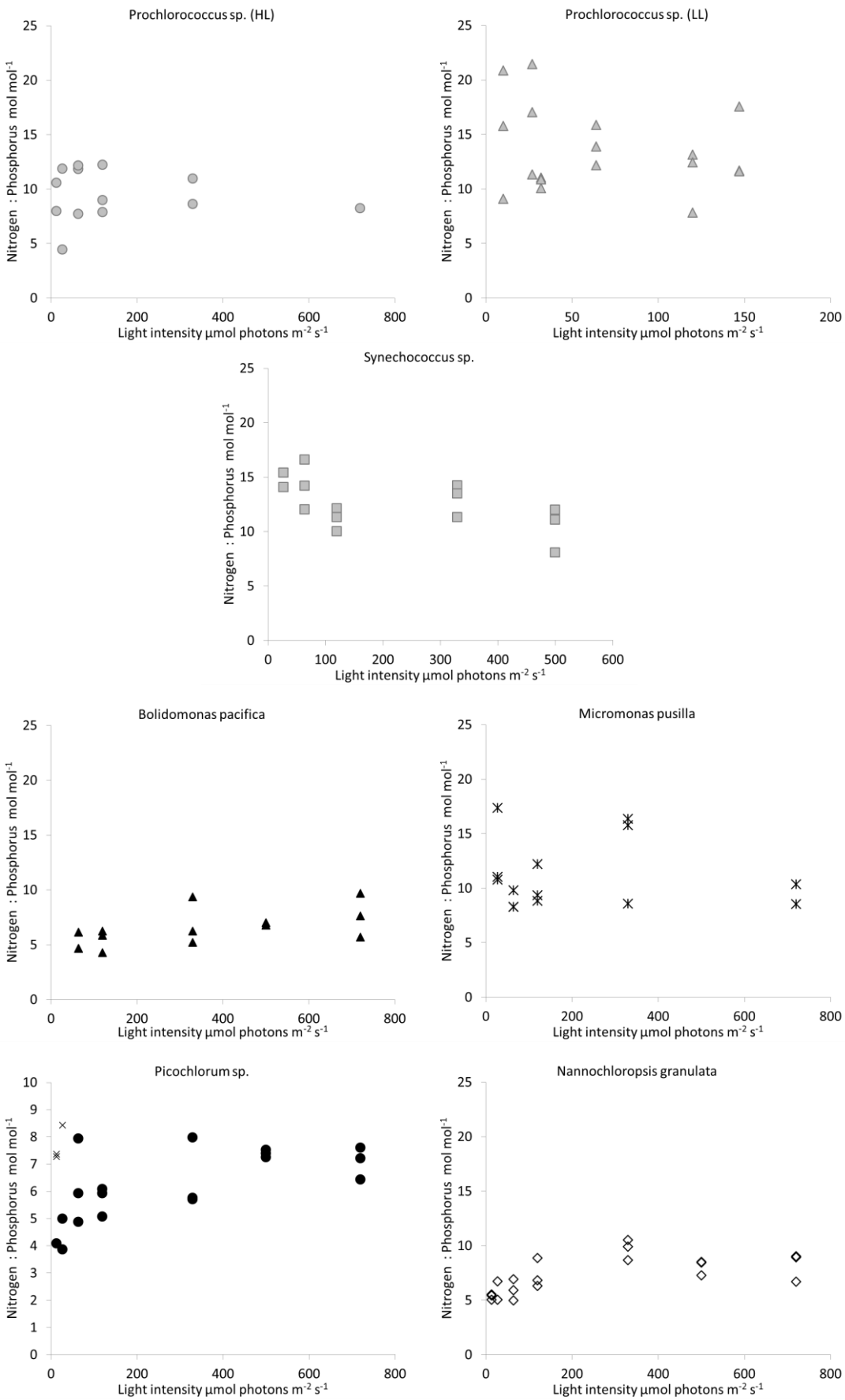

Figure 4. 10 Species specific nitrogen to phosphorus ratios [mol mol^{-1}] depending on light intensity: top three: picoprokaryotes, below: picoeukaryotes

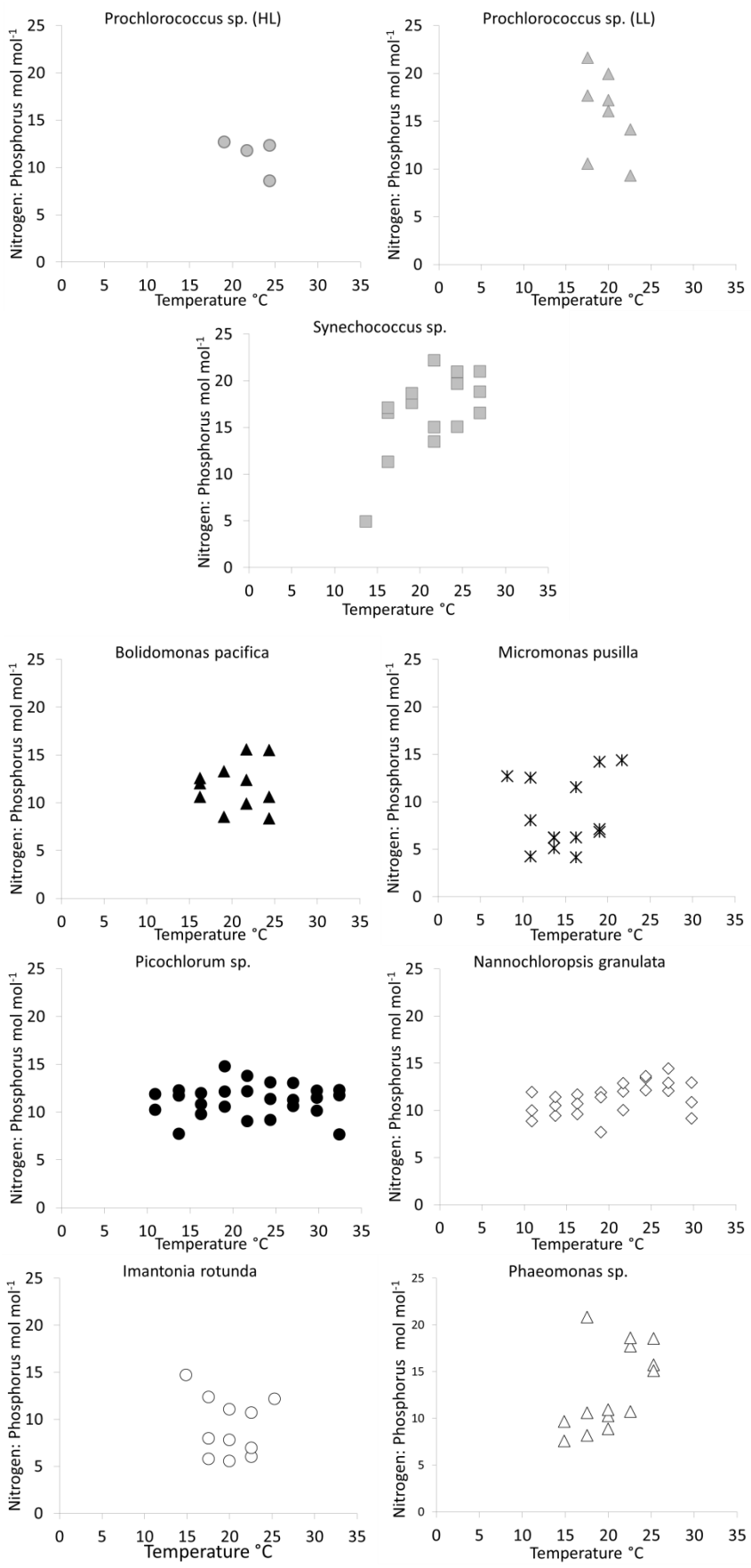

Figure 4. 11 Species specific nitrogen to phosphorus ratios [mol mol^{-1}] depending on temperature: top: three: picoprokaryotes, below: picoeukaryotes.

5. MODELLING THE IMPLICATIONS OF CLIMATE CHANGE ON PICOPHYTOPLANKTON USING AN RCP8.5 SIMULATION

5.1. Abstract

The aim of this chapter is to explore the impact of climate change on picophytoplankton using parameter values which were estimated in the previously discussed light and temperature chapters. Four pairs of model simulations in the biogeochemical model *PISCES* coupled to the NEMO general circulation model were run to compare preindustrial conditions (1800) to the RCP8.5 climate change scenario (2100) with different parameters for picophytoplankton physiology. As this model only considers two plankton functional types, it needs to be taken into account that there are limitations for the representation of this specific phytoplankton group, due to missing interactions. Hence, it is not an attempt to improve the model itself, but to identify the potential impact of climate change on small phytoplankton with physiological characteristics of picophytoplankton. The model is able to reproduce global distribution patterns of picophytoplankton compared to the MAREDAT database. The biomass distributions differ substantially from the initial parameterisation of the ocean biogeochemical model *PISCES* if temperature response parameters are changed. Climate change leads to enhanced stratification of the water column, reduced availability of nutrients and an increased contribution of picophytoplankton to total phytoplankton biomass. It agrees with the assumption that chlorophyll will decrease in the surface ocean with global warming but also shows that it will be counterbalanced for picophytoplankton with a shift towards deeper layers with the exception of the North Atlantic. Further, the new parameterisations shows that the export of carbon below 100m is correlated with the picophytoplankton ratio based on carbon biomass and that regions with a high contribution of picophytoplankton are effected relatively stronger by the reduction of export than regions with a initially low contribution. This, and also the fact that the reduction of export by 21.1% is higher than the decline in primary production (16.5%) shows that the community structure has a profound effect on the future carbon cycle and that there is urgent need for more complex models which consider diverse communities to identify the impact of climate change on global biogeochemical fluxes.

5.2. Introduction

As shown in the previous chapters, changes in environmental conditions including light, temperature and nutrient concentrations have significant influence on the biogeochemical composition and the physiological response of picophytoplankton. Le Quéré et al. (2005) estimated that picophytoplankton account for one third of the global phytoplankton biomass. However, a more recent study by Buitenhuis et al. (2012) calculates an almost twice as high global concentration with an average biomass of 12 ± 22 mg carbon m^{-3}. They are a central part of the microbial loop, which regulates the organic carbon export from the upper ocean (Morán et al. 2010). Unlike larger organisms, it is assumed that picophytoplankton supply less carbon to the deep ocean as a consequence of small size, lower sinking and higher turnover rates (Raven 1998; Le Quéré et al. 2005),.

Their higher nutrient uptake efficiency due to their small size gives them a competitive advantage over other phytoplankton groups (Raven 1998). Hence, they dominate in oligotrophic ocean areas (Alvain et al. 2005) which represent ~70% of the global ocean (Grossman et al. 2010). They decrease in biomass polewards (Buitenhuis et al. 2012) which can also be partly attributed to their low tolerance to cold temperatures. Also, the ability of especially the smaller picoprokaryotes to use light with a high efficiency allows them to grow at the deep chlorophyll maximum.

Particle size has an influence on the export of carbon particles from the ocean surface and consequently on pCO_2 which controls the level of CO_2 that is absorbed from the atmosphere and available for primary production. Hence, the relative contribution of picophytoplankton to total phytoplankton biomass has a direct feedback on the global carbon cycle.

The aim of this chapter is to identify the potential impact of climate change on the geographical distribution of picophytoplankton, their relative contribution to biomass and as a consequence, the influence on export of carbon to the deep ocean. For this, preindustrial conditions from 1800 were compared to a Representative Concentration Pathway simulation with a radiative forcing of 8.5 W m^{-2} in 2100 (RCP8.5). This simulation assumes a global population increase to 12 billion people with high energy demands and has the highest greenhouse gas emissions of all pathways. Hence it was defined as the baseline if no mitigation target is set (Riahi et al. 2011). It is not an attempt to improve the parameterization of the small phytoplankton group in the model itself.

Up to five physiologically relevant parameters of the small phytoplankton group in the global ocean biogeochemical model PISCES were changed to values obtained in this thesis. Hence, for simplicity, this group will be referred to as picophytoplankton.

5.3. Methods

For simulation of the impact of climate change on picophytoplankton the ocean biogeochemical model *PISCES* (Pelagic Interactions Scheme for Carbon and Ecosystem studies) coupled to the NEMO general circulation model (version 3.5) was used (Aumont et al. 2003). It consists of 4 plankton functional types (PFT's), picophytoplankton, diatoms, microzooplankton and mesozooplankton and twenty other prognostic variables. The phytoplankton growth rates are controlled by temperature, light intensity and external nitrate, ammonium, phosphate, silicate and iron concentrations. The C: Chl: Fe stoichiometry is variable while the C: N: P stoichiometry is fixed to 122: 16: 1. All equations and default values are described in the PISCES user manual (Aumont 2012, figure 1).

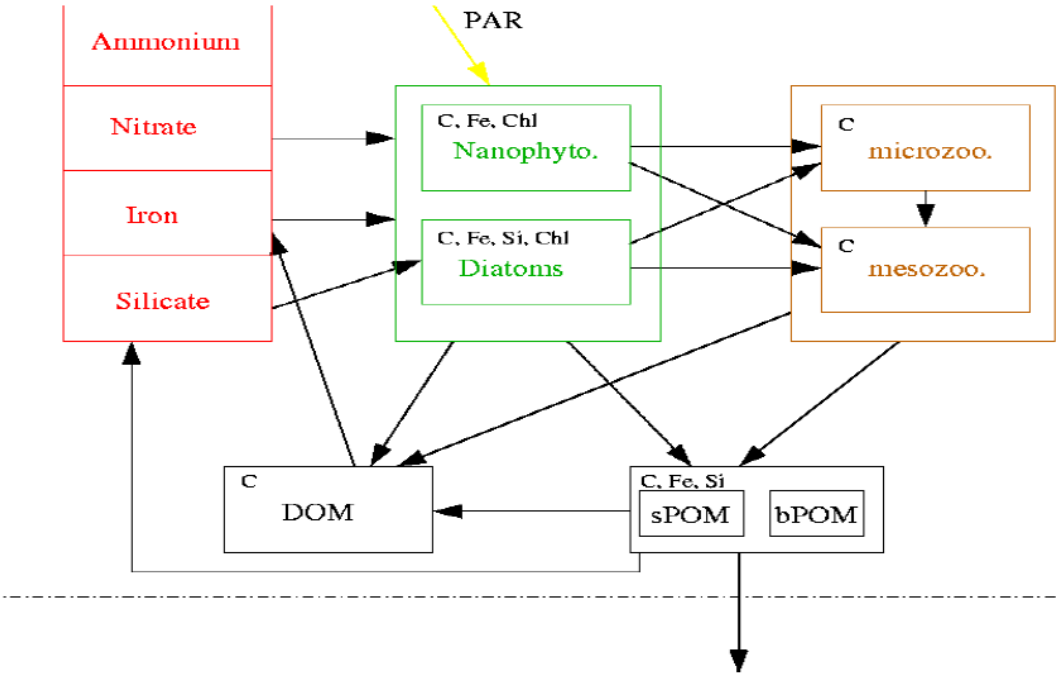

Figure 5. 1 Architecture of the PISCES model taken from the PISCES user manual (Aumont 2012, figure 1)

For simulation of the ocean physics and circulation the IPSL-CM5A-LR model (Institut Pierre Simon Laplace coupled model version 5) was used.

Four pairs of simulations were run with four different sets of parameter values for picophytoplankton physiology and two climate scenarios, corresponding to preindustrial conditions in the year 1800 and the high emission scenario RCP8.5.

Scenario A included the initial (standard) parameterisation (Aumont 2012), scenario B included changes in light and temperature relevant parameters. In scenario B1 only light relevant and in scenario B2 only temperature relevant parameters were changed(Table 5. 1and Table 5. 2). Since PISCES has fixed C: N: P stoichiometry, the results from the nutrient chapter were not used.

Table 5. 1Model simulation scenarios

Scenario	Modifications
A	Standard conditions with nanophytoplankton
B	All parameters changed
B1	Only light dependent parameters changed
B2	Only temperature dependent parameters changed

Table 5. 2 Physiologically relevant parameters changed in the PISCES model to represent picophytoplankton as the smaller phytoplankton group

Parameter	Inital value	Modified value	Unit
α^{Chl}	2	2.906	g C m²(mol photons g Chl)$^{-1}$
θ_{min}	0.0033	0.009	g C g Chl^{-1}
θ_{max}	0.33	0.045	g C g Chl^{-1}
μ_{max0}	0.66	0.141	d^{-1}
$Q_{10}^{0.1}$	1.066	1.076	-

Concerning light physiology the initial slope of the photosynthesis versus irradiance curve, (α^{Chl}) and minimum and maximum achievable chlorophyll to carbon ratio (θ) were modified. Temperature relevant parameters included the maximum growth rate at 0°C (μ_{max0}) and $Q_{10}^{0.1}$ (Table 5. 2).

For all simulations mean values of the last 5 years between 1806 - 1810 and 2095- 2100 were calculated.

5.4. Results

The increase of the initial slope of the photosynthesis versus light relationship by 45% leads to a stronger increase in photosynthesis under lower light. Also, higher chlorophyll concentrations within the cells contribute to a better light use. Changes in temperature relevant parameters caused major changes to the biomass distribution patterns due to the large decrease in μmax0. As there is no validation of the preindustrial results with observations, the major focus will be given to scenario B1, including only changes in 3 major growth parameters.

5.4.1. Chlorophyll a

Surface Chlorophyll a concentration, as observed by the Seawifs satellite under historical conditions, is shown in Figure 5. 2 as an example to identify regions of high and low surface chlorophyll and compared to the preindustrial simulation A and B1.

The *PISCES* model is able to reproduce high concentrations along the South American and African coasts, in the North Atlantic and North Pacific. It also identifies low concentrations in the subtropical open oceans. However, it overestimates chlorophyll in the Southern Ocean and underestimates it along all coastlines of the Northern hemisphere. Still, *PISCES* projects a historical global annual mean surface concentration of 0.3 mg Chl m^{-3} (Vogt et al. 2013).This is in agreement with the estimation by Hirata et al. (2011). The preindustrial concentrations in the initial scenarios A and B1 (Figure 5. 2) are slightly lower (0.27 - 0.28 mg Chl m^{-3}). The main difference in scenario B1 compared to scenario A is a higher concentration of chlorophyll in areas where it was initially low and lower concentrations where chlorophyll was high. However, differences in most areas are in the range of ± 20% and distribution patterns are still the same. In all tested RCP8.5 scenarios chlorophyll decreases by ~22% until 2100 (Table 5. 3). Mean surface chlorophyll concentrations are higher in scenario B and B2.

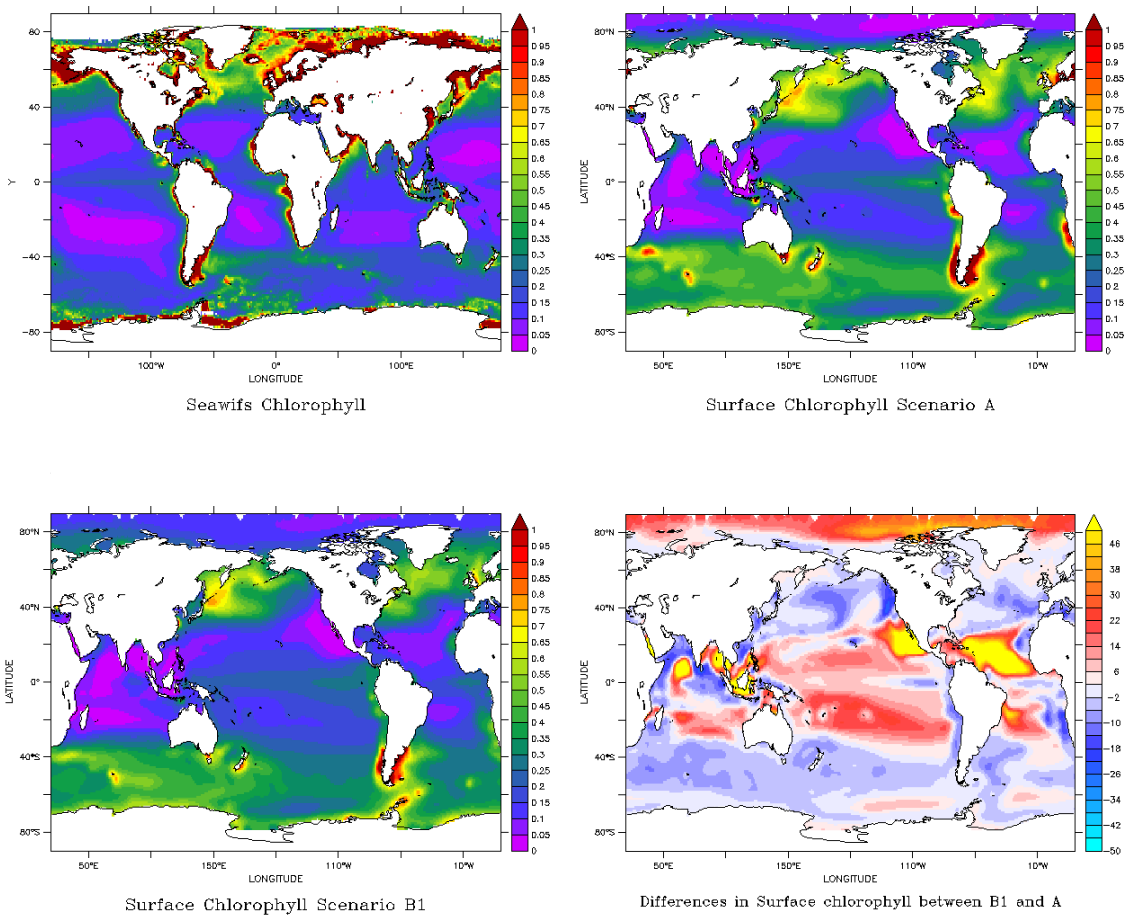

Figure 5. 2 Surface Chlorophyll concentration from historical Seawifs data and preindustrial conditions in the PISCES simulation A, B1 [mg m^{-3}] and differences in the scenario B1 compared to scenario A in [%].

Table 5. 3 Mean surface chlorophyll [mg/m³] and relative difference between 1800 and 2100

Scenario	1800 mg/m³	2100 mg/m³	Δ Chl [%]	historical observation
A	0.28	0.21	-22.2	-
B	0.33	0.26	-22.2	-
B1	0.27	0.21	-22.6	-
B2	0.32	0.25	-21.6	-
PISCES	-	-	-	0.30
Hirata (2011)	-	-	-	0.30
Seawifs [year 1998]	-	-	-	0.35

Only a part of the total chlorophyll is located near the surface. Even though the surface chlorophyll concentration decreases by one fifth by 2100, the average concentration within the top 200m is only reduced by ~10% (Table 5. 4) as phytoplankton is shifted

towards deeper layers (two examples in Figure 5. 3). At a depth of approximately 200m the chlorophyll concentration is equally low under future and preindustrial conditions.

The picophytoplankton chlorophyll concentration down to 200m decreases by 2.2 - 4.1 % in scenarios A and B1 and increases by 7.6 - 11.5 % in scenarios B and B2. The diatom chlorophyll in turn is reduced by 15.5 - 21.3% in all scenarios. Thus, with the new parameterization in scenario B1 the mean chlorophyll concentration decreases slightly stronger than in the initial parameterization.

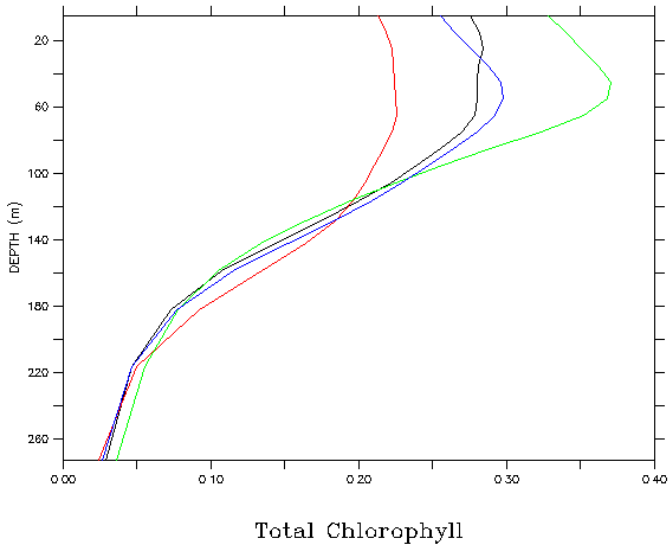

Figure 5. 3 Global average, 5-yearly mean total Chlorophyll (Picophytoplankton + Diatom) concentration over depth; black: preindustrial B1, red: rcp B1, green: preindustrial B, blue: rcp B [mg m^{-3}]

Table 5. 4 Global average, 5-yearly mean Picophytoplankon , Diatom and mean total Chlorophyll concentration in the top 200m in 1800, 2100 and relative differences

	Picophytoplankton			Diatoms			Total Chlorophyll		
Scenario	1800 mg/m³	2100 mg/m³	Δ Chl [%]	1800 mg/m³	2100 mg/m³	Δ Chl [%]	1800 mg/m³	2100 mg/m³	Δ Chl [%]
A	0.13	0.12	-2.2	0.07	0.06	-20.6	0.20	0.18	-9.0
B	0.05	0.05	7.7	0.18	0.16	-15.5	0.23	0.21	-10.6
B1	0.14	0.13	-4.1	0.07	0.05	-21.3	0.20	0.18	-9.8
B2	0.04	0.05	11.5	0.18	0.16	-15.5	0.23	0.20	-10.6

5.4.2. Carbon biomass

In all scenarios the carbon biomass of both groups decreases with depth, but reaches an equally low concentration at approximately 200m depth (two examples in Figure 5. 4).

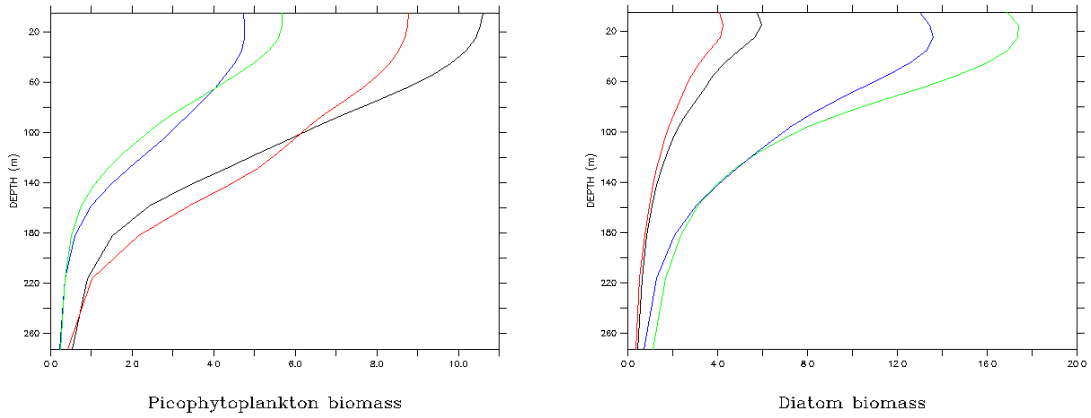

Figure 5. 4 Global average, 5-yearly mean picophytoplankton and diatom biomass over depth; black: preindustrial B1, red: rcp B1, green: preindustrial B, blue: rcp B [mg C m^{-3}]

The mean phytoplankton biomass is similar in the scenarios A and B1 (Table 5. 5). Under preindustrial conditions, picophytoplankton make up 5.99 - 6.22 mg carbon m^{-3} and diatoms account for one third of the total biomass. With climate change picophytoplankton biomass decreases by 3.2 - 4.6% and of diatoms by 23.2 - 24.7% leading to a decrease of the total phytoplankton biomass by 10.3 - 10.5%.

The adjustment of light relevant parameters in scenario B1 leads to a slight increase in picophytoplankton biomass compared to the initial scenario but a relatively higher decrease in 2100.

In the other two scenarios, which include changes in the temperature parameters, the mean total biomass is higher with picophytoplankton accounting for not more than 22 - 24% and diatoms having 3 times the biomass they achieved in scenario A. With climate change picophytoplankton gain 0.4 - 2.3% of biomass and diatoms loose 16.2 - 16.6%, leading to a total decrease of biomass by 12.2 - 12.6%.

Table 5. 5 Mean picophytoplankton, diatom and total biomass in 1800, 2100 and relative differences

Scenario	Picophytoplankton			Diatoms			Total biomass		
	1800 mg m^{-3}	2100 mg m^{-3}	Δ biomass [%]	1800 mg m^{-3}	2100 mg m^{-3}	Δ biomass [%]	1800 mg m^{-3}	2100 mg m^{-3}	Δ biomass [%]
A	5.99	5.79	-3.2	2.91	2.19	-24.7	8.90	7.99	-10.3
B	2.81	2.82	0.4	9.10	7.59	-16.6	11.91	10.42	-12.6
B1	6.22	5.94	-4.6	2.75	2.11	-23.2	8.97	8.05	-10.3
B2	2.49	2.55	2.3	8.97	7.51	-16.2	11.46	10.07	-12.2

In both the A and B1 scenario the highest decrease in picophytoplankton between 1800 and 2100 takes place in the North Atlantic, the North Pacific and the Indian Ocean. Biomass increases in the South Atlantic and South Pacific Ocean, the Arctic Ocean and along the Antarctic coastline (Figure 5. 5). The same general patterns are found in the two less realistic scenarios. However, the changes are more extreme.

Inorganic nitrogen and phosphorus distribution patterns decrease in almost all ocean areas, except of parts of the North Atlantic and the Southern ocean (Appendix, Figure 5. 15 and Figure 5. 16)

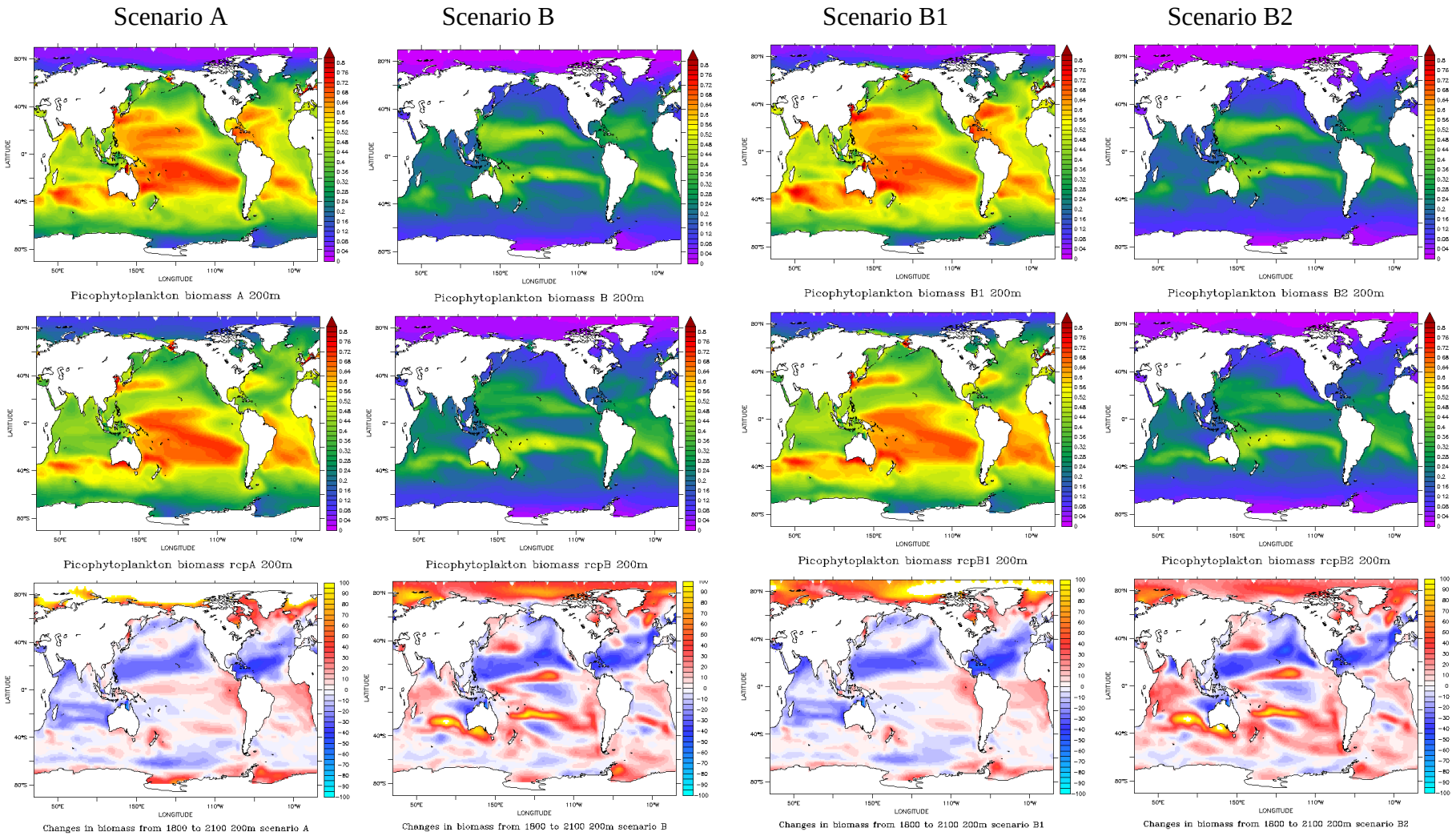

Figure 5. 5 5-Yearly mean picophytoplankton biomass (average over 200m) in mmol m^{-3} in 1800 (top) 2100 (middle) and relative changes between 1800 and 2100 (below).

Changes in light relevant parameters in scenario B1 lead to a lower predicted picophytoplankton biomass concentration between 40°N and 40°S in the central Pacific and North Atlantic, as well as around 20° north and south in the Indian Ocean and the Arctic Ocean (Figure 5. 6). In the other regions the biomass increases. Generally the differences between the two scenarios are smaller than between the preindustrial and historical conditions.

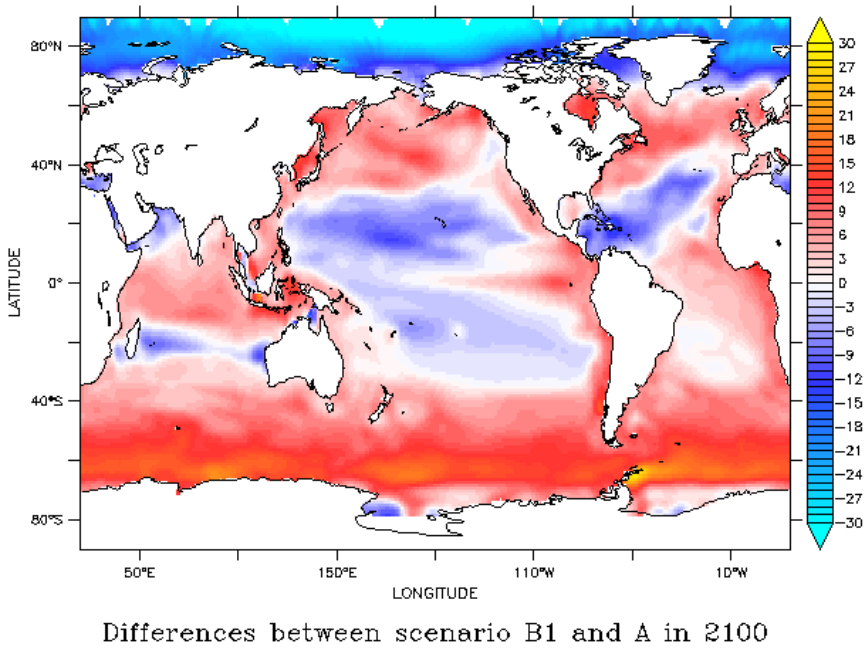

Figure 5. 6 Difference in picophytoplankton biomass in the rcp8.5 projections of scenario B1 related to the initial scenario rcp A in %

Latitudinal differences in environmental parameters and biomass are shown for scenario A and B1 in (Figure 5. 7 and Figure 5. 8). The temperature increases almost constantly over the entire latitudinal range in 2100 compared to 1800. Nitrogen, phosphorus and diatom concentrations are generally lower in 2100 with the exception of the Polar Regions. The opposite trend applies to the depth of the euphotic layer, as it increases in a clearer water column.

The average picophytoplankton biomass in the top 200m is highest in the subtropical regions between 20° and 40° and lowest in the Polar Regions. Climate change has the strongest effect in the North Atlantic from 5 to 40°N, where it causes a decrease in biomass. This decrease is also visible in the southern hemisphere but to a much smaller

extent. It increases around the Equator and in the Arctic. Diatoms in contrast have highest concentrations in the mid latitudes and lowest in the subtropical regions. In the rcp8.5 scenarios it is generally lower between the 0 and 60° and higher in the Polar Regions.

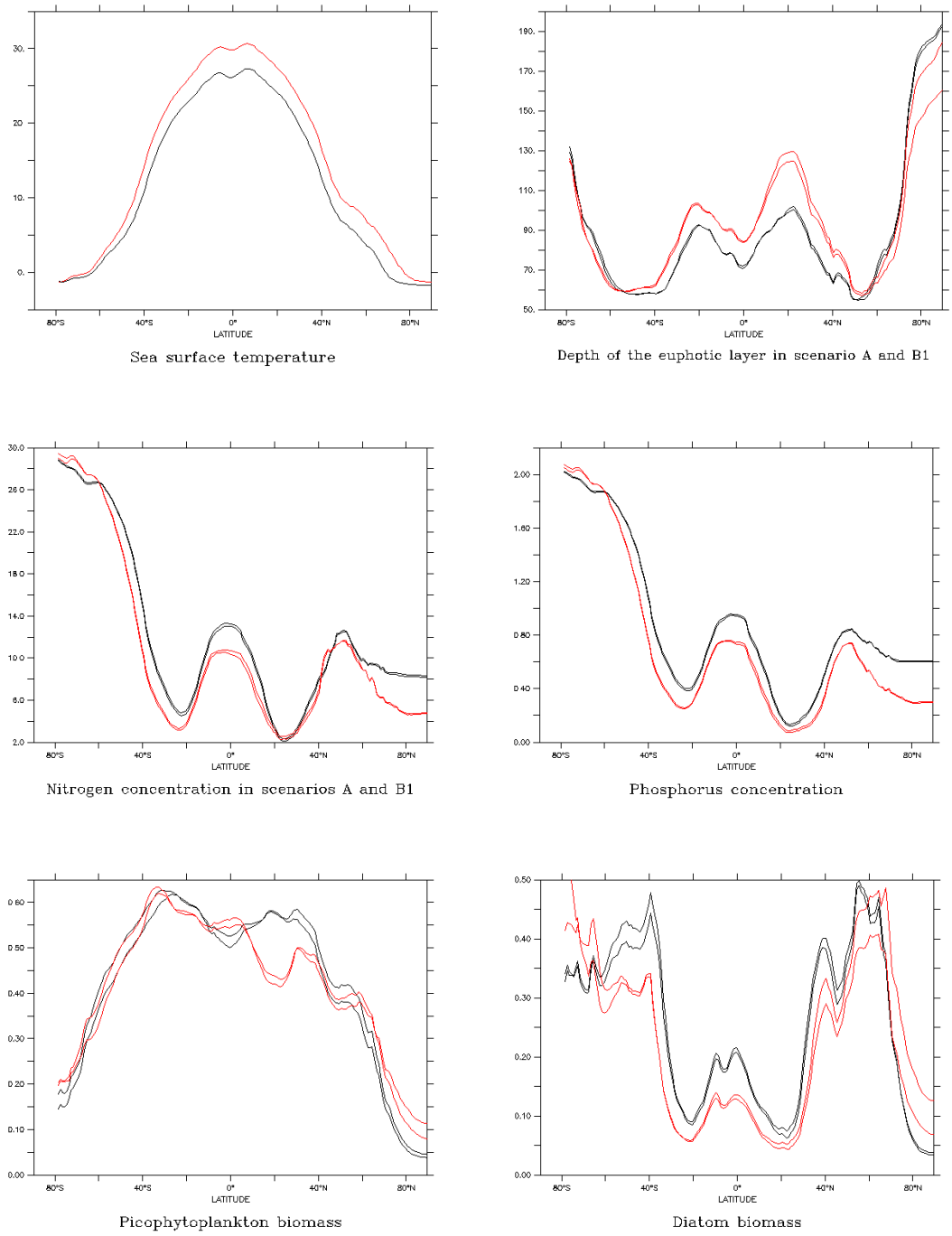

Figure 5. 7 Average environmental conditions including Sea surface temperature [°C], depth of the euphotic layer [m], mean total dissolved nitrogen [mmol m^{-3}], phosphorus [mmol m^{-3}] concentration and mean picophytoplankton biomass [mmol m^{-3}] in the top 200m in scenario A and B1 over latitude; black: 1800, red: 2100.

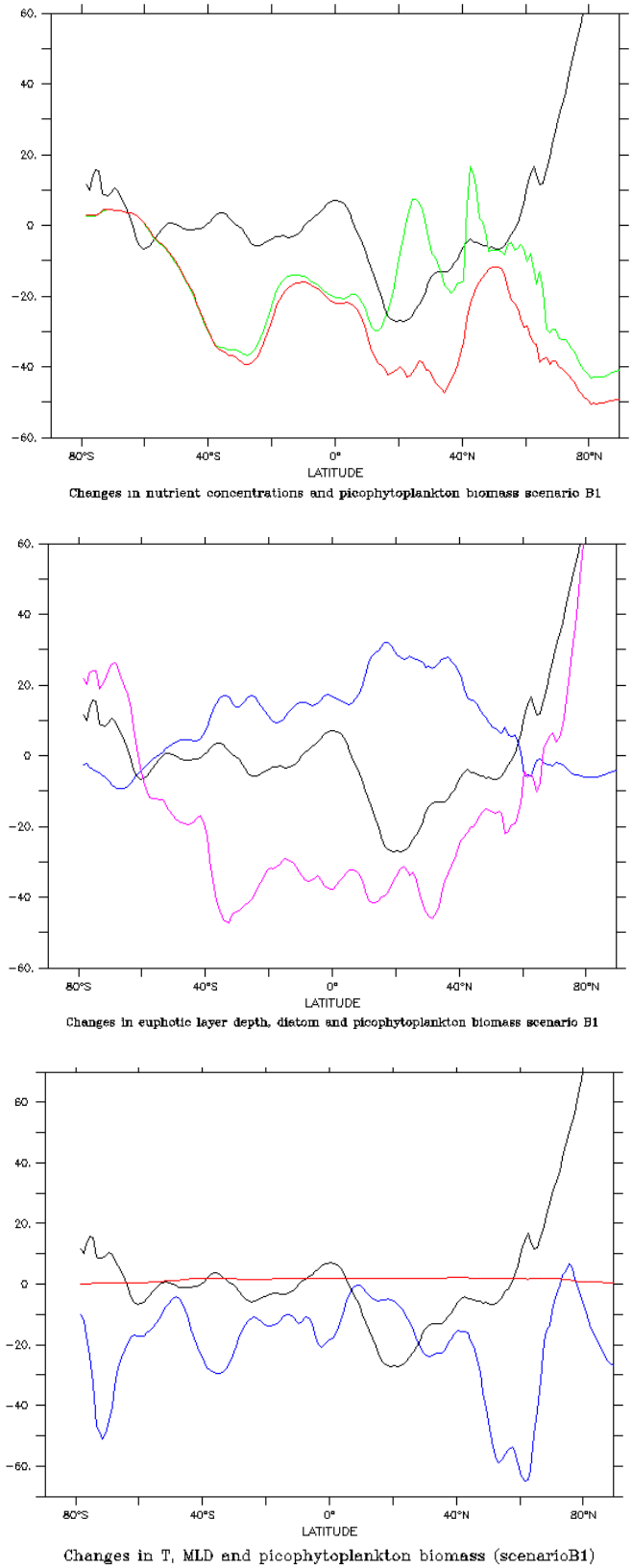

Figure 5. 8 all: Changes in picophytoplankton biomass (black) between 1800 and 2100, top: changes in nitrogen (green) and phosphorus (red) concentration, middle: changes in depth of the euphotic layer (blue) and diatom biomass (purple), below: changes in temperature (red) and mixed layer depth (blue). All values are calculated from 5-yearly averages in the top 200m over a latitudinal gradient in % from scenario B.1.

Compared to changes in nutrient concentration, the changes in picophytoplankton biomass can be regarded as almost constantly low in the southern hemisphere up to 60°S. The only strong difference between preindustrial and future conditions is found in the North Atlantic where picophytoplankton biomass decreases strongly and nitrogen availability is highest. Diatom biomass in turn decreases strongly between 60°N and 60°S and allows the euphotic layer depth to increase (Figure 5. 9).

There is no general correlation between temperature, nutrient concentration, depth of the euphotic or mixed layer or diatom concentration with picophytoplankton biomass regarding the 5-yearly average mean concentrations over 200m on a latitudinal gradient in either the initial scenario A or in scenario B1.

However, decreasing nutrient concentrations in the surface and the extension of the euphotic layer cause a shift in picophytoplankton biomass towards deeper layers (Figure 5. 10).

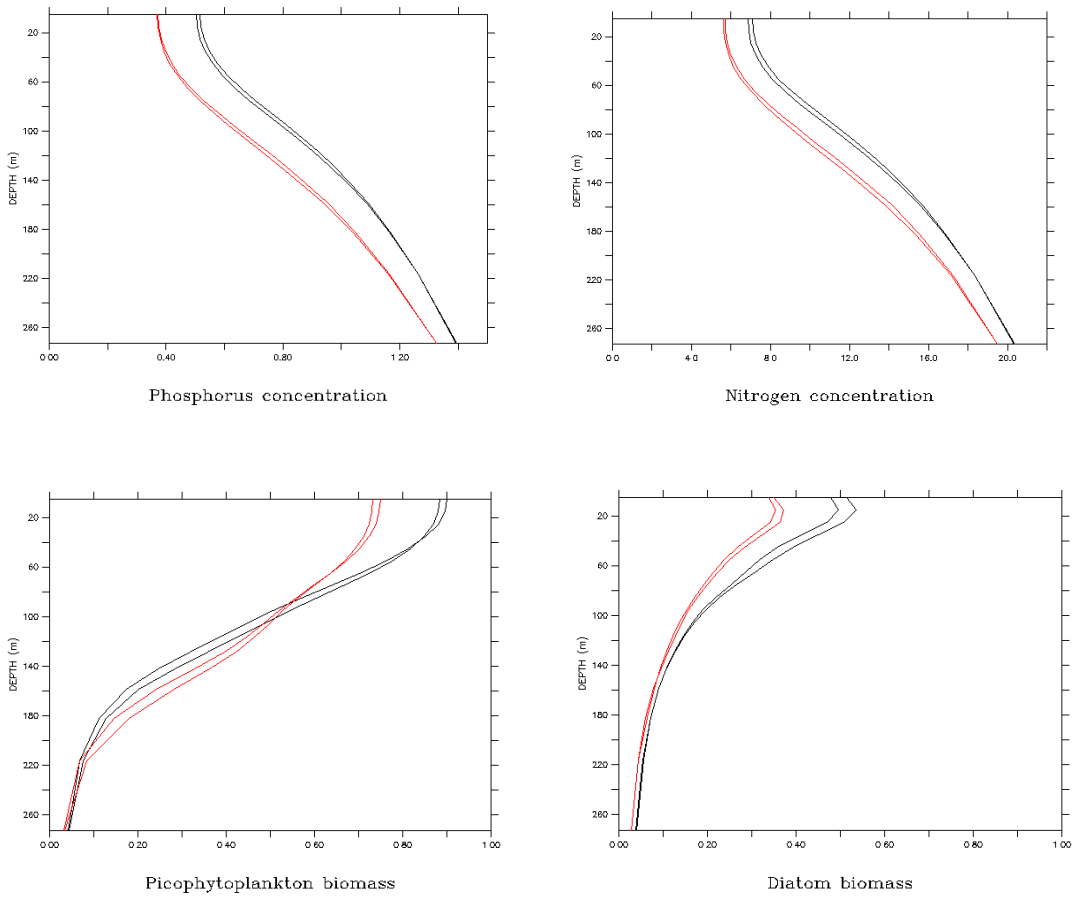

Figure 5. 9 5-Yearly average mean total dissolved nitrogen [mmol m^{-3}], phosphorus [mmol m^{-3}] concentration and mean picophytoplankton biomass over depth [mmol m^{-3}] in 1800 (black) and 2100 (red) in Scenario A,B1.

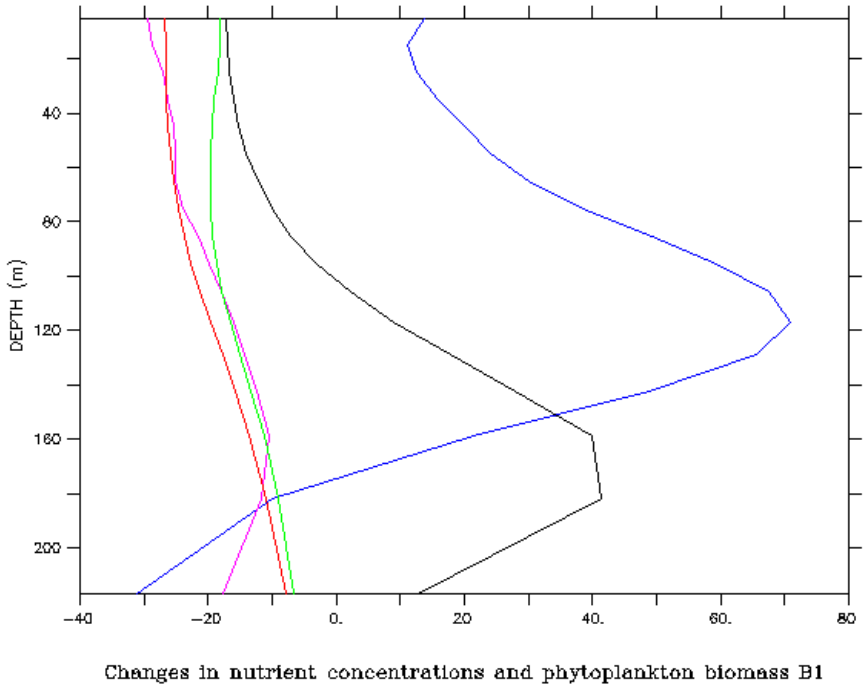

Figure 5. 10 Changes in picophytoplankton biomass (black), nitrogen (green) and phosphorus (red) concentration, photosynthetically active radiation (blue) and diatom biomass (purple) between 1800 and 2100. All values are calculated from 5-yearly global averages on a depth gradient in % from scenario B1

Nutrient concentrations and diatom biomass decrease strongest at the surface and reach the point of lowest decrease at the same depth. Those concentrations are lower in 2100 over the entire depth gradient. Picophytoplankton also decreases in biomass at the surface but increases its biomass below 110m in the future scenario with a peak increase 160m below the surface. The decline of biomass below the peak in both diatoms and picophytoplankton is a consequence in reduction of photosynthetically active radiation.

5.4.3. Contribution of picophytoplankton to total phytoplankton biomass (picophytoplankton ratio) and export of carbon particles below 100m

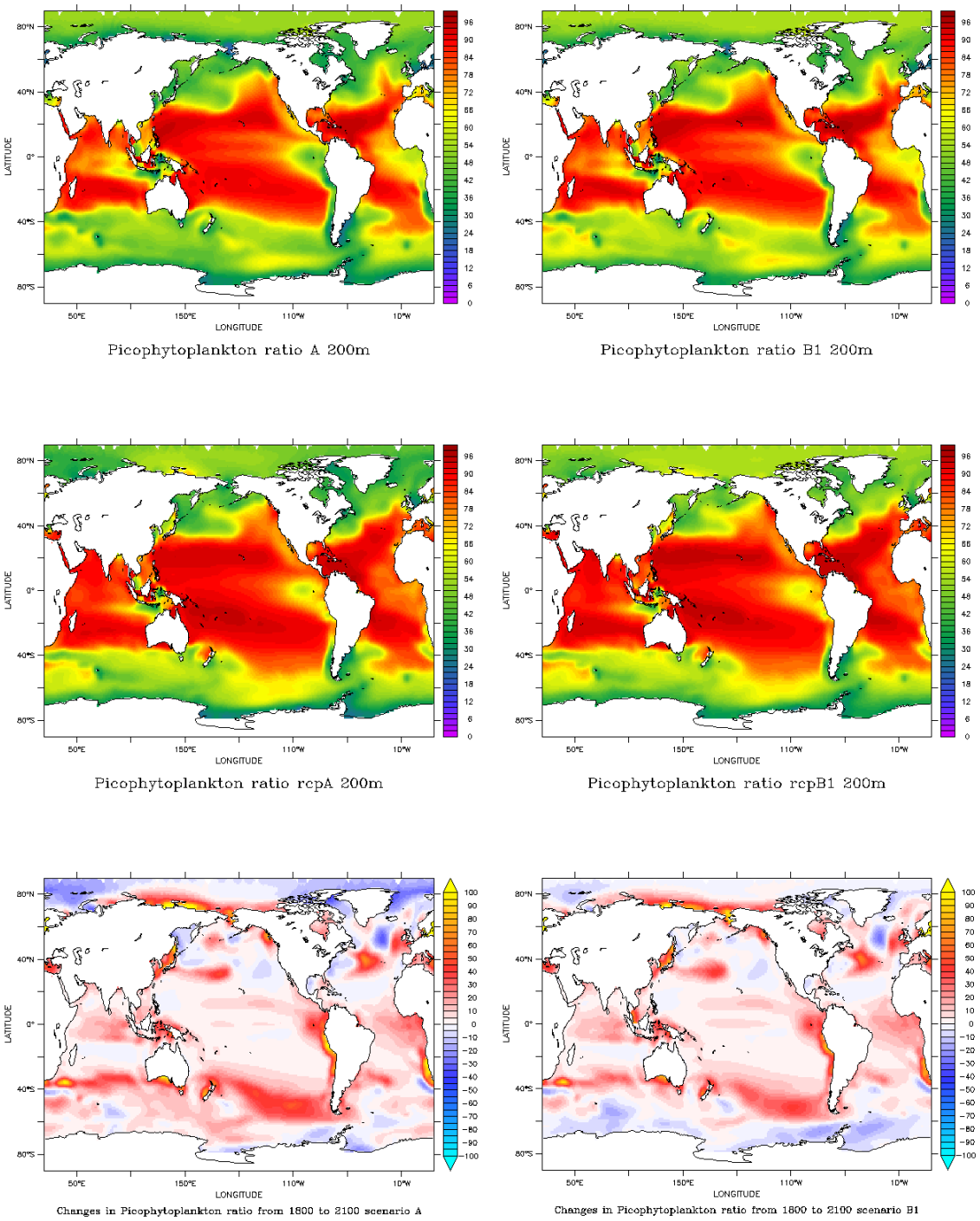

Figure 5. 11 Mean contribution of Picophytoplankton to total Phytoplankton biomass in the top 200m (picophytoplankton ratio, 5-yearly average) in scenario A (left) and B1 (right) in 1800 (top) and 2100 (middle) and changes between 1800 and 2100 in % (bottom).

The mean contribution of picophytoplankton to total phytoplankton biomass (picophytoplankton ratio) is shown in Figure 5. 11 and Figure 5. 12. Picophytoplankton dominate the phytoplankton biomass strongly in most ocean areas between 40°N and 40°S. Their contribution to total phytoplankton biomass is lower along the west coasts of Africa and South America and South East Asia in 1800. In 2100 it gains importance especially in those regions but also extends its dominance towards higher latitudes.

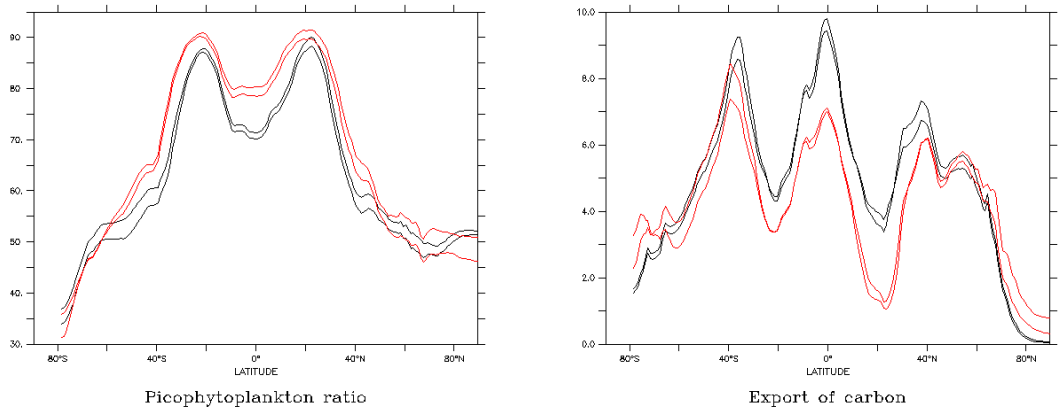

Figure 5. 12 Yearly mean picophytoplankton ratio [%] (left) and export of carbon particles below 100m [mmol m^{-2} day^{-1}] (right) over latitude in 1800 (black) and 2100 (red) in Scenario A and B1.

Table 5. 6 Global 5-yearly average Picophytoplankton ratio over all latitudes and between 40°N and 40°S in 1800, 2100 and differences between years in %.

	All latitudes			40°N - 40°S		
	1800	2100	difference	1800	2100	difference
	%	%	%	%	%	%
A	67.3	72.5	5.3	75.4	82.1	6.7
B	23.6	27.1	3.5	28.7	34.7	6.0
B1	69.4	73.8	4.4	76.9	83.1	6.2
B2	21.8	25.4	3.6	27.0	33.0	6.0

Table 5. 7 Global yearly export of carbon particles [Gt C yr^{-1}] below 100m over all latitudes and between 40°N and 40°S in 1800, 2100 and differences between years in %.

Scenario	All latitudes			40°N - 40°S		
	1800	2100	Δ export	1800	2100	Δ export
	Gt C yr^{-1}	Gt C yr^{-1}	%	Gt C yr^{-1}	Gt C yr^{-1}	%
A	8.95	7.20	-19.6	1.42	1.04	-26.5
B	10.11	7.97	-21.1	1.46	1.01	-30.8
B1	9.28	7.44	-19.8	1.45	1.06	-27.3
B2	9.81	7.81	-20.4	1.43	1.01	-29.8

The global, annual average picophytoplankton ratio in the top 200m is 67.3% in 1800 and increases by 5.3% up to 72.5% in 2100 in the initial scenario (Table 5. 6). In Scenario B1 it is higher in 1800 and increases up to 73.8% by a relatively lower 4.4%. In the other two scenarios the increase is similar (3.5 - 3.6%) even though the relative contribution is substantially lower.

The global yearly export of carbon particles below 100m in scenario A is 8.95 Gt C yr^{-1} and decreases by 19.6% to 7.2 Gt C yr^{-1} (Table 5. 7). In scenario B1 it decreases to a similar extend by 19.8% from 9.28 to 7.44 Gt C yr^{-1}. This decrease in export of carbon exceeds the decrease in primary production (-15.2%, -16.5%) and needs to be at least partly attributed to changes in community structure. In the other two scenarios export and its decrease is slightly higher due to the higher contribution of diatoms.

In the regions in which picophytoplankton dominates over diatoms, between 40°N and 40°S, the mean picophytoplankton ratio is higher (75.4 - 76.9% and 27 - 28.7%) in all scenarios and increases more strongly by 6.0 - 6.7%.

In the top 100m it is strongly correlated (scenarios A, B, B1, B2: 1800: R^2 = 0.6, 0.7, 0.7, 0.7; 2100: R^2 = 0.55, 0.58, 0.65, 0.67) with the amount of carbon that is exported below 100m (Figure 5. 14). The higher the contribution of picophytoplankton, the lower the carbon export rate. This is also reflected in a lower absolute yearly export of carbon in these latitudes. It contributes only 12.7 - 15.9% to the total global export of carbon particles below 100m, even though the area between 40°N and 40°S is 67% of the global ocean.

Also, the impact of climate change is highly correlated with a significant decrease of export related to a defined initial picophytoplankton ratio in scenario A and B1 where picophytoplankton is dominant (Figure 5. 13, equations below). The decrease was also significant in scenario B (p = 0.02), but not well correlated with the change in picophytoplankton contribution (R^2 = 0.089). Hence, a higher reduction in global export of carbon by 26.5% - 27.3% was calculated between 40°N and 40° S. Changes in the parameterisation in scenario B1 indicate a lower export rate for a defined picophytoplankton ratio than in the initial scenario.

The changes in export of carbon below 100m related to preindustrial picophytoplankton ratio can be described by the following equations:

scenario A $-1.31\ x + 76.04$ ($R^2 = 0.522$, $p < 0.01$)

scenario B1 $-1.59\ x + 98.49$ ($R^2 = 0.527$, $p < 0.01$)

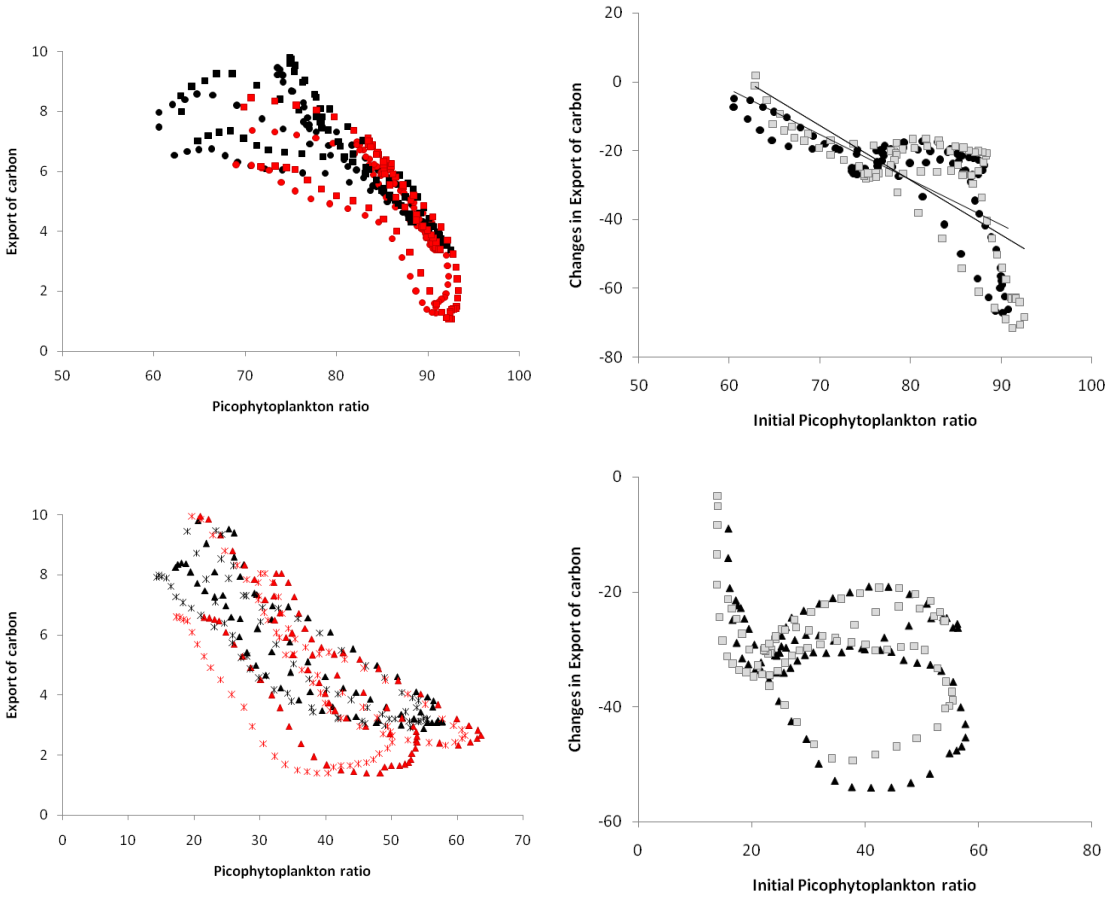

Figure 5. 13 left: 5-Yearly average mean picophytoplankton ratio [%] in the top 100m versus export of carbon particles below 100m [mol m^{-2} day^{-1}] over latitude between 40°N and 40°S in 1800 (black) and 2100 (red) right: Changes in Export ratio [%] between 1800 and 2100 vs. initial picophytoplankton ratio[%], in top: Scenario A (circles) and B1 (squares), bottom: B (triangles), B2 (stars)

5.5. Discussion

The initial parameterization of the *PISCES* model was evaluated against historical observations (e.g. Bopp et al. 2005; Buitenhuis et al. 2006; Schneider et al. 2008; Vogt et al. 2013) and showed general agreement with distribution patterns of phytoplankton. Hence it was successfully used to conduct climate change simulations.

Generally with the initial *PISCES* parameterisation chlorophyll concentrations reproduce diatom blooms in the high latitudes but are underestimated in oligotrophic subtropical regions, and even stronger in the equatorial Atlantic and Arabian Sea (Aumont 2012). With the adjustment of light parameters towards values typical for picophytoplankton, surface chlorophyll concentration increases especially in those regions under preindustrial conditions. Also in the Southern Ocean where the initial parameterization of *PISCES* overestimates chlorophyll, a decrease was found in the B1 scenario. However, as there is neither a historical simulation with the new parameterisation nor are there satellite observations from preindustrial condition this does not necessarily imply that the scenario B1 matches better with observations.

A global annual mean surface chlorophyll concentration from satellite observations is 0.3 mg Chl m^{-3} (Hirata et al. 2011) and agrees well with historical simulations in PISCES (Vogt et al. 2013). The simulated preindustrial concentrations are lower in both the initial and the B1 run and decrease to a similar extent by 2100. This is in agreement with the study by Behrenfeld et al. (2006) who report a general decrease in chlorophyll concentration with increasing ocean temperature.

Even though the surface chlorophyll concentration is similar in scenarios B and B2, the contribution of picophytoplankton chlorophyll is substantially lower.

The mean picophytoplankton concentration in the top 200m in the PISCES model scenarios A and B1 are much closer to the observed picophytoplankton biomass which was summarised in the MAREDAT database (Buitenhuis et al. 2013) and shown in Figure 5. 14. The other two scenarios underestimate the average picophytoplankton biomass substantially. They also underestimate the picophytoplankton biomass in all ocean regions, showing that the temperature parameterisation used is not appropriate.

The reason for the strong decline in picophytoplankton biomass or chlorophyll in those scenarios is the extreme difference in μmax_0 compared to the initial run. *PISCES* only consists of two plankton functional types. Therefore a realistic parameterization does not

necessarily lead to a realistic representation of picophytoplankton within the global biogeochemical cycles, due to missing interactions with other groups.

For this reason, the scenario B1, in which only light relevant parameters were changed, it was considered as the most realistic one to explore how climate change may influence picophytoplankton or small phytoplankton in general.

On a global scale *PISCES* represents the distribution of picophytoplankton biomass fairly well. It shows high concentrations in the western North Atlantic, the central Pacific, the east coast of Australia and Japan and the west coast of the Arabian Sea. Lower concentrations are also well represented at the west coast of South Africa and the Polar Regions, but overestimated in the central north Atlantic. However, in the future scenarios concentrations are lower in the North Atlantic (Figure 5. 5).

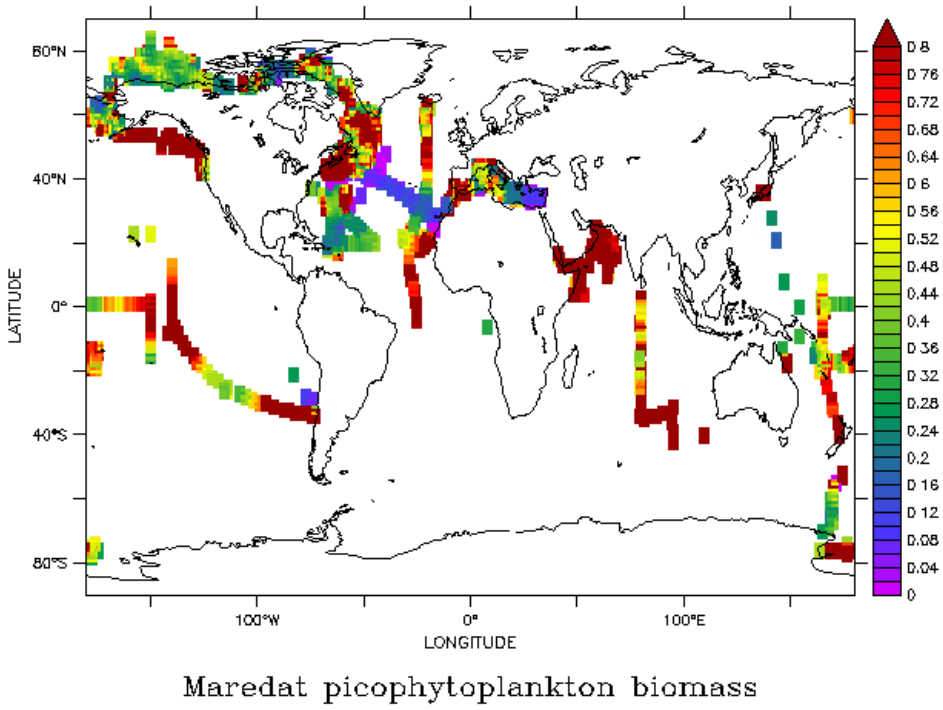

Figure 5. 14 Average surface picophytoplankton biomass from Maredat database in mmol m^{-3}

In general, even if the preindustrial simulations in *PISCES* do not match the quantities of the historical observations they do identify the regions of dominance of picophytoplankton. Hence it is possible to allow future predictions on the relative distribution using the scenarios A and B1. As B1 includes the new parameterization obtained in the previous chapters, the main focus is given to this scenario.

Picophytoplankton is well known to dominate oligotrophic ocean areas (Alvain et al. 2005). Especially in those areas, total phytoplankton biomass is supposed to decline strongest with climate change (Behrenfeld et al. 2006). This is in agreement with our simulations, but it needs to be considered that this model only consists of two plankton functional types. Hence, the global contribution of picophytoplankton is higher in this study than previously estimated (Buitenhuis et al. 2012).

However, their relative contribution to total phytoplankton was shown to increase with ocean warming (Agawin et al. 2000; Morán et al. 2010; Bopp et al. 2005).

The reason behind this is not only the increase in temperature, but also the deepening of the mixed layer which restricts nutrient supply to the upper ocean. Picophytoplankton are well adapted to use light and nutrients more efficiently than bigger phytoplankton groups due to their small size which gives them an advantage in the future ocean.

Hence, the decline in mean picophytoplankton biomass is relatively low compared to diatoms. The strong decline in the North Atlantic or the Southern Ocean can be explained by stronger mixing, with higher nutrient supply and lower grazing pressure which is advantageous for diatoms (Laufkötter et al. 2013).

The increased picophytoplankton ratio also has a major effect on the marine carbon cycle. Particulate carbon, fixed in the euphotic zone by primary production sinks down and is removed from the surface. The sinking speed depends on the size of the particle. Small particles sink slowly and are grazed and remineralised at shallower depths than bigger cells, which sink faster and export carbon to the interior ocean. The remineralisation of small carbon particles in the surface ocean influences the pCO_2 and restricts the uptake of atmospheric carbon.

A study which compared results from different CMIP5 models within different climate change (RCP) scenarios found the general agreement, that compared to preindustrial (1860) conditions, climate change induces a reduction of net primary production by 2 - 13%. This is a consequence of enhanced stratification, reduced nutrient supply and the reduction of ocean ventilation (Bopp et al. 2013). Our estimate even suggest a slightly higher decline of global annual mean primary production between 40°N and 40°W. This is accompanied with a global decline in export production, which is strongest in the low latitudes (Bopp et al. 2001). Globally our estimated export is within the range of previously reviewed information of 6 - 13 Gt C yr^{-1} (Schneider et al. 2008).

Bopp et al. (2005) used the same model as in this study, but a less severe climate change simulation over 140 years (IPSL-CM4, 4x CO_2, +3.2°C) and simulated an extension of

the oligotrophic ocean areas due to enhanced water column stratification, which restricts the resupply of nutrients to the surface. This decline was directly correlated with the decline in diatom biomass. Even though the growing season in the high latitudes was extended through reduction of the ice cover their global abundance was reduced by 10% and the relative contribution of small phytoplankton to chlorophyll increased from 73% to 76% leading to a reduction of export of carbon to the sea floor which was larger than the reduction of primary production.

These results agree with the findings in this study, also with the new parameterization (scenario B1) of the model. However, they consider the contribution of small phytoplankton to total chlorophyll, which is slightly higher than the contribution to carbon biomass. As satellites measure chlorophyll concentration it is logical to refer to this parameter. Chlorophyll concentration is only a small and very variable component of the phytoplankton cell. It does not only vary between species, but also with acclimation state of the cell. Carbon in turn is a major component of all cells and more important with regard to climate change. Hence this study focuses on the relative contribution of picophytoplankton to biomass in units of carbon.

There was no direct correlation between picophytoplankton ratio and any other prognostic variable or the physical environment represented by temperature and mixed layer depth in this study, but Bopp et al. (2005) reported that there is a correlation between nutrients and the decrease in diatom chlorophyll concentration.

However, this study shows that the impact of climate change on the export of carbon particles can also be estimated from the initial mean picophytoplankton ratio based on carbon biomass between 40°N and 40°S, where picophytoplankton dominates phytoplankton biomass and the export of carbon is lower. Also the changes in the parameterization (scenario B1) towards physiological characteristics of picophytoplankton related to light shows that the export is reduced by a higher extent with climate change than estimated by the initial parameterisation (Scenario A).

5.6. Conclusion

The model simulation with the physiological characteristics of picophytoplankton related to light is able to identify global distribution patterns of picophytoplankton if compared to data from the MAREDAT database. It also visualises the enhanced stratification of the water column, reduced availability of nutrients and the increased contribution of picophytoplankton to total phytoplankton biomass by 4.4% and even 6.2% in low latitudes. It agrees with the assumption that chlorophyll will decrease in the surface ocean with global warming, but also shows that it will be counterbalanced for picophytoplankton with a shift towards deeper layers with the exception of the North Atlantic.

Furthermore, the new parameterization shows that the export of carbon particles below 100m is negatively correlated with the picophytoplankton ratio. Those regions are affected relatively more strongly by the reduction of export of carbon with climate change than regions with an initially low contribution. This, and also the fact that the global reduction of export by 21.1% is higher than the average decline in primary production (16.5%) shows that the community structure has a profound effect on the future carbon cycle and that there is urgent need for more complex models which consider diverse communities to identify the impact of climate change on global biogeochemical fluxes.

5.7 Appendix

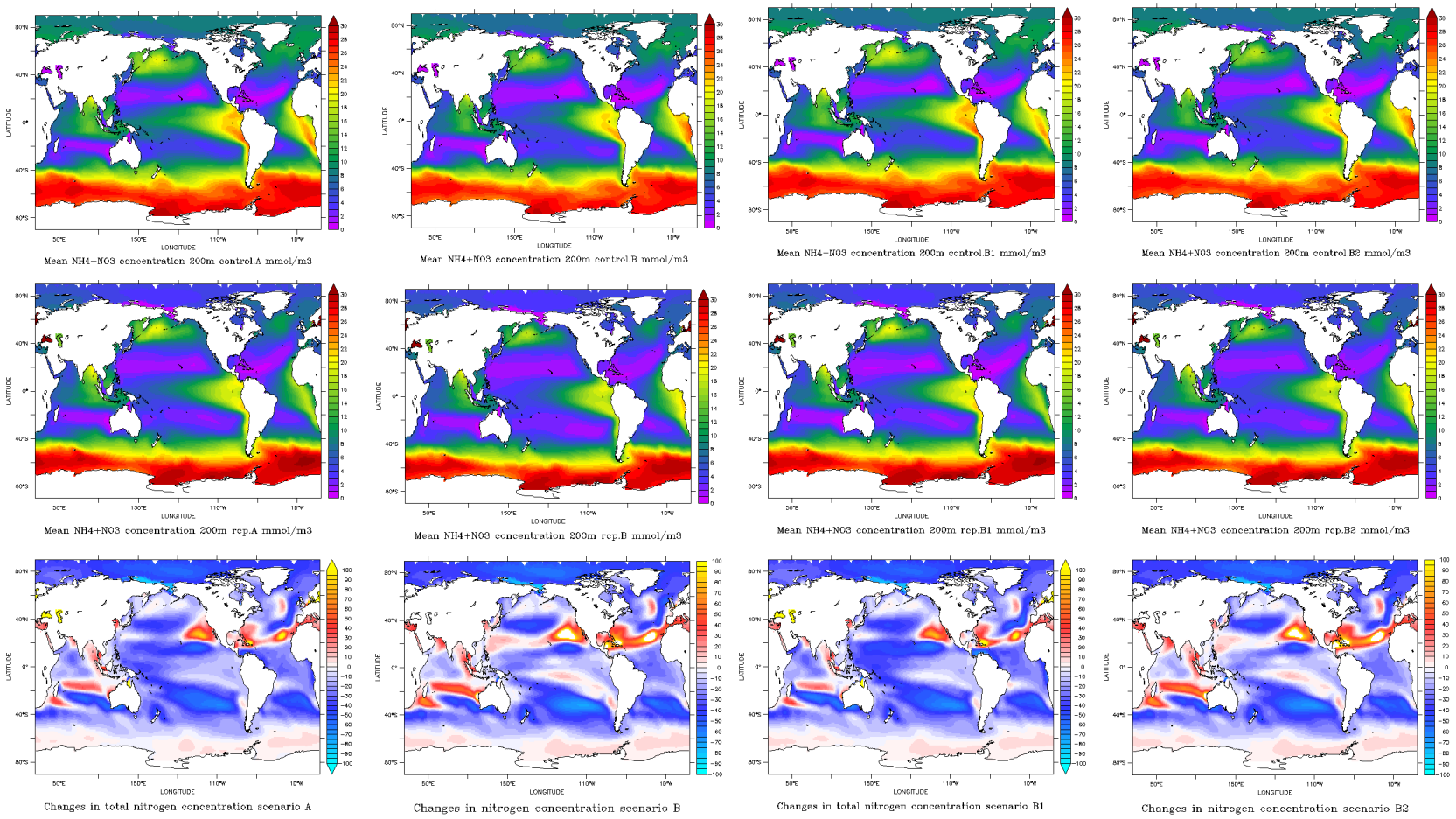

Figure 5. 15 5-Yearly mean nitrogen (NO3 + NH4) concentrations (average over 200m) in mmol m^{-3} in scenario A, B, B1 and B2 (from left to right) in 1800 (top) 2100 (middle) and relative changes between 1800 and 2100 (bottom).

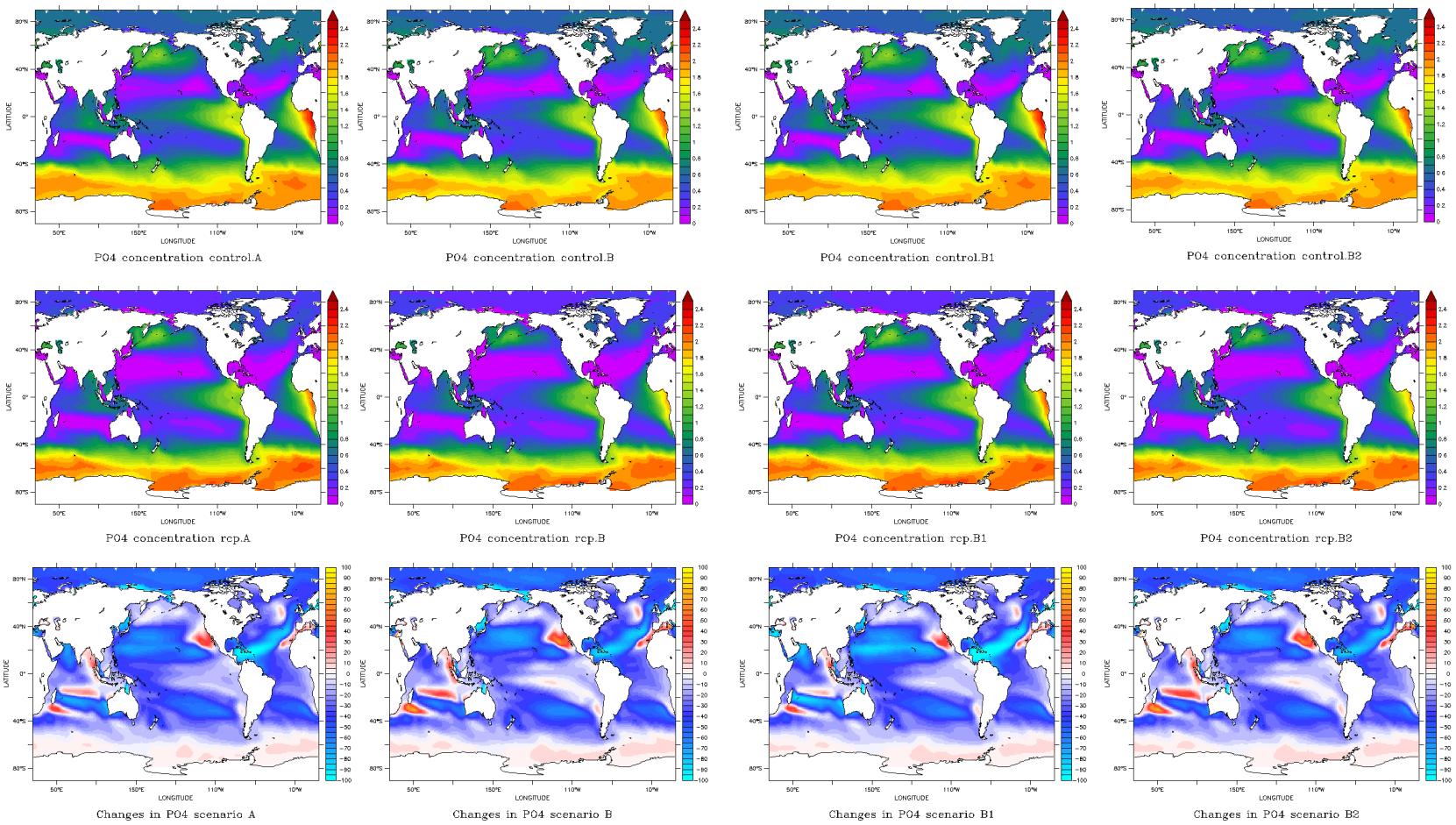

Figure 5. 16 5-Yearly mean phosphorus concentrations (average over 200m) in mmol m^{-3} in scenario A, B, B1 and B2 (from left to right) in 1800 (top) 2100 (middle) and relative changes between 1800 and 2100 (bottom).

6. CONCLUSIONS

6.1. Summary

6.1.1. THE INFLUENCE OF LIGHT ON THE PHYSIOLOGY OF PICOPHYTOPLANKTON

Light limitation experiments (Chapter 2) were conducted over a range of light intensities as they are represented in the euphotic zone of the ocean. Growth rates were measured in cultures which have been acclimated to specific light intensities together with an instantaneous photosynthesis response to changes in light. From this photosynthetic parameters were derived for an acclimated and dynamic response.

The first hypothesis

- We are able to reproduce the physiological response of picophytoplankton to changing environmental conditions with a dynamic photosynthesis model to improve the understanding on translating chlorophyll *a* concentration into carbon biomass and primary production. With the inclusion of a light inhibition term and validation against this extensive new dataset I am able to improve the understanding on translating chlorophyll *a* concentration into carbon biomass and primary production

has not been fully confirmed within this study and showed limitations of the dynamic photosynthesis response model. The parameters obtained by the dynamic photosynthesis model were comparable to an acclimated response for maximum rates of photosynthesis and the affinity for light. However it showed differences for respiration and photoinhibition. Photoinhibition was not represented as strongly in instantaneous photosynthesis measurements as in acclimated growth response curves and led to the underestimation of long term damage due to acclimation to high light conditions in the dynamic model. With this type of model, environmental feedback on pigment and nutrient stoichiometry within the cells can also be considered over time under unbalanced growth conditions. Hence, a better validation with laboratory data, as within this study will contribute to a better understanding of translating chlorophyll *a* concentration from observations into biomass and primary production.

The second hypothesis

- Picoeukaryotes differ significantly from picoprokaryotes in terms of physiological parameterization in specific light environments

has been confirmed. It has been shown that picoprokaryotes and picoeukaryotes differ significantly in their physiological response to light. The maximum carbon specific rate of photosynthesis is significantly lower for picoprokaryotes, while their affinity to light is higher. Hence, their growth is saturated at lower light levels. These findings agree with theoretical assumptions related to size, which give picoprokaryotes an advantage in oligotrophic light limited environments.

6.1.2. The influence of temperature on the Physiology of Picophytoplankton

In Chapter 3 temperature experiments were conducted on three picoprokaryotes and nine picoeukaryotes over a broad temperature range to test whether Eppley's assumptions on phytoplankton growth as a function of temperature are applicable to picophytoplankton. A linear, exponential and an optimum function were fit to the obtained data, and substantial support for the third hypothesis in this thesis was found.

- The temperature dependent maximum growth rates of single phytoplankton species follow an optimum function.

It was also shown that picoeukaryotes have significantly higher optimum growth rates compared to picoprokaryotes, but do not differ in mean optimum growth temperature. However, the temperature tolerance range is higher for picoeukaryotes, consistent with their biogeographical distribution. While picoprokaryotes are more restricted towards warmer ocean regions, picoeukaryotes extend further towards higher latitudes. Another important parameter in biogeochemical models is the temperature dependence of the chlorophyll to carbon ratio, which increases with increasing temperature. This study shows that there may also be a drop above the optimum temperature.

Also the fourth hypothesis

- The temperature dependent maximum growth rates of a phytoplankton community approach an exponential function

has been confirmed in this study. Applying a 99th quantile regression, the maximum picophytoplankton community growth is lower than the curve estimated by Eppley, but has a higher Q_{10} value of 2.3. For picoprokaryotes this value is even more than twice as high (4.9). The increase of ocean temperature due to climate change will be beneficial for picophytoplankton because of a higher Q_{10} compared to other phytoplankton groups. It will also have a stronger effect on picoprokaryotes and may shift their distribution because of their narrow temperature tolerance range.

6.1.3. Light and temperature induced variability of the elemental composition of picophytoplankton and their minimum requirements based on nutrient limitation experiments.

Fifth, in Chapter 4 the investigation of the elemental composition of picophytoplankton under nutrient saturation addressed the hypothesis

- Both groups show a high flexibility in their nutrient stoichiometry under a broad light and temperature range under nutrient replete conditions, but picoprokaryotes have lower phosphorus requirements.

It revealed that under nutrient saturated conditions, there is a significant deviation from the Redfield ratio. In general, nitrogen and phosphorus are taken up in excess. It also shows that picoprokaryotes and picoeukaryotes have similar mean C: N but significantly different N: P ratios under nutrient saturated conditions, which reflects the lower phosphorus demand of picoprokaryotes. C: N increases within the groups with increasing light intensity and decreasing temperature but this trend is not significant in picoprokaryotes as their temperature tolerance range is restricted. Also, N: P increases with increasing temperature in picoeukaryotes. These changes are consistent with previously suggested physiological changes in the concentration of nitrogen rich light and nutrient acquisition components, and phosphorus rich ribosomes for protein synthesis.

Sixth, the hypothesis

- Nutrient limitation affects C: N: P ratios and leads to a decrease in Chlorophyll *a* : carbon ratios.

has been investigated to confirm that under nutrient limited conditions nitrogen relative to carbon decreases by 15 − 42% and phosphorus by 37 − 65% compared to nutrient saturated conditions in picoeukaryotes. Also the Chlorophyll *a* : carbon ratio is significantly lower under both nitrogen (-50 − -82%) and phosphorus (-62 − -91%) limitation compared to saturated conditions due to a lower availability of nitrogen and lower synthesis rates when phosphorus is limited. The half-saturation constants for nitrogen for *Picochlorum sp.* (0.19 ± 0.23 µmol $NH_4^+L^{-1}$) and *Micromonas pusilla* (0.07 ± 0.05 µmol $NH_4^+ L^{-1}$), found in this study agree with previous estimates. It is substantially lower for *Nannochloropsis granulata* (0.01 ± 0.02 µmol $NH_4^+L^{-1}$).

6.1.4. MODELLING THE IMPLICATIONS OF CLIMATE CHANGE ON PICOPHYTOPLANKTON USING AN RCP8.5 SIMULATION

In Chapter 5 the ocean biogeochemical model *PISCES* was used to compare preindustrial climate conditions to a future high emissions scenario to investigate the seventh hypothesis

- Climate change has an influence on the relative contribution of picophytoplankton to total phytoplankton biomass and as a consequence, on the export of carbon to the deep ocean.

It was confirmed that climate change leads to enhanced stratification of the water column, reduced availability of nutrients and an increased contribution of picophytoplankton to total phytoplankton biomass. It agrees with the assumption that chlorophyll will decrease in the surface ocean with global warming, but also shows that it will be counterbalanced for picophytoplankton with a shift towards deeper layers with the exception of the North Atlantic. Furthermore, it shows that the export of carbon below 100m is anti-correlated with the picophytoplankton contribution to phytoplankton carbon biomass and that

regions with a high contribution of picophytoplankton are affected relatively more strongly by the reduction of export than regions with an initially low contribution. The fact that the reduction of export is higher than the decline in primary production shows that the community structure has a profound effect on the future carbon cycle and that there is urgent need for more complex models which consider diverse communities to identify the impact of climate change on global biogeochemical fluxes.

6.2. General conclusion and Future work

This study has shown strong evidence that picophytoplankton is well adapted to low light, relatively high temperatures and low nutrient availability. It has also shown that there are significant differences between picoprokaryotes and picoeukaryotes which are reflected in and consistent with their geographical distribution. Generally higher growth rates (Figure 6. 1 A and B) and photosynthesis rates of picoeukaryotes (Figure 6. 1C) explain their dominance in biomass over picoprokaryotes on a global scale. However, picoprokaryotes have a higher affinity to light and are consequently light saturated at lower light intensities (Figure 6. 1D). This gives them an advantage in deeper layers of the water column. Further, they show a stronger physiological response to increased temperature (Figure 6. 2A) than was estimated by Eppley for a general phytoplankton community with a twice as high temperature coefficient for picoprokaryotes (Q_{10}) than for picoeukaryotes. Lower phosphorus requirements of picoprokaryotes are reflected in significantly higher N: P ratios of picoprokaryotes as shown over both a light (Figure 6. 2B) and temperature gradient. This is an advantage in regard to climate change expecting stronger nutrient limitation due to enhanced vertical stratification. Altogether, climate change will favour small phytoplankton cells, meaning the entire group of picophytoplankton, over larger cells such as diatoms (Figure 6. 2 C) which will lead to the decrease in export production (Figure 6. 2D), and will be highest in regions where picophytoplankton already dominates.

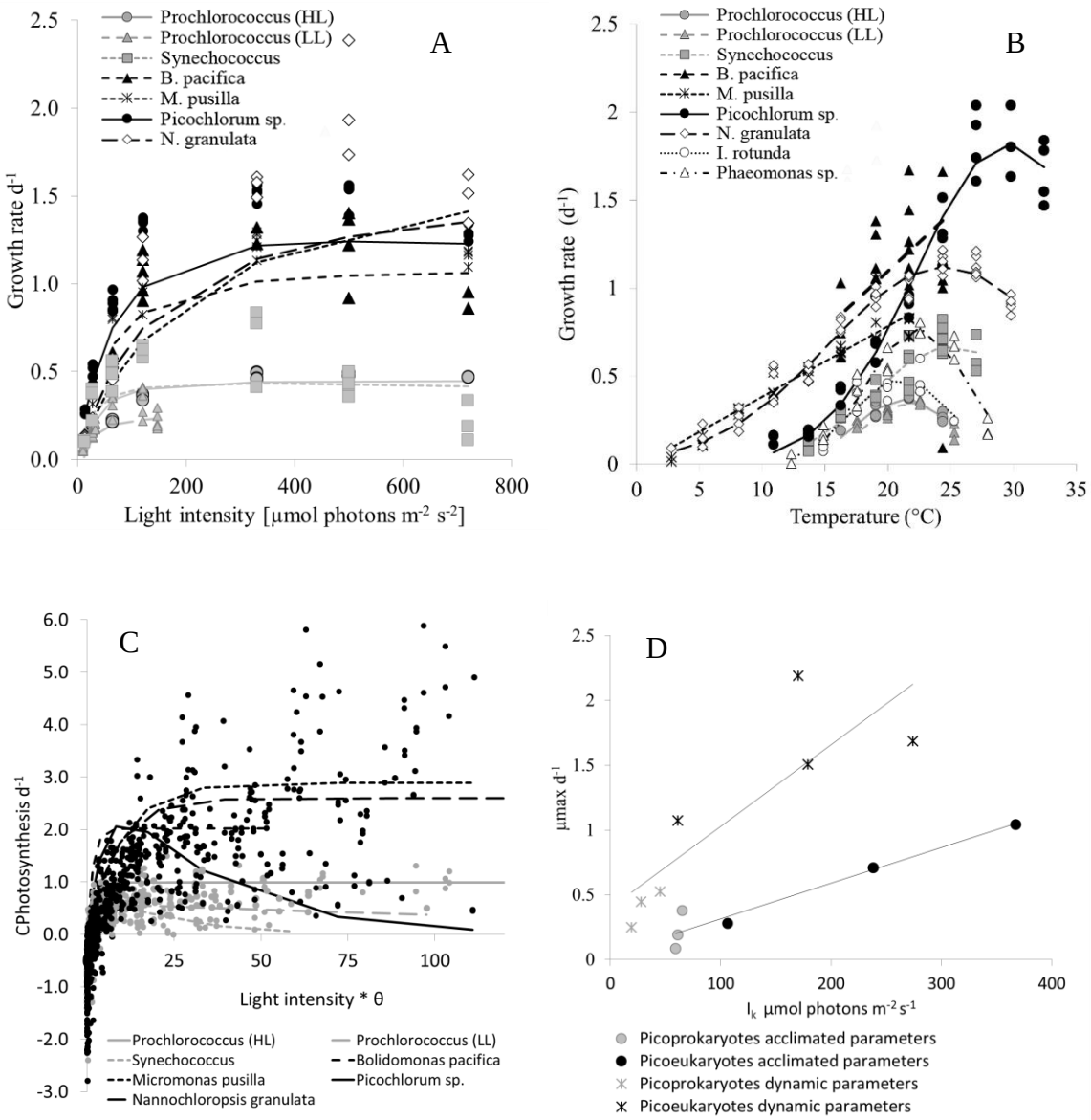

Figure 6. 1 A: Light and B: temperature dependent growth rates of picoprokaryotes (*Prochlorococcus sp.* and *Synechococcus sp.*, grey) and picoeukaryotes (*Bolidomonas pacifica*, *Micromonas pusilla*, *Picochlorum sp.*, *Nannochloropsis granulata*, *Imantonia rotunda* and *Phaeomonas sp.*, black and white). C: Photosynthesis response to light picoprokaryotes, D: light saturation levels related to maximum growth rate using parameters calculated by an acclimated and dynamic model.

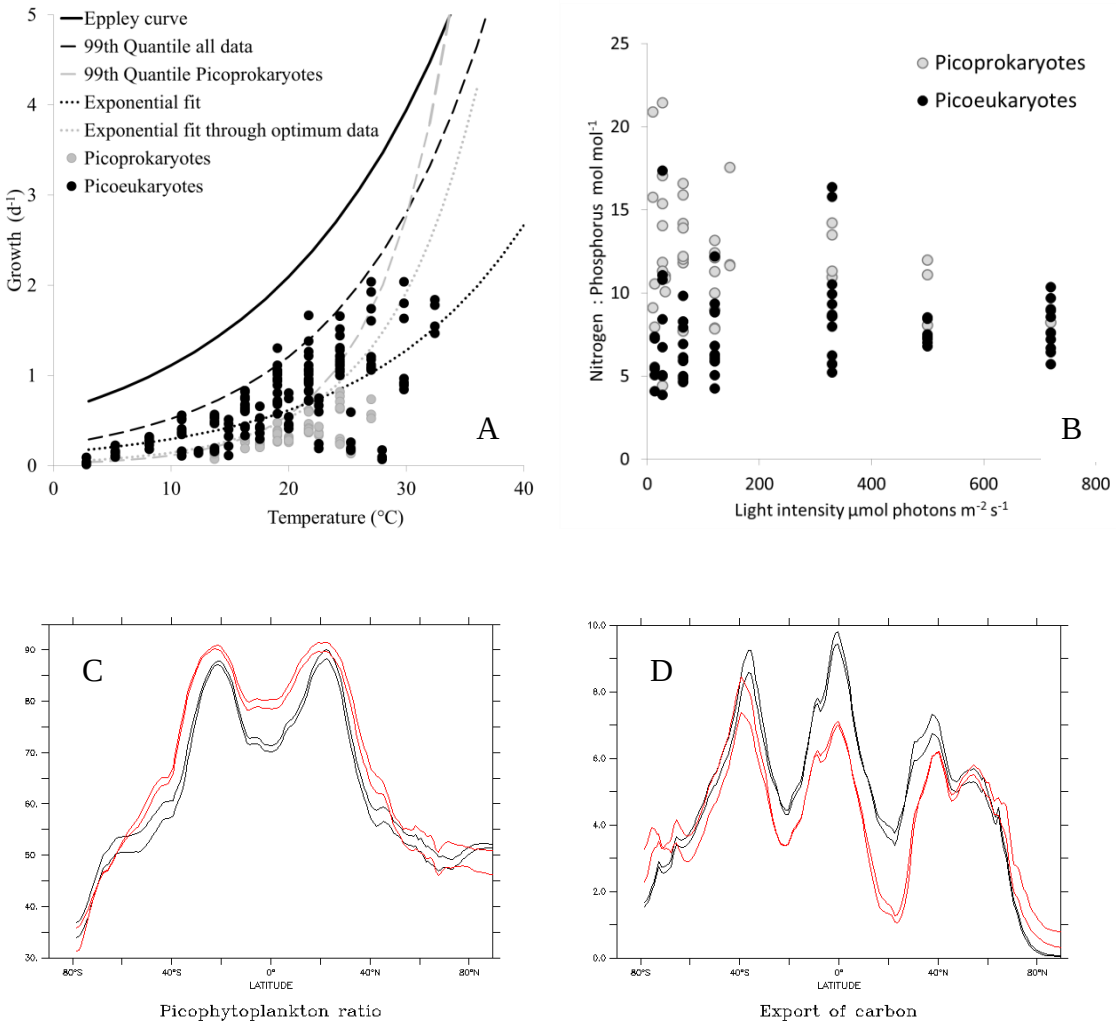

Figure 6. 2 A: Temperature dependent group specific maximum community growth of picoprokaryotes (*Prochlorococcus sp*. and *Synechococcus sp*., grey) and picoeukaryotes (*Bolidomonas pacifica, Micromonas pusilla, Picochlorum sp., Nannochloropsis granulata, Imantonia rotunda* and *Phaeomonas sp.*, black) compared to Eppley's curve. B: Light dependent N:P ratios of both groups, C: Picophytoplankton ratio and D: Export of carbon from the surface ocean, both across a latitudinal gradient in the *PISCES* model under preindustrial (black) conditions and in a future climate change simulation (RCP 8.5) (red).

All species have higher temperature optima than their incubation temperatures in the culture collection, which is plausible as culture collections tend to grow species under suboptimal conditions to decrease growth rates. *Picochlorum sp*. even showed a 50% higher optimum temperature in experiments compared to stock culture temperature after 17 years in collection. Also, species cultured at lower temperatures reached similar optimum temperatures as species grown at a 5°C higher temperature in collection. Further, there was no correlation between affinity to light or light saturation level and light level in culture collection. Potential evolutionary adaptation processes under laboratory conditions are a caveat that affects all studies working on cultured strains of phytoplankton. However, the missing correlations between previous culturing conditions

and physiological optima allow us to exclude major adaptation processes in the investigated strains even though they were held in culture collection for 4 - 25 years.

Even though a few studies distinguish between the physiological response of picoprokaryotes and picoeukaryotes, these two groups are summarized due to their small size as picophytoplankton in most observations and plankton functional type models or even classified as small phytoplankton together with larger phytoplankton groups. As there is less physiological information available on picoeukaryotes than on picoprokaryotes one can assume that they are biased towards the physiological characteristics of the smaller group. The increasing importance of picophytoplankton relative to larger phytoplankton groups highlights the need to better parameterize this plankton functional type in ocean biogeochemical models. Picoeukaryotes constitute a higher biomass than picoprokaryotes and contribute substantially to primary production. Hence it is important to investigate and include the physiological response of this diverse group to fully understand the biogeochemical cycles within the ocean and the impact of the biological pump on the global carbon cycle.

Future studies on the physiological response of a variety of picoeukaryotic species would need to be conducted to be able to include more information on picoeukaryotes in ocean biogeochemical models. For instance, more information is needed on cold water picophytoplankton to improve the understanding of their distribution in higher latitudes.

In addition, the nutrient stoichiometry of the cells is often simplified by applying the Redfield ratio for different plankton functional types, but it varies between groups and environmental conditions. This variability with light and temperature and nutrient availability would further need to be considered. A few studies on nitrogen and phosphorus limitation and the response of carbon nitrogen, phosphorus and chlorophyll *a* content to environmental conditions are available. However, iron limitation is far less studied and would help to improve the understanding of their physiological response in high nutrient low chlorophyll (HNLC) environments.

The light experiments in chapter 2 reveal limitations of the representation of light inhibition in the dynamic photosynthesis model which is commonly implemented in marine biogeochemical models. This could be improved by a more specific investigation of the threshold and a better distinction between short-time light inhibition and irreversible damage through long term inhibition.

Also additional measurements such as the photosynthetic efficiency (Fv/Fm) which relates the absorbed photons to the proportion of available reaction centres in the cell

(Genty et al. 1989) could be included to quantify stress levels in photosystem II. It could further be used to estimate optimum growth conditions and photoinhibition thresholds. It would also allow to identify the acclimation state of the living cell before sampling for cell component analyses or photosynthesis versus irradiance measurements and hence might improve reproducibility of the results. The fraction of energy which is emitted as fluorescence is a variable fraction of the energy which is absorbed by the cell and increases if the fraction which can be used for photosynthesis and heat dissipation decreases (Maxwell & Johnson 2000). As growth rates were measured by daily chlorophyll *a* fluorescence signal, a control of photosynthetic efficiency could have been included to improved the robustness of the results.

Recent studies (Moore et al. 1995:Johnson et al. 2006; Zinser et al. 2007) and the results in chapter 3 indicate that there is a slight discrepancy between optimum temperatures and peak abundance in the field. Also, contrary to laboratory studies, growth rates of picoprokaryotes have been shown to exceed those of picoeukaryotes in a certain area of the oligotrophic ocean (Zubkov 2014). For a better understanding of the combined influence of the three investigated environmental parameters (light, temperature and nutrients) multifactorial laboratory studies would be needed to improve the definition of their fundamental ecological niches.

There was a first attempt to investigate the realised ecological niches of different phytoplankton groups based on a global set of field observations linked to multiple environmental variables such as temperature, nutrients or mixed layer depth (Brun et al. in press). This study identified a broad niche space for picophytoplankton, however it was not able to clearly define it yet. With the extension of available field measurements of picophytoplankton carbon biomass, a better comparison of laboratory studies with observations would be possible. For this it would be necessary to further encourage scientist to report their data to a standardised global database such as the MARine Ecosystem biomass DATa (MAREDAT) initiative (Buitenhuis et al. 2013) on a regular basis.

Finally, it would also be interesting to investigate the competition between picoprokaryotes and picoeukaryotes and the resulting community structure in laboratory experiments. This could also be combined with alternative modelling approaches with emergent phytoplankton communities which evolve through natural selection processes due to interactions with the environment on stochastic self-organizing maps. For this a very large number of plankton functional types is used initially. This allows more

flexibility of diverse physiological traits and does not require the grouping into few specific plankton functional types which are usually constrained with a very limited amount of information. Diverse selection processes result in a community structure specific for a given environment (Follows et al. 2007) and might be compared to field observations on a global scale rather than just locally once a better dataset is available. It would further allow to distinguish better between the ecological niches of picoprokaryotes, picoeukaryotes and may even be used on a level of certain species or even ecotypes. Also, niches of an observed but yet uncultured ecotype with a similar common set of traits but one individual divergent trait could be uncovered as shown for a nitrate-utilizing *Prochlorococcus* in a certain area (Follows et al. 2007). However, the research question would need to justify the higher computational costs of such models (Follows & Dutkiewicz 2011).

Generally, we need to continuously improve the understanding of all physiological mechanisms which govern the whole phytoplankton community structure and biogeochemical fluxes between biological communities and the marine environment. This thesis is a small but important contribution to the understanding of such in picophytoplankton as an important contributor to the phytoplankton community and I hope that it will encourage other researchers to continue resolving open questions.

7. References

Agawin, N., Duarte, C.M. & Agustí, S., 2000. Nutrient and temperature control of the contribution of picoplankton to phytoplankton biomass and production. Limnology and Oceanography, 45(3), pp.591–600.

Alvain, S. et al., 2005. Remote sensing of phytoplankton groups in case 1 waters from global SeaWiFS imagery. Deep Sea Research Part I: Oceanographic Research Papers, 52(11), pp.1989–2004.

Aumont, O., 2012. An ocean biogeochemical model for carbon and ecosystem studies. PISCES user manual, (Version 2).

Aumont, O. et al., 2003. An ecosystem model of the global ocean including Fe, Si, P colimitations. Global Biogeochemical Cycles, 17(2), pp.29–1 – 29–15.

Azam, F. et al., 1983. The Ecological Role of Water-Column Microbes in the Sea. Marine Ecology Progress Series, 10, pp.257–263.

Balzano, S. et al., 2012. Composition of the summer photosynthetic pico and nanoplankton communities in the Beaufort Sea assessed by T-RFLP and sequences of the 18S rRNA gene from flow cytometry sorted samples. The ISME journal, 6(8), pp.1480–98.

Bec, B. et al., 2008. Growth rate peaks at intermediate cell size in Marine photosynthetic picoeukaryotes. Limnology and Oceanography, 53(2), pp.863–867.

Behrenfeld, M.J. et al., 2006. Climate-driven trends in contemporary ocean productivity. Nature, 444(7120), pp.752–5.

Berges, J.A., Franklin, D. & Harrison, P.J., 2001. Evolution of an artificial seawater medium: Improvements in enriched seawater, artificial water over the last two decades. Journal of phycology, 37, pp.1138–1145.

Bertilsson, S. et al., 2003. Elemental composition of marine Prochlorococcus and Synechococcus: Implications for the ecological stoichiometry of the sea. Limnology and Oceanography, 48(5), pp.1721–1731.

Bissinger, J.E. et al., 2008. Predicting marine phytoplankton maximum growth rates from temperature : Improving on the Eppley curve using quantile regression. Limnology and Oceanography, 53(2), pp.487–493.

Bopp, L. et al., 2013. Multiple stressors of ocean ecosystems in the 21st century : Dynamics projections with CMIP5 models. Biogeoschiences Discussions, (10), pp.3627–3676.

Bopp, L. et al., 2005. Response of diatoms distribution to global warming and potential implications : A global model study. Geophysical Research Letters, 32, pp.2–5.

Bopp, L. et al., 2001. Potential impact of climate change on marine export production. Global Biogeochemical Cycles, 15(1), pp.81–99.

Bouman, H. et al., 2011. Water-column stratification governs the community structure of subtropical marine picophytoplankton. Environmental Microbiology Reports, 241, pp.1–10.

Brun, P. et al., (in press.) Ecological niches of open ocean phytoplankton taxa. Limnology and Oceanography.

Buitenhuis, E.T. et al., 2013. MAREDAT: towards a world atlas of MARine Ecosystem DATa. Earth System Science Data, 5(2), pp.227–239.

Buitenhuis, E.T. et al., 2012. Picophytoplankton biomass distribution in the global ocean. Earth System Science Data, (4), pp.37–46.

Buitenhuis, E.T. & Geider, R.J., 2010. A model of phytoplankton acclimation to iron – light colimitation. Limnology and Oceanography, 55(2), pp.714–724.

Buitenhuis, E.T. et al., 2008. Growth rates of six coccolithophorid strains as a function of temperature. Limnology and Oceanography, 53(3), pp.1181–1185.

Buitenhuis, E.T. et al., 2006. Biogeochemical fluxes through mesozooplankton. Global Biogeochemical Cycles, 20(2), pp.1–18.

Buitenhuis, E.T., (in prep.) Compensation light intensity as a function of temperature in Chlorella stigmatophora.

Burnham, K. & Anderson, D., 1998. Akaike's Information Criterion. In Model Selection and Multimodel Inference: A Practical Information-Theoretic Approach. Springer Verlag, pp. 42–49.

Butcher, R.W., 1952. Contributions to our knowledge of the smaller marine algae. Journal of the Marine Biological Association of the United Kingdom, 31(1).

Canadell, J.G. et al., 2010. Interactions of the carbon cycle, human activity, and the climate system: a research portfolio. Current Opinion in Environmental Sustainability, 2(4), pp.301–311.

Chen, B. et al., 2014. Temperature effects on the growth rate of marine picoplankton. Marine Ecology Progress Series, 505, pp.37–47.].

Chen, B. & Liu, H., 2010. Relationships between phytoplankton growth and cell size in surface oceans: Interactive effects of temperature, nutrients, and grazing. Limnology and Oceanography, 55(3), pp.965–972.

Chisholm, S.W., 1992. Phytoplankton size. In P. G. Falkowski & A. Woodhead, eds. Primary productivity and biogeochemical cycles in the sea. New York: Plenum Press, pp. 213–237

Chisholm, S.W. et al., 1988. A novel free-living prochlorophyte abundant in the oceanic euphotic zone. Nature, 334(6180), pp.340–343.

Cochlan, W.P. & Harrison, P.J., 1991. Kinetics of nitrogen (nitrate, ammonium and urea) uptake by the picoflagellate Micromonas pusilla (Prasinophyceae). Journal of Experimental Marine Biology and Ecology, 153(2), pp.129–141..

Cullen, J.J., 1995. Status of the iron hypothesis after the Open-Ocean Enrichment Experiment. Limnology and Oceanography, 40(7), pp.1336–1343.

Cullen, J.J., 1990. On models of growth and photosynthesis in phytoplankton. Deep Sea Research, 37(4), pp.667–683.

Davey, M. et al., 2008. Nutrient limitation of picophytoplankton photosynthesis and growth in the tropical North Atlantic. Limnology and Oceanography, 53(5), pp.1722–1733.

Doney, S.C., 2006. Plankton in a warmer world. Nature, 444, pp.695–696.

Duarte, C.M., 2012. How Cyanobacteria Made Planet Earth Habitable. In C. M. Duarte, ed. The Role of Marine Biota in the Functioning of the Biosphere. Bilbao: Publisher: Fundación BBVA, pp. 55–70.

Dutkiewicz, S., Follows, M.J. & Bragg, J.G., 2009. Modeling the coupling of ocean ecology and biogeochemistry. Global Biogeochemical Cycles, 23(4), pp.1–15.

Enright, C. et al., 2009. PlankTOM10 User Manual. Version 1.02.

Eppley, R., 1972. Temperature and phytoplankton growth in the sea. Fishery Bulletin, 70(4), pp.1063–1085.

Falkowski, P.G. & Oliver, M.J., 2007. Mix and match: how climate selects phytoplankton. Nature reviews. Microbiology, 5(10), pp.813–9.

Falkowski, P.G., Barber, R. & Smetacek, V., 1998. Biogeochemical Controls and Feedbacks on Ocean Primary Production. Science (New York, N.Y.), 281(5374), pp.200–7.

Falkowski, P.G. & La Roche, J., 1991. Acclimation to spectral irradiance in algae. Journal of phycology, pp.8–14.

Fenchel, T., 2008. The microbial loop – 25 years later. Journal of Experimental Marine Biology and Ecology, 366(1-2), pp.99–103.

Field, C. B., 1998. Primary Production of the Biosphere: Integrating Terrestrial and Oceanic Components. Science, 281(5374), pp.237–240.

Finkel, Z. V et al., 2010. Phytoplankton in a changing world : cell size and elemental stoichiometry. Journal of Plankton Research, 32(1), pp.119–137.

Follows, M. J. & Dutkiewicz, S., 2011. Modeling Diverse Communities of Marine Microbes. Annual Review of Marine Science, 3, pp.427–451.

Follows, M. J. et al., 2007. Emergent biogeography of microbial communities in a model ocean. Science (New York, N.Y.), 315(5820), pp.1843–6.

Friedlingstein, P. et al., 2001. Positive feedback between future climate change and the carbon cycle Climate Impact on Land Uptake. Geophysical Research Letters, 28(8), pp.1543–1546.

Furnas, M.J., 1990. In situ growth rates of marine phytoplankton: approaches to measurement, community and species growth rates. Journal of Plankton Research, 12(6), pp.1117–1151.

Geider, R.J. & La Roche, J., 2002. Redfield revisited : variability of C : N : P in marine microalgae and its biochemical basis. European Journal of Phycology, 37, pp.1–17.

Geider, R.J., MacIntyre, H.L. & Kana, T.M., 1998. A dynamic regulatory model of phytoplanktonic acclimation to light, nutrients, and temperature. Limnology and Oceanography, 43(4), pp.679–694.

Geider, R.J., MacIntyre, H.L. & Kana, T.M., 1997. Dynamic model of phytoplankton growth and acclimation:responses of the balanced growth rate and the chlorophyll a:carbon ratio to light, nutrient-limitation and temperature. Marine Ecology Progress Series, 148, pp.187–200.

Geider, R.J., MacIntyre, H.L. & Kana, T.M., 1996. A Dynamic Model of Photoadaptation in Phytoplankton. Limnology and Oceanography, 41(1), pp.1–15.

Geider, R.J., 1987. Light and Temperature Dependence of the Carbon to Chlorophyll a Ratio in Microalgae and Cyanobacteria : Implications for Physiology and Growth of Phytoplankton. New Phytologist, 106(1), pp.1–34.

Genty, B., Briantais, J.-M. & Baker, N.R., 1989. The relationship between the quantum yield of photosynthetic electron transport and quenching of chlorophyll fluorescence. Biochimica et Biophysica Acta (BBA) - General Subjects, 990(1), pp.87–92.

Glover, H.E., Keller, M. & Spinrad, R., 1987. The effects of light quality and intensity on photosynthesis and growth of marine eukaryotic and prokaryotic phytoplankton clones. Journal of Experimental Marine Biology and Ecology, 105(2-3), pp.137–159.

Goldman, C.R., 1986. On phytoplankton growth rates and particulate ratios at low light ' C : N : P. Limnology and Oceanography, (Goldman 1980), pp.1358–1363.

Gómez-Pereira, P.R. et al., 2013. Flow cytometric identification of Mamiellales clade II in the Southern Atlantic Ocean. FEMS microbiology ecology, 83(3), pp.664–71.

Grossman, A.R., Mackey, K.R.M. & Bailey, S., 2010. A Perspective on Photosynthesis in the Oligotrophic Oceans: Hypotheses Concerning Alternate Routes of Electron Flow1. Journal of Phycology, 46, pp.629–634.

Guillou, L. et al., 1999. Bolidomonas: A new genus with two scpecies belonging to a new algal class, The Bolidophyceae (Heterokonta). Journal of Phycology, 35, pp.368–381.

Hays, G.C., Richardson, A.J. & Robinson, C., 2005. Climate change and marine plankton. Trends in ecology & evolution (Personal edition), 20(6), pp.337–44.

Heldal, M. et al., 2003. Elemental composition of single cells of various strains of marine Prochlorococcus and Synechococcus using X-ray microanalysis. Limnology and Oceanography, 48(5), pp.1732–1743.

Henley, W.J. et al., 2004. Phylogenetic analysis of the ' Nannochloris-like ' algae and diagnoses of Picochlorum oklahomensis gen. et sp. nov. (Trebouxiophyceae, Chlorophyta). Phycologia, 43(6), pp.641–652.

Hirata, T. et al., 2011. Synoptic relationships between surface Chlorophyll-a and diagnostic pigments specific to phytoplankton functional types. Biogeosciences, 8(2), pp.311–327.

Honda, D. & Inouye, I., 2002. Ultrastructure and taxonomy of a marine photosynthetic stramenopile Phaeomonas parva gen . et sp . nov . (Pinguiophyceae) with emphasis on the flagellar apparatus architecture. Phycological Research, (50), pp.75–89.

Jiao, N. et al., 2005. Dynamics of autotrophic picoplankton and heterotrophic bacteria in the East China Sea. Continental Shelf Research, 25(10), pp.1265–1279.

Johnson, Z.I. et al., 2006. Niche Partitioning Among Prochlorococcus Ecotypes Along Ocean-Scale Environmental Gradients. Science, 311(5768), pp.1737–40.

Karl, D. et al., 1997. The role of nitrogen fixation in biogeochemical cycling in the subtropical North Pacific Ocean. Nature, 388(6642), pp.533–538.

Karlson, B. et al., 1996. Ultrastructure, pigment composition, and 18S rRNA gene sequence for Nannochloropsis granulata sp. nov. (Monodopsidaceae, Eustigmatophyceae), a marine ultraplankter isolated from the Skagerrak, northeast Atlantic Ocean. Phycologia, 35(3), pp.253–260.

Klausmeier, C.A. et al., 2004. Phytoplankton growth and stoichiometry under multiple nutrient limitation. Limnology and Oceanography, 49(1), pp.1463–1470.

Kraemer, S.M., 2004. Iron oxide dissolution and solubility in the presence of siderophores. Aquatic Sciences - Research Across Boundaries, 66(1), pp.3–18.

Krom, M., 1980. Spectrophotometric Determination of Ammonia: A Study of Modified Berthelot Reaction Using Salicylate and Dichloroisocyanurate. Analyst, 105, pp.305–316.

Kulk, G. et al., 2012. Temperature-dependent growth and photophysiology of prokaryotic and eukaryotic oceanic picophytoplankton. Marine Ecology Progress Series, 466, pp.43–55.

Lakeman, M.B., von Dassow, P. & Cattolico, R.A., 2009. The strain concept in phytoplankton ecology. Harmful Algae, 8(5), pp.746–758.

Landry, M. et al., 2000. Biological response to iron fertilization in the eastern equatorial Pacific (IronEx II). I. Microplankton community abundances and biomass. Marine Ecology Progress Series, 201, pp.27–42.

Laufkötter, C., Vogt, M. & Gruber, N., 2013. Long-term trends in ocean plankton production and particle export between 1960–2006. Biogeosciences, 10(11), pp.7373–7393.

Laws, E. a, 2013. Evaluation of in situ phytoplankton growth rates: a synthesis of data from varied approaches. Annual review of marine science, 5, pp.247–68.

Laws, E.A., 1991. Photosynthetic quotients, new production and net community production in the open ocean. Deep-Sea Research, 38(1), pp.143–167.

Libes, S.M., 2009. Introduction to marine biogeochemistry 2nd ed., Amsterdam: Elsevier, Acad. Press.

Mackey, K.R.M. et al., 2013. Effect of temperature on photosynthesis and growth in marine Synechococcus spp. Plant physiology, 163(2), pp.815–29.

Malinsky-Rushansky, N. et al., 2002. Physiological characteristics of picophytoplankton , isolated from Lake Kinneret : responses to light and temperature. Journal of Plankton Research, 24(11), pp.1173–1183.

Manton, I. & Parke, M., 1960. Further observations on small green flagellates with special reference to possible relatives of Chromulina pusilla Butcher. Journal of the Marine Biological Association of the United Kingdom, (39), pp.275–298.

Marañón, E. et al., 2013. Unimodal size scaling of phytoplankton growth and the size dependence of nutrient uptake and use. Ecology letters, 16(3), pp.371–9.

Marañón, E., 2005. Phytoplankton growth rates in the Atlantic subtropical gyres. Limnology and Oceanography, 50(1), pp.299–310.

Marie, D. et al., 2010. Use of flow cytometric sorting to better assess the diversity of small photosynthetic eukaryotes in the English Channel. FEMS microbiology ecology, 72(Paris 06), pp.165–178.

Marie, D., Simon, N. & Vaulot, D., 2005. Phytoplankton Cell Counting by Flow Cytometry. In R. Andersen & Provasoli-Guillard, eds. Algal culturing techniques. West Boothbay Harbor, ME USA: Elsevier/Academic Press, pp. 253–556.

Martin, J. & Fitzwater, S., 1988. Iron deficiency limits phytoplankton growth in the north-east Pacific subarctic. Nature, (331), pp.341–343.

Massana, R., 2011. Eukaryotic Picoplankton in Surface Oceans. Annual Review of Microbiology, 65(1), pp.91–110.

Maxwell, K. & Johnson, G.N., 2000. Chlorophyll fluorescence — a practical guide. Journal of Experimental Botany, 51(345), pp.659–668.

Montagnes, D.J.S., Kimmance, S.A. & Atkinson, D., 2003. Using Q 10 : Can growth rates increase linearly with temperature ? Aquatic Microbial Ecology, 32, pp.307–313.

Moore, L.R. & Chisholm, S.W., 1999. Photophysiology of the Marine Cyanobacterium Prochlorococcus: Ecotypic Differences among Cultured Isolate. Limnology, 44(3), pp.628–638.

Moore, L.R., Goericke, R. & Chisholm, S.W., 1995. Comparative physiology of Synechococcus and Prochlorococcus: influence of light and temperature on growth, pigments, fluorescence and absorptive properties. Marine Ecology progress series, 116, pp.259–275.

Van Mooy, B. a S. et al., 2006. Sulfolipids dramatically decrease phosphorus demand by picocyanobacteria in oligotrophic marine environments. Proceedings of the National Academy of Sciences of the United States of America, 103(23), pp.8607–12.

Morán, X.A.G. et al., 2010. Increasing importance of small phytoplankton in a warmer ocean. Global Change Biology, 16(3), pp.1137–1144.

Morán, X.A.G., 2007. Annual cycle of picophytoplankton photosynthesis and growth rates in a temperate coastal ecosystem: a major contribution to carbon fluxes. Aquatic Microbial Ecology, 49, pp.267–279.

Morel, A., 1987. Kinetics of nutrient uptake and growth in phytoplankton. Journal of phycology, (23), pp.137–150.

Nägeli, C., 1849. Gattungen einzelliger Algen, physiologisch und systematisch bearbeitet. Neue Denkschriften der Allg. Schweizerischen Gesellschaft für die Gesammten Naturwissenschaften, 10(7), pp.i–viii, 1–139, pls I–VIII.

Parson, T.R., Maita, Y. & Lalli C.M., 1984. A Manual of Chemical and Biological Methods for Seawater Analysis. Chapter 4 Plant Pigments, Oxford: Pergamon Press.

Partensky, F., Hess, W.R. & Vaulot, D., 1999. Prochlorococcus, a marine photosynthetic prokaryote of global significance. Microbiology and molecular biology reviews : MMBR, 63(1), pp.106–27.

Partensky, F., J., B. & Vaulot, D., 1999. Differential distribution and ecology of Prochlorococcus and Synechococcus in oceanic waters : a review. Bulletin de l'Institud océanographique, 19, pp.457–475.

Partensky, F. et al., 1993. Photoacclimation of Prochlorococcus sp.(Prochlorophyta) strains isolated from the North Atlantic and the Mediterranean Sea. Plant Physiology, 101(1), p.285.

Platt, T., Gallegos, C.L. & Harrison, W.G., 1980. Photoinhibition and photosynthesis in natural assemblages of marine phytoplankton. Journal of Marine Research, (38), pp.687–701.

Ploug, H. et al., 2008. Production , oxygen respiration rates , and sinking velocity of copepod fecal pellets : Direct measurements of ballasting by opal and calcite. Limnology and Oceanography, 53(2), pp.469–476.

Poulton, S.W. & R., R., 2002. The low temperature geochemical cycle of iron: From continental fluxes to marine sediment deposition. American Journal of Science, 302, pp.774–805.

Le Quéré, C. et al., 2010. Impact of climate change and variability on the global oceanic sink of CO 2. Global Biogeochemical Cycles, 24(4), pp.1–10.

Le Quéré, C. et al., 2005. Ecosystem dynamics based on plankton functional types for global ocean biogeochemistry models. Global Change Biology, (11), pp.2016–2040.

Raven, J. & Falkowski, P.G., 1999. Oceanic sinks for atmospheric CO2. Plant, Cell and Environment, 22(6), pp.741–755.

Raven, J., 1998. The twelfth Tansley Lecture. Small is beautiful: the picophytoplankton. Functional Ecology, 12(4), pp.503–513.

Raven, J. & Geider, R.J., 1988. Temperature and algal growth. New Phytologist, 110(4), pp.441–461.

Raven, J., 1984. A cost-benefit analysis of photon absoption by photosynthetic unicells. New Phytologist, 98, pp.593–625.

Reckermann, M. & Veldhuis, M.J.W., 1997. Trophic interactions between picophytoplankton and micro- and nanozooplankton in the western Arabian Sea during the NE monsoon 1993. , 12, pp.263–273.

Redfield, A.C., 1958. The biological control of chemical factors in the environment. American Scientist, 46(3), pp.205–221.

Reynolds, N., 1974. Imantonia rotunda gen. et sp. nov., a new member of the Haptophyceae. British Phycological Journal, 9(4), pp.429–434.

Riahi, K. et al., 2011. RCP 8.5—A scenario of comparatively high greenhouse gas emissions. Climatic Change, 109(1-2), pp.33–57.

Schneider, B. et al., 2008. Climate-induced interannual variability of marine primary and export production in three global coupled climate carbon cycle models. Biogeosciences, pp.597–614.

Schoemann, V. et al., 2005. Phaeocystis blooms in the global ocean and their controlling mechanisms: a review. Journal of Sea Research, 53(1-2), pp.43–66.

Shimada, A., Maruyama, T. & Miyachi, S., 1996. Vertical distributions and photosynthetic action spectre of two oceanic picophytopianlcters, Prochlorococcus marinus and Synechococcus sp. Marine Biology, 127(1), pp.15–23.

Sommer, U., 2005. Physikalische und chemische Eigenschaften des Lebensraums Meer. In Biologische Meereskunde. pp. 18–43.

Speight, M.R. & Henderson, P.A., 2010. Primary production and chemosynthesis. In Marine Ecology: Concepts and Applications. Wiley-Blackwell, pp. 49–64.

Strickland, J.D.H. & Parson, T.R., 1972. A practical handbook of seawater analysis Bulletin 1., Ottawa (Canada): Fisheries Research Board of Canada.

Suzumura, M., 2008. Persulfate chemical wet oxidation method for the determination of particulate phosphorus in comparison with a high-temperature dry combustion method. Limnology and Oceanography: Methods, 6, pp.619–629.

Tagliabue, A., Bopp, L. & Gehlen, M., 2011. The response of marine carbon and nutrient cycles to ocean acidification: Large uncertainties related to phytoplankton physiological assumptions. Global Biogeochemical Cycles, 25(3)

Taniguchi, D. et al., 2014. Size-specific growth and grazing rates for picophytoplankton in coastal and oceanic regions of the eastern Pacific. Marine Ecology Progress Series, 509, pp.87–101.

Timmermans, K. et al., 2005. Physiological responses of three species of marine pico-phytoplankton to ammonium, phosphate, iron and light limitation. Journal of Sea Research, 53(1-2), pp.109–120.

Toseland, A. et al., 2013. The impact of temperature on marine phytoplankton resource allocation and metabolism. Nature Climate Change, 3(11), pp.979–984.

Vaulot, D. et al., 2008. The diversity of small eukaryotic phytoplankton (< 3 μm) in marine ecosystems. FEMS microbiology reviews, 32(5), pp.795–820.

Vaulot, D. et al., 2004. The Roscoff Culture Collection (RCC): A collection dedicated to marine picoplankton. Nova Hedwigia, 79(1-2), pp.49–70.

Vázquez-Domínguez, E., Morán, X. & López-Urrutia, a, 2013. Photoacclimation of picophytoplankton in the central Cantabrian Sea. Marine Ecology Progress Series, 493, pp.43–56.

Veldhuis, M. et al., 2005. Picophytoplankton; a comparative study of their biochemical composition and photosynthetic properties. Journal of Sea Research, 53(1-2), pp.7–24.

Vogt, M. et al., 2013. The distribution, dominance patterns and ecological niches of plankton functional types in Dynamic Green Ocean Models and satellite estimates. Biogeosciences Discussions, 10(11), pp.17193–17247.

Waterbury, J.B. et al., 1986. Biologial and Ecological Characterization of the Marine Unicellular Cyanobacterium Synechococcus. In T. Platt & W. Li, eds. Photosynthetic Picoplankton. Can. J. Fish. Aquat. Sci. Bull. 214, pp. 71–120.

Worden, A.Z., 2008. Ecology and diversity of picoeukaryotes. Protist.

Worden, A.Z., Nolan, J.K. & Palenik, B., 2004. Assessing the Dynamics and Ecology of Marine Picophytoplankton: The Importance of the Eukaryotic Component. Limnology, 49(1), pp.168–179.

Zinser, E.R. et al., 2007. Influence of light and temperature on Prochlorococcus ecotype distributions in the Atlantic Ocean. Limnology and Oceanography, 52(5), pp.2205–2220.

Zubkov, M. V, 2014. Faster growth of the major prokaryotic versus eukaryotic CO2 fixers in the oligotrophic ocean. Nature communications, 5(3776).

Zubkov, M. V et al., 2007. Microbial control of phosphate in the nutrient-depleted North Atlantic subtropical gyre. Environmental Microbiology, 9(8), pp.2079–2089

Zubkov, M. V et al., 2003. High Rate of Uptake of Organic Nitrogen Compounds by Prochlorococcus Cyanobacteria as a Key to Their Dominance in Oligotrophic Oceanic Waters. Applied and environmental microbiology, 69(2), pp.1299–1304.